

Spectral Networks and Snakes

Davide Gaiotto,^{1,2} **Gregory W. Moore**² and **Andrew Neitzke**³

¹*School of Natural Sciences, Institute for Advanced Study,
Princeton, NJ 08540, USA*

²*Perimeter Institute for Theoretical Physics,
Waterloo, Ontario, Canada N2L 2Y5*

³*NHETC and Department of Physics and Astronomy, Rutgers University,
Piscataway, NJ 08855–0849, USA*

⁴*Department of Mathematics, University of Texas at Austin,
Austin, TX 78712, USA*

E-mail: dgaiotto@ias.edu, gmoore@physics.rutgers.edu,
neitzke@math.utexas.edu

ABSTRACT: We apply and illustrate the techniques of spectral networks in a large collection of A_{K-1} theories of class S , which we call “lifted A_1 theories.” Our construction makes contact with Fock and Goncharov’s work on higher Teichmüller theory. In particular we show that the Darboux coordinates on moduli spaces of flat connections which come from certain special spectral networks coincide with the Fock-Goncharov coordinates. We show, moreover, how these techniques can be used to study the BPS spectra of lifted A_1 theories. In particular, we determine the spectrum generators for all the lifts of a simple superconformal field theory.

Contents

1	Introduction and Summary	2
2	The level K lifts of A_1 theories	4
3	Coulomb branch and mass deformations of the level K lift of AD_1	7
4	Spectral networks for the level K lift of AD_1	12
4.1	Definition of minimal spectral networks	12
4.2	Realizing minimal spectral networks as WKB spectral networks	16
4.3	Cycles on the SW curve associated to a minimal spectral network	16
5	Flags, flat sections, and cluster coordinates associated with a minimal spectral network	18
5.1	Flat connections and Hitchin solutions	18
5.2	The flags $A_\bullet, B_\bullet, C_\bullet$	19
5.3	Twistings	21
5.4	Line decompositions from the nonabelianization map	22
5.5	Transformation of line decompositions across \mathcal{S} -walls	23
5.6	The plane in \mathcal{E} associated to a branch point	24
5.7	Snakes and the planes	25
5.8	Identifying our triangle with Fock-Goncharov's	27
5.9	Identifying Darboux sections with canonical homs	28
5.10	Identifying Fock-Goncharov triangle coordinates with Darboux coordinates	30
5.11	Another viewpoint on the Darboux coordinates	31
5.12	Compact regions	32
5.13	WKB asymptotics	32
5.14	Formal monodromy	33
5.15	The <i>Yang</i> case	33
6	Example: \mathcal{S}-walls and coordinates for the level 3 lift of AD_1	34
7	How to find the BPS spectrum of the level K lift of AD_1	38
7.1	The spectrum generator	38
7.2	Morphisms of WKB spectral networks for the level 3 lift of AD_1	38
7.3	Determining the spectrum generator	40
7.3.1	Example: $K = 3$	41
7.3.2	Example: $K = 4$	41
7.3.3	Example: $K = 5$	44
8	Gluing of triangles, amalgamation, and identifying Fock-Goncharov edge coordinates with Darboux coordinates	44

9 BPS spectra of level K lifts	48
10 Lifting wall-crossing identities	51
10.1 Conjugating (Yin, Yin) to ($Yin, Yang$)	52
10.2 Level 3 lift of the pentagon identity	52
10.3 Flips and Darboux coordinates	53
11 Open problems and future directions	55
A Linear algebra of three flags in general position	58
A.1 m -triangles	58
A.2 m -triangles associated with three flags	60
A.2.1 Canonical homs	61
A.3 Fock and Goncharov's triple ratio	62
A.3.1 Three alternative formulations of the triple ratio	62
A.3.2 Fock and Goncharov's triple ratios for $K > 3$	64
A.3.3 An alternative coordinate system for $K > 3$	64
A.3.4 Relation between the coordinate systems	65
A.4 Fock and Goncharov's snakes	67
A.4.1 Examples of snakes for $K = 3$ and $K = 4$	70
A.5 Duality	72
B Explicit form of cable transformations	73
B.1 $K = 3$	73
B.2 $K = 4$	74
B.3 The point $r^{x,y,z} = 1$	75

1 Introduction and Summary

In the past few years there has been a renaissance in the subject of four-dimensional field theory with $\mathcal{N} = 2$ supersymmetry and its mathematical applications. In part this development has been driven by many new and important insights into the spectrum of BPS states in these theories. Nevertheless, explicit examples of the many new mathematical structures that are emerging have tended to focus on theories of class S of A_1 type. In an effort to understand more deeply theories of higher rank (for example, $SU(K)$ $\mathcal{N} = 2$ super-Yang-Mills theories with $K > 2$), reference [1] introduced a combinatorial object called a *spectral network*. One of the virtues of spectral networks is that they provide an algorithmic approach to describing the BPS degeneracies of all theories of class S of A type. Another virtue is that they have potentially interesting mathematical applications to the theory of character varieties, moduli spaces of flat connections on Riemann surfaces, Hitchin systems, and higher Teichmüller theory (as considered in [2].)

Spectral networks are unfamiliar objects and [1] provided only a few examples. The present paper is a continuation of [1]. The purposes of this paper are:

1. To exhibit a rich set of examples of A_{K-1} theories of class S with $K > 2$, where the associated spectral networks are nontrivial but tractable. We call these theories “lifted A_1 theories.”
2. To make a direct connection to the work of Fock and Goncharov on higher Teichmüller theory [2]. As explained in [1], spectral networks facilitate the construction of new coordinate systems on moduli spaces of flat connections. Here we will explain how some special cases of these coordinates agree precisely with the coordinates introduced by Fock and Goncharov.
3. To study the BPS degeneracies in special regions of the Coulomb branch of the lifted A_1 theories.

We will now give a brief summary of the paper. We will assume the reader is familiar with the basic definitions of spectral networks and will not review the subject here. See [1] and references therein for background material.

In §2 we define the *lifted A_1 theories of class S* . A lifted theory consists of a special A_{K-1} theory of class S together with a distinguished “lift locus” on its Coulomb branch. The central idea is that while the spectral networks of A_{K-1} theories are in general exceedingly complicated objects, near the lift locus they can be tamed and brought under good control, because in this region they are closely related to the much simpler spectral networks of the parent A_1 theory. The latter networks are simply dual to ideal triangulations of the ultraviolet curve C used to define the theory.

In §3 we focus on the lifts of the “Argyres-Douglas series” of A_1 theories. This is a series of superconformal $d = 4$, $\mathcal{N} = 2$ theories AD_N , $N = 1, 2, 3, \dots$, studied in [3–5]. These theories have Seiberg-Witten curves $\lambda^2 = z^N(dz)^2$ at their superconformal points (often written in local coordinates as $y^2 = z^N$.) The theory AD_1 is somewhat trivial

from the four-dimensional viewpoint (it has no Coulomb branch, no IR gauge fields and no BPS spectrum) and for this reason has not really been discussed in the literature before; however it does admit interesting surface defects. Such a defect can be viewed as a purely two-dimensional Landau-Ginzburg theory with cubic superpotential [6]. All of the AD_N theories are A_1 theories of class S [5, 7]. The reader is urged not to confuse “ A_1 theory” and “ AD_1 theory” in what follows: the former refers to the whole class of theories $S[A_1, C, D]$ while the latter refers to a particular theory in that class.

In §3 we spell out the spectral curves and the normalizable, mass, and non-normalizable deformations of the level K lifts of AD_N theories. We also count the number of parameters in the Stokes matrices of the associated Hitchin system on $C = \mathbb{CP}^1$ with irregular singular point at infinity. A crucial result is (3.27) which gives the rank of the lattice Γ of charges.

In §4 we narrow our focus yet further, to the level K lifts of the AD_1 theory. These theories are already nontrivial and provide the foundation for our approach to the more general lifted A_1 theories. We begin by defining a very special class of *minimal spectral networks*. These come in two types, which we dub *Yin* and *Yang*. These minimal spectral networks are the very simplest spectral networks associated to the level K lifts of AD_1 theories and, while somewhat elaborate, are nevertheless tractable, as the remainder of the paper amply demonstrates. Indeed, in §5 we use these minimal spectral networks to examine some special coordinate systems on moduli spaces of solutions of Hitchin equations associated to the level K lifts of AD_1 theories. This section is really the heart of the paper: it makes direct contact between spectral networks and the work of Fock and Goncharov on higher Teichmüller theory. The main result is equation (5.43), identifying our coordinates on the Hitchin moduli space with those of Fock-Goncharov. In the course of proving this result we find that certain combinatorial objects introduced by Fock and Goncharov, especially “ $(K - 1)$ -triangles of lines” and “snakes,” arise extremely naturally from the viewpoint of spectral networks.

For the convenience of the reader we have reviewed those constructions of Fock and Goncharov which are essential to our present story in Appendix A. Although this appendix is a review, we do add a slightly different approach to the construction of the Fock-Goncharov coordinates on moduli spaces of three flags in a complex vector space. The relation between the new and old approaches is a bit subtle and involves the comparison between flags in a vector space V and the corresponding dual flags in V^* . This is described in §A.3.4 and §A.5. The new approach, based on compositions of canonical homs around closed loops, is better suited to matching with spectral networks.

In §6 we illustrate some of the general reasoning of §5 in the first nontrivial case, $K = 3$.

In §7 we move on to show how spectral networks allow us to determine, in principle, the BPS spectrum of the lifted AD_1 theories in the special region of the Coulomb branch where essentially minimal spectral networks exist. The key result is an algorithm, given in (A.74), for determining the “spectrum generator” of a lifted AD_1 theory. (The spectrum generator is a particular symplectomorphism of a torus, whose factorization in terms of Kontsevich-Soibelman symplectomorphisms encodes the BPS spectrum of the theory.)

§8, §9, and §10 are of a more programmatic and telegraphic nature than the rest of

the paper. In §8 we sketch how one can use our detailed understanding of the level K lifts of the AD_1 theory to construct Darboux coordinates for the more general level K lifts of A_1 theories. Curiously, the essential geometrical gluing operation corresponds to a procedure in cluster algebra theory known as *amalgamation* [8]. Similarly, §9 indicates how our understanding of the level K lifts of the AD_1 theory can be used to construct at least part of the BPS spectrum of the more general level K lifts of A_1 theories, again in a special region of the Coulomb branch. Finally §10 just scratches the surface of what must be a very rich combinatorial story concerning the wall-crossing identities of the the level K lifts of the A_1 theories.

Clearly, much more can be said about this subject. In §11 we indicate a few open problems which seem to us to be interesting and feasible.

2 The level K lifts of A_1 theories

This paper is based on a very simple and general idea. Suppose we have a solution (A, φ) of Hitchin's equations for a compact Lie group G and a homomorphism $\rho : G \rightarrow G'$. Then we can define a corresponding solution of Hitchin's equations for G' just by applying ρ to the transition functions of the bundle and to (A, φ) .¹

This general technique allows one to embed a Hitchin moduli space as a special locus in another Hitchin moduli space. In this paper we narrow the focus considerably and apply this procedure to the homomorphism $\rho : SU(2) \rightarrow SU(K)$ given by the K -dimensional irreducible representation of $SU(2)$, for any integer $K \geq 2$.

Let us write the corresponding spectral curves. These will be the Seiberg-Witten (SW) curves of a “lifted theory of class S .” The SW curve of an A_1 theory of class S (i.e. the spectral curve of an A_1 Hitchin system) takes the form

$$\det(\lambda 1_2 - \varphi) = \lambda^2 + \phi_2 = 0, \quad (2.1)$$

where φ is a 1-form valued (locally) in 2×2 traceless matrices, i.e. in $sl(2, \mathbb{C})$. Applying ρ we obtain a new curve:

$$\det(\lambda 1_K - \rho(\varphi)) = 0. \quad (2.2)$$

We will call this new curve the *level K lift* of the original curve (2.1).

We can write the lifted curve explicitly in terms of the quadratic differential ϕ_2 . Suppose we diagonalize φ :

$$\varphi \sim \begin{pmatrix} \sqrt{-\phi_2} & 0 \\ 0 & -\sqrt{-\phi_2} \end{pmatrix}. \quad (2.3)$$

In the K -dimensional representation the eigenvalues of $\rho(\varphi)$ are

$$(K-1)\sqrt{-\phi_2}, (K-3)\sqrt{-\phi_2}, \dots, (3-K)\sqrt{-\phi_2}, (1-K)\sqrt{-\phi_2}, \quad (2.4)$$

¹This construction is also natural in the framework of Higgs bundles: the holomorphic bundle $E \rightarrow C$ is associated to a holomorphic $G_{\mathbb{C}}$ -bundle P ; using the analytic continuation of ρ we can make a holomorphic $G'_{\mathbb{C}}$ bundle P' , and the image of the Higgs field under ρ gives the new Higgs field.

and hence if K is even the lifted curve has the form

$$(\lambda^2 + \phi_2)(\lambda^2 + 9\phi_2)(\lambda^2 + 25\phi_2) \cdots (\lambda^2 + (K-1)^2\phi_2) = 0, \quad (2.5)$$

while if K is odd the lifted curve has the form

$$\lambda(\lambda^2 + 4\phi_2)(\lambda^2 + 16\phi_2) \cdots (\lambda^2 + (K-1)^2\phi_2) = 0. \quad (2.6)$$

The first few polynomials are explicitly:

$$\begin{aligned} K = 2 : & \quad \lambda^2 + \phi_2, \\ K = 3 : & \quad \lambda^3 + 4\phi_2\lambda, \\ K = 4 : & \quad \lambda^4 + 10\phi_2\lambda^2 + 9\phi_2^2, \\ K = 5 : & \quad \lambda^5 + 20\phi_2\lambda^3 + 64\phi_2^2\lambda, \\ K = 6 : & \quad \lambda^6 + 35\phi_2\lambda^4 + 259\phi_2^2\lambda^2 + 225\phi_2^3, \\ K = 7 : & \quad \lambda^7 + 56\phi_2\lambda^5 + 784\phi_2^2\lambda^3 + 2304\phi_2^3\lambda, \\ K = 8 : & \quad \lambda^8 + 84\phi_2\lambda^6 + 1974\phi_2^2\lambda^4 + 12916\phi_2^3\lambda^2 + 11025\phi_2^4. \end{aligned} \quad (2.7)$$

Of course, the curves (2.5) and (2.6) are highly reducible. A generic small perturbation makes the curve irreducible. A second key idea in this paper is that WKB spectral networks² associated to such irreducible curves behave “at long distance” (on C) like WKB spectral networks of the A_1 theory. That is, the \mathcal{S} -walls of the lifted spectral network will — for parametrically small perturbations — coalesce to \mathcal{S} -walls of the original A_1 spectral network. Thus A_1 spectral networks, which are well understood, serve as a springboard to understand the considerably more intricate A_{K-1} spectral networks.

For example, consider the level 3 lift of the SW curve $\lambda^2 + \phi_2 = 0$ of an A_1 theory. After perturbation, the lifted curve has the form

$$\lambda^3 + (4\phi_2 + \delta\phi_2)\lambda + \delta\phi_3 = 0. \quad (2.8)$$

For $\delta\phi_2$ and $\delta\phi_3$ which are “small” in an appropriate sense, each of the branch points of the A_1 curve splits into three closely separated branch points for the lifted curve. Far away from these branch points, the \mathcal{S} -walls of the lifted spectral network are “close” to the \mathcal{S} -walls of the A_1 spectral network.

Now what is the physics of this construction? We began with an A_1 theory and produced a lifted A_{K-1} theory, at a rather special locus of the Coulomb branch. Of course, the ultraviolet curve C is the same for the original theory and the lifted one; hence the coupling constants are also the same. To understand precisely which theory we obtain, we must consider the behavior of φ near the punctures z_n . For the original A_1 theory, around a regular puncture we have locally

$$\varphi \sim \frac{dz}{z - z_n} \begin{pmatrix} m_n & 0 \\ 0 & -m_n \end{pmatrix} + \cdots \quad (2.9)$$

²We use the term “WKB spectral network” to refer to the particular spectral networks \mathcal{W}_ϑ which were the object of study in most of [1]; a WKB spectral network is uniquely determined by a choice of a point of the Coulomb branch and a phase ϑ .

where m_n is the mass parameter of the defect at the puncture z_n . The level K lift produces a puncture where φ has a simple pole, with residue

$$\text{Diag}\{(K-1)m_n, (K-3)m_n, \dots, (3-K)m_n, (1-K)m_n\}. \quad (2.10)$$

As long as $m_n \neq 0$, these eigenvalues are distinct, so we obtain a *full puncture* in the lifted theory.

We close with some remarks:

1. So far we have described how A_1 theories with only regular singularities, i.e. conformal A_1 theories, lift to conformal A_{K-1} theories. In a similar way, asymptotically free A_1 theories — which arise when φ has higher-order poles at the punctures — lift to asymptotically free A_{K-1} theories. The simplest case of lifting a higher-order pole is discussed in detail in §5 below.
2. Our lift gives an embedding of a hyperkähler manifold (the Coulomb branch of the A_1 theory reduced to three dimensions) into a higher-dimensional hyperkähler manifold (the Coulomb branch of the lifted theory reduced to three dimensions). We will refer to the image of this embedding as the *lift locus*. As the vacuum of the lifted theory approaches the lift locus, many BPS states become massless. On general principles the normal bundle to this locus is a hyperholomorphic vector bundle with connection induced from the Levi-Civita connection on the tubular neighborhood [9]. It should be possible to investigate its geometry by studying the quantum effects of these states on the hyperkähler metric in the limit that they become massless.
3. Suppose we begin with an A_1 theory at a generic point of its Coulomb branch. Then all the branch points of $\Sigma \rightarrow C$ are simple, and hence in a sufficiently small neighborhood of each branch point we have $\phi_2(z) \approx z(dz)^2$ for an appropriate local coordinate z . This is exactly the form of $\phi_2(z)$ in the first superconformal Argyres-Douglas theory AD_1 . Therefore, we can study WKB spectral networks of the lifted theory — at least in these neighborhoods — by studying WKB spectral networks of the level K lifts of AD_1 .
4. We will argue later that understanding the lifts of the AD_N theories is key to understanding the lift of general A_1 theories of class S . The AD_2 theory has a spectral network involving two branch points, and the level K lift of this theory can be understood as a result of “gluing together” two lifts of AD_1 . Similarly, the spectral network of AD_N has N branch points, and the level K lift of AD_N can be viewed as “gluing together” N level K lifts of AD_1 .
5. The notion of “gluing” just mentioned can be made somewhat precise by studying the Darboux coordinate systems $\{\mathcal{Y}_\gamma\}$ on moduli spaces of flat connections. In this context the geometrical gluing corresponds to Fock and Goncharov’s *amalgamation* procedure on cluster algebras. See §8 for further discussion.

6. The consistency of wall-crossing for the AD_N theories is guaranteed by the pentagon identity [7], which first appears in the AD_3 theory. It follows that the level K lifts of the AD_1 , AD_2 , and AD_3 theories are of fundamental importance. Most of this paper is devoted to understanding these cases. §§4–7 focuses on the level K lift of the AD_1 theory, §8 focuses on the lift of the AD_2 theory, and §10 briefly discusses the lifts of the wall-crossing identities.
7. A lifting construction similar to ours appears in [10], embedding the centered 2-monopole moduli space into the centered K -monopole moduli space.

3 Coulomb branch and mass deformations of the level K lift of AD_1

The spectral curve of the superconformal point of the AD_N theory is

$$\lambda^2 = z^N (dz)^2. \quad (3.1)$$

In this section we explain the Coulomb branch and mass deformations of the level K lift of this theory. Readers uninterested in the details should at least note the rank of the charge lattice (3.17) and its rewriting as (3.27). (An analysis similar to what we do here for some related theories has been carried out in [11].)

In organizing the perturbations it is very useful to introduce R -charge (following a strategy first used in [3].) The 1-form λ has mass dimension 1 and R -charge 1. Therefore, from (3.1), z has R -charge and dimension $2/(N+2)$. The perturbations of the lifted equations (2.5) and (2.6) should not change the behavior $\lambda \sim \kappa z^{N/2} dz$ at $z \rightarrow \infty$. (Here κ is a nonzero constant. There is an exceptional case where the growth is subleading to $z^{N/2}$, dealt with below.) This puts strong constraints on what kinds of perturbations we can consider.

Let $P_0^{(K)}$ be the polynomials (2.5) for K even and (2.6) for K odd, with $\phi_2 = -z^N (dz)^2$. These have a Newton polygon with a line as a boundary: namely, writing the equation as

$$P_0^{(K)} = \lambda^K + \sum_{p=2}^K \sum_{a \geq 0} c_{p,a}^{(0)} \lambda^{K-p} z^a (dz)^p = 0, \quad (3.2)$$

the nonzero terms have $2a = Np$. Requiring that $\lambda \sim \kappa z^{N/2} dz$ as $z \rightarrow \infty$ means we should only allow perturbations within the Newton polygon: that is, writing the spectral curve in the form

$$P_0^{(K)} + \sum_{p=0}^K \lambda^{K-p} \delta \phi_p = 0, \quad (3.3)$$

we can only add perturbations of the form

$$\delta \phi_p = \sum_{a=0}^{\left[\frac{Np}{2}\right]} \delta c_{p,a} z^a (dz)^p. \quad (3.4)$$

Let us verify that — as guaranteed by Newton — the asymptotic growth of the roots λ for $z \rightarrow \infty$ is not changed by the perturbations (3.4). Let $P^{(K)}$ be the general polynomial obtained by such perturbations:

$$P^{(k)} = \lambda^K + \sum_{p=2}^K \sum_{a=0}^{\left[\frac{Np}{2}\right]} c_{p,a} z^a (dz)^p \lambda^{K-p}, \quad (3.5)$$

with $c_{p,a} = c_{p,a}^{(0)} + \delta c_{p,a}$. Let $\lambda_0 = \kappa z^{N/2} dz$ be one of the roots of the unperturbed equation. If the $\delta c_{p,a}$ are small then we can compute the perturbed $\lambda = \lambda_0 + \delta\lambda$ from

$$\frac{\partial P_0^{(K)}}{\partial \lambda} \delta\lambda + \sum_{p=2}^K \sum_{a=0}^{\left[\frac{Np}{2}\right]} \delta c_{p,a} z^a (dz)^p \lambda_0^{K-p} = 0. \quad (3.6)$$

Using this, we can easily confirm that, if $\lambda_0 = \kappa z^{N/2} dz$ with $\kappa \neq 0$, then $\delta\lambda$ also grows at most like $z^{N/2} dz$ as $z \rightarrow \infty$.³

A useful interpretation of this constraint on the allowed perturbations is obtained by considering the dimension of $c_{p,a}$. Recall that ϕ_p has mass dimension $[\phi_p] = p$ (e.g. because it is a Casimir made from p powers of φ , and in 5D SYM φ has mass dimension 1), and therefore $c_{p,a}$ has mass dimension

$$[c_{p,a}] = p - \frac{2}{N+2}(a+p) = \frac{Np-2a}{N+2} := D[p, a]. \quad (3.7)$$

Thus (3.4) is the general perturbation whose coefficients have nonnegative mass dimension,

$$D[p, a] \geq 0. \quad (3.8)$$

Now let us analyze normalizable and non-normalizable deformations. We consider a polynomial $P^{(K)}$ of the above type and perturb it to

$$P^{(K)} + \epsilon_{p,a} z^a (dz)^p \lambda^{K-p}. \quad (3.9)$$

By the same analysis we just performed, the change in the asymptotic behavior of the roots is

$$\frac{\partial P^{(K)}}{\partial \lambda} \delta\lambda + \epsilon_{p,a} z^a (dz)^p \lambda^{K-p} = 0. \quad (3.10)$$

If $\lambda \sim z^{N/2} dz$ at infinity then we find the asymptotic behavior

$$\delta\lambda \sim \text{const} \cdot z^{a+\frac{N}{2}-\frac{Np}{2}} dz, \quad (3.11)$$

³There is one special case we should address. If K is odd, then one of the roots is $\lambda_0 = 0$. In this case $\frac{\partial P_0^{(K)}}{\partial \lambda}|_{\lambda_0} \neq 0$ because there is a constant term in $P_0^{(K)}$. Likewise, the only terms which can contribute to $\delta\lambda$ are those with $p = K$. The most dangerous of these is the one with $a = \left[\frac{NK}{2}\right]$. One easily checks that this give $\delta\lambda \sim z^{\left[N/2\right]} dz$ as $z \rightarrow \infty$, so no root grows faster than $z^{N/2} dz$, although the perturbation of this special root might grow more slowly than $z^{N/2} dz$.

where the constant depends on which root we perturb around. Note that the power of z can be written as $\frac{N}{2} - \frac{N+2}{2}D[p, a]$. The perturbation is considered to be *normalizable* if

$$\int_{\Sigma} |\delta\lambda|^2 < \infty. \quad (3.12)$$

The only source of divergence is the integration on the sheets covering the region $|z| \rightarrow \infty$. Therefore the potential divergence of (3.12) is controlled by the potential divergence of the integral

$$\int^{\infty} \frac{d|z|}{|z|^{(N+2)D[p, a] - (N+1)}} \quad (3.13)$$

from the region at infinity. and therefore we conclude that:⁴

1. If $D[p, a] > 1$ the perturbation is *normalizable*.
2. If $D[p, a] = 1$ the perturbation leads to a log-divergent integral. These are called *mass perturbations*.
3. If $D[p, a] < 1$ the perturbation is *non-normalizable*.

Now we can count the allowed perturbations. The number of pairs (p, a) with $p = 3, \dots, K$ and $a = 0, 1, \dots, \left[\frac{Np}{2}\right]$ with $D[p, a] > 1$ gives the number of normalizable deformations. These are local coordinates in the normal bundle to the lift locus in the Coulomb branch of the lifted A_{K-1} theory. Similarly, the pairs with $D[p, a] = 1$ give the mass perturbations.

The mass perturbations are the ones with $a = \frac{1}{2}N(p-1) - 1$ for $p = 2, \dots, K$. Since a must be integral, in the case when N is odd we only have mass parameters for odd values of p . Thus the number of mass parameters is:

$$\text{Mass}(N, K) = \begin{cases} K-1 & N = 0 \bmod 2, \\ \frac{(K-2)}{2} & N = 1 \bmod 2, K = 0 \bmod 2, \\ \frac{(K-1)}{2} & N = 1 \bmod 2, K = 1 \bmod 2. \end{cases} \quad (3.14)$$

Similarly, counting the number of normalizable parameters we find

$$\text{Norm}(N, K) = \begin{cases} \frac{1}{4}NK(K-1) - (K-1) & N = 0 \bmod 2, \\ \frac{1}{4}(N-1)K(K-1) + \frac{(K-2)^2}{4} & N = 1 \bmod 2, K = 0 \bmod 2, \\ \frac{1}{4}(N-1)K(K-1) + \frac{(K-1)(K-3)}{4} & N = 1 \bmod 2, K = 1 \bmod 2. \end{cases} \quad (3.15)$$

In the A_{K-1} theory there is an IR charge lattice Γ . Γ should have an electric and magnetic charge generator for each independent normalizable deformation, and a flavor charge generator for each independent mass deformation. We therefore expect that the rank of Γ will be

$$\text{rank}(\Gamma) = 2 \text{Norm}(N, K) + \text{Mass}(N, K). \quad (3.16)$$

⁴Note that if we use the root growing like $z^{[N/2]}dz$ and N is odd then the estimate (3.11) is changed. However, a parameter is non-normalizable if for *some* root the integral (3.12) is divergent.

Using (3.14) and (3.15) this works out to

$$\text{rank}(\Gamma) = \left(\frac{1}{2} NK - 1 \right) (K - 1), \quad (3.17)$$

in all cases.

Now, the AD_N theory is associated with a Hitchin system on \mathbb{CP}^1 , of rank $K = 2$, with an irregular singularity at $z = \infty$ supporting $N + 2$ Stokes sectors, as described in [7]. In particular, each \mathcal{S} -wall of a WKB spectral network in this theory is asymptotic to one of the Stokes rays as $z \rightarrow \infty$. As we have explained, the level K lift does not change the number of Stokes sectors at infinity: the \mathcal{S} -walls of the lifted network asymptote to the same Stokes rays as those of the original network. We now check that the result (3.17) is indeed as expected for a rank K Hitchin system on the complex plane with $N + 2$ Stokes sectors at infinity.

Viewing the Hitchin system as a moduli space of flat connections, the moduli can be encoded in a set of $K \times K$ Stokes matrices S_n , $n = 1, \dots, N + 2$, cyclically ordered. The S_n alternate between upper and lower triangular, with 1 on the diagonal. We must discuss the cases N even and odd separately.

For N even the product of the Stokes matrices is the formal monodromy at infinity, which we diagonalize:

$$\prod_{n=1}^{N+2} S_n = \text{Diag}\{\mu_1, \dots, \mu_K\}. \quad (3.18)$$

This formal monodromy encodes the mass parameters. Since $\prod_{i=1}^K \mu_i = 1$ there are $(K - 1)$ independent mass parameters in agreement with (3.14). Having diagonalized the formal monodromy most of the gauge freedom has been fixed. We may still conjugate by diagonal matrices in $SL(K, \mathbb{C})$. Thus we expect a moduli space with complex dimension

$$(N + 2) \cdot \frac{K(K - 1)}{2} - (K^2 - 1) - (K - 1), \quad (3.19)$$

and the reader can check that this nicely coincides with $2\text{Norm}(N, K)$ in the case N is even.

Now let us consider the case when N is odd. In this case there is branching at infinity. For the AD_N theories with N odd the monodromy exchanges the two branches. How should we lift this permutation? We can again use the homomorphism ρ . The formal monodromy for the AD_N theory with N odd is

$$\begin{pmatrix} 0 & 1 \\ -1 & 0 \end{pmatrix}. \quad (3.20)$$

The level K lift of this group element is an antidiagonal matrix of alternating +1 and -1's:

$$W_0^{(K)} := e_{K,1} - e_{K-1,2} + e_{K-2,3} \pm \dots + (-1)^{K-1} e_{1,K} \quad (3.21)$$

Therefore, the branching at infinity is given by the permutation

$$w_0^{(K)} : \{1, 2, \dots, K - 1, K\} \mapsto \{K, K - 1, \dots, 2, 1\}. \quad (3.22)$$

This permutation will play an important role in our analysis and similarly the matrix $W_0^{(K)}$ will be important in subsequent sections. When K is understood we drop the superscript and just write W_0 . Note that $(W_0^{(K)})^2 = (-1)^{K-1}$.

From this discussion follows that the monodromy constraint along the lift locus is

$$\prod_{n=1}^{N+2} S_n = W_0^{(K)}. \quad (3.23)$$

When counting deformation parameters it is more useful to enlarge our scope of theories by turning on mass parameters. The monodromy constraint for this broader class of theories is then of the form

$$\prod_{n=1}^{N+2} S_n = \text{AntiDiag}\{\mu_1, \dots, \mu_K\}. \quad (3.24)$$

The remaining gauge symmetry in (3.24) is conjugation by diagonal $SL(K, \mathbb{C})$ transformations. We can usefully fix it further by gauging so that the masses are w_0 -invariant, i.e.

$$\mu_1 = \mu_K, \mu_2 = \mu_{K-1}, \dots \quad (3.25)$$

This gives $(K-2)/2$ mass parameters for K even and $(K-1)/2$ for K odd, in agreement with (3.14). Having chosen a generic set of w_0 -invariant mass parameters there are still $(K-2)/2$ independent diagonal gauge degrees of freedom for K even and $(K-1)/2$ independent diagonal gauge degrees of freedom for K odd. Thus we expect that the dimension of the moduli space for N odd is

$$2 \text{Norm}(N, K) = (N+2) \cdot \frac{K(K-1)}{2} - (K^2 - 1) - \begin{cases} \frac{K-2}{2} & K = 0 \pmod{2} \\ \frac{K-1}{2} & K = 1 \pmod{2} \end{cases} \quad (3.26)$$

which indeed agrees with (3.15).

Finally, let us briefly consider the expected structure of the “Darboux coordinates” in this case. These are locally-defined functions \mathcal{Y}_γ on the Hitchin moduli spaces, discussed extensively in [1, 7, 12]. We rewrite the rank of Γ , (3.17), as

$$\text{rank}(\Gamma) = N \frac{(K-1)(K-2)}{2} + (N-1)(K-1). \quad (3.27)$$

So this is the number of independent coordinates we expect. As we have stressed, for small $\delta c_{p,a}$, the WKB spectral network of the lifted theory approximates that of the original A_1 theory. In particular, the WKB spectral network of the AD_N theory (considered as a particular example of an A_1 theory) determines an ideal triangulation of the disk with $N+2$ vertices. These vertices represent the asymptotic directions of the \mathcal{S} -walls on the plane. There are N triangles in this triangulation, and $N-1$ internal edges. Now, recall that for A_1 theories each internal edge of the triangulation is associated with one independent coordinate \mathcal{Y}_γ , and there are no coordinates associated with triangles; so in the original A_1 theory there are a total of $N-1$ coordinates. The result (3.27) suggests how this statement extends to the level K lift: each triangle will contribute $\frac{(K-1)(K-2)}{2}$ independent “triangle coordinates,” and each internal edge will contribute $(K-1)$ independent “edge coordinates.” In the following sections we will verify that this is indeed the case.

4 Spectral networks for the level K lift of AD_1

In this section we make use of m -triangles. This is a concept introduced and used extensively in the work of Fock and Goncharov on higher Teichmüller theory [2]. See Appendix A.1 for m -triangles, and Appendix A for important background on some associated linear algebra.

4.1 Definition of minimal spectral networks

Our first order of business is to define *minimal spectral networks* of the level K lift of the AD_1 theory. Recall that the AD_1 theory has spectral curve

$$\lambda^2 = z(\mathrm{d}z)^2, \quad (4.1)$$

or equivalently $\phi_2 = -z(\mathrm{d}z)^2$. The lifted polynomial is order K in λ , as are its perturbations. Its discriminant therefore is a polynomial in z of degree $\frac{1}{2}K(K-1)$, and hence for generic perturbations there are $\frac{1}{2}K(K-1)$ simple branch points.

In general, the corresponding spectral networks are very complex. Still, there are a few general things we can say. Three \mathcal{S} -walls emerge from each branch point. At large $|z|$ each of them asymptotes to one of the three \mathcal{S} -walls of the AD_1 theory. We will refer to each collection of \mathcal{S} -walls asymptoting to a single AD_1 \mathcal{S} -wall as a *cable*. The lift of AD_1 thus has three cables, each consisting of at least $\frac{1}{2}K(K-1)$ \mathcal{S} -walls; in general each cable contains more than $\frac{1}{2}K(K-1)$ \mathcal{S} -walls, because there can be secondary \mathcal{S} -walls emanating from joints.

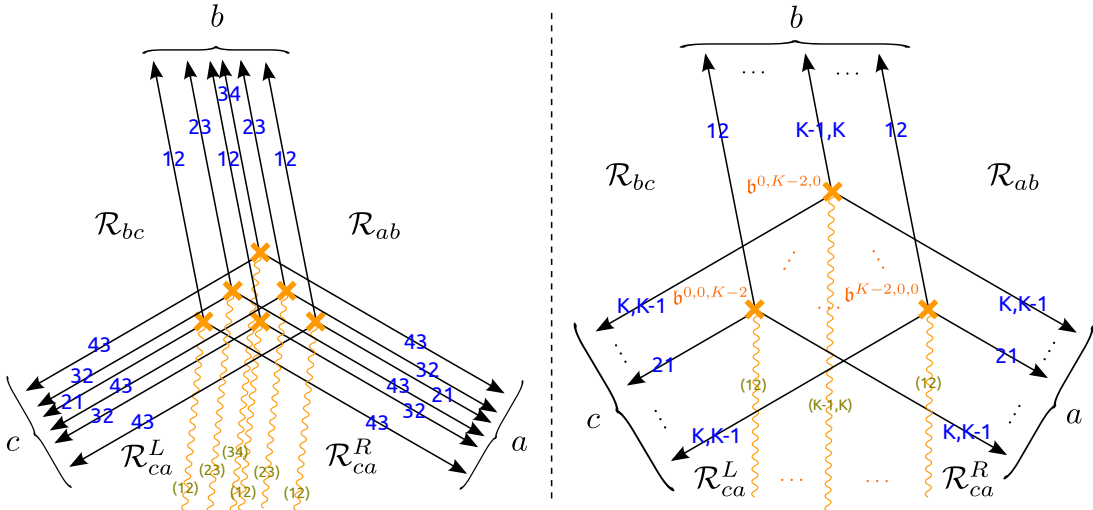


Figure 1. Minimal spectral networks of *Yin* type, for $K = 4$ (left) and general K (right).

We now define a *minimal level K spectral network*. In fact we will need to distinguish between two basic types, which we call minimal spectral networks of *Yin*-type and *Yang*-type. See Figures 1 and 2. A minimal spectral network is a spectral network of the level K lift of the AD_1 theory, with the following properties:

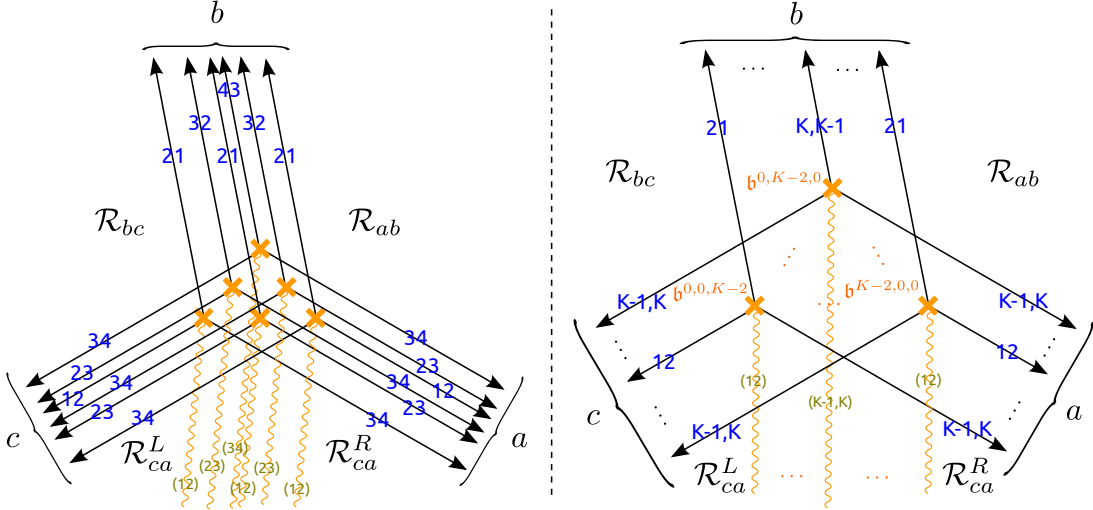


Figure 2. Minimal spectral networks of Yang type, for $K = 4$ (left) and general K (right).

1. Each of the three cables consists of precisely $\frac{1}{2}K(K-1)$ \mathcal{S} -walls.
2. Each branch point is associated with a point in a $(K-2)$ -triangle. We label the branch points $b^{x,y,z}$, where x, y, z are nonnegative integers with $x + y + z = K - 2$.
3. The branch points sit in an approximate triangular array in the z -plane, with $b^{0,K-2,0}$ the topmost vertex, $b^{0,0,K-2}$ the bottom left vertex and $b^{K-2,0,0}$ the bottom right vertex. The three cables are labeled a, b, c with b pointing (roughly) to the north, a to the southeast and c to the southwest. There are consequently three “large” open regions near $z = \infty$. We call the region between the a - and b -cables \mathcal{R}_{ab} , lying in the northeast. The region between the b - and c -cables is denoted \mathcal{R}_{bc} , and lies in the northwest. Finally, \mathcal{R}_{ca} lies in the south.
4. There exists a trivialization of the branched cover $\Sigma \rightarrow \mathbb{C}$ (i.e. choice of branch cuts) such that each branch point is of type $(i, i+1)$ for some i . In this trivialization $b^{x,y,z}$ is a branch point of type $(y+1, y+2)$, where $0 \leq y \leq K-2$. Thus, the top vertex is of type $(K-1, K)$, the next row has two branch points of type $(K-2, K-1)$, the next row has three branch points of type $(K-3, K-2)$, and so on until the bottom row has $K-1$ branch points of type $(1, 2)$. The cuts point down and slightly to the southwest, and asymptote to a single line, also pointing down and slightly to the southwest. The cuts thus divide the region \mathcal{R}_{ca} into western and eastern halves. Moving from the southwest to the southeast, we encounter cuts of type

$$\omega_{K-1}\omega_{K-2} \cdots \omega_2\omega_1, \quad (4.2)$$

where

$$\begin{aligned}
\omega_{K-1} &= (1, 2)(2, 3) \cdots (K-1, K), \\
\omega_{K-2} &= (1, 2)(2, 3) \cdots (K-2, K-1), \\
&\vdots \\
\omega_2 &= (1, 2)(2, 3), \\
\omega_1 &= (1, 2).
\end{aligned} \tag{4.3}$$

Reading these words from left to right describes the cuts encountered as one moves on the z -plane from left to right, i.e. counterclockwise relative to an origin inside the triangle. (See the cuts in Figures 1 and 2.)

5. The net transformation of sheets across all the cuts is the permutation $w_0^{(K)}$, which takes $(1, 2, \dots, K-1, K) \rightarrow (K, K-1, \dots, 2, 1)$. Equivalently it is the product of $[K/2]$ transpositions:

$$w_0^{(K)} = \begin{cases} (1, K)(2, K-1) \cdots (\frac{K}{2}, \frac{K}{2}+1) & K = 0 \bmod 2, \\ (1, K)(2, K-1) \cdots (\frac{K-1}{2}, \frac{K+3}{2}) & K = 1 \bmod 2. \end{cases} \tag{4.4}$$

6. There are two essentially different kinds of minimal spectral networks, which we call *Yin*-type and *Yang*-type. In the *Yin*-type, in each of the three cables there is a unique \mathcal{S} -wall either of type $K-1, K$ or of type 21. In the *Yang*-type, each cable contains a unique \mathcal{S} -wall of type $K, K-1$ or of type 12. See Figures 1 and 2. In the following we describe in detail the structure of the cables for the *Yin*-type spectral network. The *Yang*-type is obtained by “transposing” all the \mathcal{S} -walls $ij \rightarrow ji$.

7. With the same trivialization of $\Sigma \rightarrow C$ used above, $\mathfrak{b}^{x,y,z}$ is associated with an \mathcal{S} -wall in the b -cable, of type $K-y-1, K-y$. One can attach to each wall of type ij an “ \mathcal{S} -factor” of type ij , which concretely means a matrix whose only nonzero off-diagonal entry is in the ij position. We abuse notation by representing any such matrix as S_{ij} . (A precise definition of these matrices can be found in (A.48) below.) Then the product of \mathcal{S} -factors which one encounters in crossing the b -cable is

$$T_{b\text{-cable}} = \beta_1 \beta_2 \cdots \beta_{K-2} \beta_{K-1}, \tag{4.5}$$

where

$$\begin{aligned}
\beta_{K-1} &= S_{K-1,K} S_{K-2,K-1} S_{K-3,K-2} \cdots S_{2,3} S_{1,2}, \\
\beta_{K-2} &= S_{K-2,K-1} S_{K-3,K-2} \cdots S_{2,3} S_{1,2}, \\
\beta_{K-3} &= S_{K-3,K-2} \cdots S_{2,3} S_{1,2}, \\
&\vdots \\
\beta_2 &= S_{2,3} S_{1,2}, \\
\beta_1 &= S_{1,2}.
\end{aligned} \tag{4.6}$$

Reading this product from right to left gives the \mathcal{S} -factors encountered in moving from \mathcal{R}_{ab} to \mathcal{R}_{bc} at large $|z|$ from right to left, that is, counterclockwise.

8. The \mathcal{S} -walls for the a -cable are

$$T_{a\text{-cable}} = \alpha_1 \alpha_2 \cdots \alpha_{K-2} \alpha_{K-1}, \quad (4.7)$$

$$\begin{aligned} \alpha_{K-1} &= S_{K,K-1}, \\ \alpha_{K-2} &= S_{K,K-1} S_{K-1,K-2}, \\ &\vdots \\ \alpha_2 &= S_{K,K-1} S_{K-1,K-2} \cdots S_{3,2}, \\ \alpha_1 &= S_{K,K-1} S_{K-1,K-2} \cdots S_{3,2} S_{2,1}. \end{aligned} \quad (4.8)$$

Reading the product (4.7) from right to left gives the \mathcal{S} -factors encountered as one moves counterclockwise from the region \mathcal{R}_{ca}^R (to the right of the cuts) to \mathcal{R}_{ab} .

9. The \mathcal{S} -walls for the c -cable are

$$T_{c\text{-cable}} = \gamma_1 \gamma_2 \cdots \gamma_{K-2} \gamma_{K-1}, \quad (4.9)$$

$$\begin{aligned} \gamma_{K-1} &= S_{2,1} S_{3,2} \cdots S_{K-1,K-2} S_{K,K-1}, \\ \gamma_{K-2} &= S_{3,2} \cdots S_{K,K-1}, \\ &\vdots \\ \gamma_2 &= S_{K-1,K-2} S_{K,K-1}, \\ \gamma_1 &= S_{K,K-1}. \end{aligned} \quad (4.10)$$

Here again, reading the product from right to left gives the pattern of \mathcal{S} -walls encountered as one moves counterclockwise from region \mathcal{R}_{bc} to \mathcal{R}_{ca}^L (to the left of the cuts).

We would like to make a number of remarks about the minimal spectral network.

1. In a minimal spectral network there are many intersections of \mathcal{S} -walls. As explained in [1], the rules of spectral networks demand that intersections of \mathcal{S} -walls in general generate new \mathcal{S} -walls. However, in the minimal spectral network the intersections are always such that no new \mathcal{S} -walls are produced. This is the reason this network is called “minimal.”
2. In accounting for the configuration of \mathcal{S} -wall factors in the a - and c -cables it is crucial to take into account the branch cuts. This is evident e.g. in Figures 1 and 2.
3. In Section 4.2 we give some evidence, for small values of K , that there are indeed branched covers $\Sigma \rightarrow C$ which are small perturbations of the level K lift, and for which the corresponding WKB spectral network is a minimal spectral network. Of course, the minimal level K spectral networks are perfectly legitimate spectral networks in the sense of [1], irrespective of whether they arise as WKB spectral networks or not.

4. There are $4 = 2 \times 2$ possible definitions we could have used for “minimal spectral network.” First, there is a two-fold choice of whether to have $(K - 1)$ branch points of type (12) and one branch point of type $(K - 1, K)$ or to have $(K - 1)$ branch points of type $(K - 1, K)$ and one of type (12) . This choice is only a convention: one can reverse it just by relabeling the sheets. There is another two-fold choice of whether the cable which is not adjacent to the cuts involves \mathcal{S} -walls of type $i, i + 1$ or $i + 1, i$. This choice is *not* a convention: reversing it exchanges the *Yin* and *Yang* type minimal spectral networks, which are really different from one another.
5. There are $8 = 2^3$ possible types of cable products, such as $T_{a\text{-cable}}, T_{b\text{-cable}}, T_{c\text{-cable}}$ above, which we could encounter. Let us denote factors such as $\beta_{K-1}, \dots, \beta_1$ in (4.5) as “strings” and let us define their “length” to be the number of \mathcal{S} -factors in β_i . Then the 8 possibilities arise as follows: First, the strings can be growing or shrinking in length as i increases. Second, the \mathcal{S} -factors can be of type $S_{i,i+1}$ or $S_{i+1,i}$. Third, the string of length 1 can be of type $(1, 2)$ or $(K - 1, K)$.

4.2 Realizing minimal spectral networks as WKB spectral networks

Much of this paper depends only on the existence of minimal spectral networks as spectral networks in the sense of §9 of [1]. Nevertheless it is interesting to ask whether this spectral network actually arises as a WKB spectral network at some point of the Coulomb branch of the lifted theory. This will be important if, for example, we want to use minimal spectral networks to study the BPS spectrum.

More precisely, we do not really care whether our networks are strictly minimal: for all of our purposes in this paper it will be enough to consider networks which are *equivalent* to a minimal spectral network, in the sense of [1]. We call such networks *essentially minimal*.

We have no general proof that there are such points in the Coulomb branch. However, we have found explicitly that they exist for all $K \leq 5$. The WKB spectral networks in question are illustrated in Figure 3 for $K = 4, K = 5$.

We have not gotten beyond $K = 5$ with this approach; however, to go further, we can also generalize the lift locus to the more general family of SW curves

$$(\lambda^2 + c_1^2 \phi_2)(\lambda^2 + c_2^2 \phi_2) \cdots (\lambda^2 + c_{K/2}^2 \phi_2) \quad (4.11)$$

where $c_i \in \mathbb{R}$ and K is even, with a similar generalization for K odd. (Taking $c_i = 2i - 1$ we recover the lift locus.) By considering small perturbations of this family we have realized essentially minimal spectral networks as WKB spectral networks for $K \leq 9$. Nevertheless, it remains an open problem to find a systematic procedure for finding minimal or essentially minimal spectral networks as WKB spectral networks.

4.3 Cycles on the SW curve associated to a minimal spectral network

We now give a basis for the lattice Γ associated to the SW cover $\Sigma \rightarrow C$ associated with a minimal spectral network.

The branch points of the cover are in 1-1 correspondence with the points of a $(K - 2)$ -triangle. Let us consider the upwards-pointing triangles in this $(K - 2)$ -triangle. These

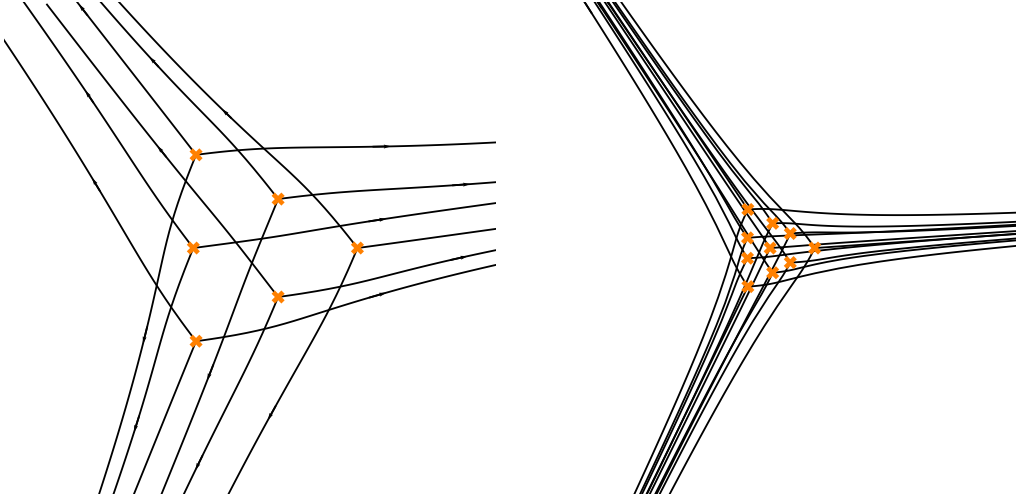


Figure 3. Two essentially minimal WKB spectral networks. **Left:** the WKB spectral network for the $K = 4$ lift of AD_1 theory, with SW curve $\lambda^4 - 10z(dz)^2\lambda^2 + 4(dz)^3\lambda + 9z^2(dz)^4 = 0$, and $\vartheta = 0.2$. **Right:** the WKB spectral network for the $K = 5$ lift of AD_1 theory, with SW curve $\lambda^5 - 20z(dz)^2\lambda^3 + (dz)^3\lambda^2 + 64z^2(dz)^4\lambda - 2z(dz)^5 = 0$, and $\vartheta = 0.1$.

are in 1-1 correspondence with the points of a $(K - 3)$ -triangle. If (x, y, z) is a point in the $(K - 3)$ -triangle, the three branch points at the vertices of the corresponding shaded triangle are of the form $\mathfrak{b}^{x,y+1,z}$, $\mathfrak{b}^{x+1,y,z}$, and $\mathfrak{b}^{x,y,z+1}$ where $x + y + z = K - 3$. Setting $i = K - 1 - y$, the branch point at the top vertex is of type $(i - 1, i)$, while the branch points at the bottom left and right vertices are of type $(i, i + 1)$. Note that the monodromy of the cover $\Sigma \rightarrow C$ around a small path \wp looping counterclockwise once around these three branch points is the transposition $(i - 1, i + 1)$. Therefore, the closed path \wp lifts to a *closed* path $\wp^{(i)}$ on the i^{th} sheet of Σ . We denote the homology class of this path $\gamma^{\mathfrak{v}}$ where $\mathfrak{v} = (x, y, z)$. There are $\frac{1}{2}(K - 2)(K - 1)$ such cycles, which can be shown to be linearly independent.⁵ Thus, given equation (3.27) (taking $N = 1$), they form a basis for Γ (at least rationally). In fact, there is a nice formula for the intersection matrix of the basis of cycles $\gamma^{\mathfrak{v}}$:

$$\langle \gamma^{\mathfrak{v}_1}, \gamma^{\mathfrak{v}_2} \rangle = \begin{cases} +1 & [\mathfrak{v}_1, \mathfrak{v}_2] \text{ oriented edge} \\ -1 & [\mathfrak{v}_1, \mathfrak{v}_2] \text{ anti oriented edge} \\ 0 & \text{otherwise} \end{cases} \quad (4.12)$$

where ‘‘edge’’ refers to edges of the $(K - 3)$ -triangle of cycles, oriented counterclockwise.

We will also need basepoints for the relative homology torsors $\Gamma(z, z)$ and $\Gamma(z_1, z_2)$. (For definitions of these torsors see [1], §§3.2 and 3.3.) These basepoints will depend on a choice of a cable. For each branch point \mathfrak{b} and each z on a (primary) \mathcal{S} -wall emerging from \mathfrak{b} , we let $\gamma_{i,i+1}^{\mathfrak{b}} \in \Gamma(z, z)$ denote the open homology class on Σ which projects to the

⁵One proof makes use of the result (5.43) below and the fact that the $r^{\mathfrak{v}}$ are an independent set of coordinates for the moduli space of three flags in a K -dimensional vector space. It would be nice to have a more direct geometrical argument that the cycles are linearly independent on the covering surface Σ .

\mathcal{S} -wall and begins at $z^{(i)}$ (the preimage of z on the i^{th} sheet), goes down to the ramification point over \mathfrak{b} , and comes back on the $(i+1)^{th}$ sheet to end at the preimage $z^{(i+1)}$. Similarly define $\gamma_{i+1,i}^{\mathfrak{b}} \in \Gamma(z, z)$. The class $\gamma_{i,i+1}^{\mathfrak{b}}$ serves as a convenient basepoint for $\Gamma_{i,i+1}(z, z)$ as a Γ -torsor, when z is on or near the \mathcal{S} -wall. Of course there are three \mathcal{S} -walls emerging from \mathfrak{b} ; when we need to distinguish them, we denote the basepoints on, say, the a -cable by $\gamma_{ij}^{\mathfrak{b},a}$.

Now, suppose that \mathfrak{b} and \mathfrak{b}' are neighboring branch points of type $(i, i+1)$ on the $(K-2)$ -triangle of branch points, and suppose the points z and z' are large and located along a common cable. We continue them to a common point z_* while staying within the cable, in the region near infinity. Then

$$\gamma_{i,i+1}^{\mathfrak{b}}(z_*) + \gamma_{i+1,i}^{\mathfrak{b}'}(z_*) = \gamma^{\mathfrak{v}}, \quad (4.13)$$

where \mathfrak{v} is the lattice point in a $(K-3)$ -triangle labeling the triangle in the $(K-2)$ -triangle determined by the pair $\mathfrak{b}, \mathfrak{b}'$.

5 Flags, flat sections, and cluster coordinates associated with a minimal spectral network

5.1 Flat connections and Hitchin solutions

Fix some ϑ and a point of the Coulomb branch of the level K lift of the AD_1 theory near the lift locus, and assume that the corresponding WKB spectral network $\mathcal{W} = \mathcal{W}_\vartheta$ is an essentially minimal spectral network.

Recall that given a solution (A, φ) of the Hitchin equations with gauge group $SU(K)$ we can form the flat $SL(K, \mathbb{C})$ connection⁶ $\nabla = d + \mathcal{A}$, where

$$\mathcal{A} = \frac{R}{\zeta} \varphi + A + R\zeta \bar{\varphi} \quad (5.1)$$

on the complex vector bundle $E \rightarrow C$. Here we use the complex structure of C to split $\phi = \varphi + \bar{\varphi}$ into its $(1, 0)$ and $(0, 1)$ parts. We call the solutions s of the ordinary differential equation $\nabla s = 0$ on C “flat sections” of (E, ∇) .

The flat connection ∇ has a singularity only at infinity. Therefore, there is a K -dimensional vector space \mathcal{E} of global flat sections. In what follows we will introduce some special bases of \mathcal{E} which are attached to regions in the complement of the spectral network \mathcal{W} . The change-of-basis matrix relating the bases attached to two neighboring regions is particularly simple; we think of this matrix as associated to “crossing the \mathcal{S} -wall” separating the regions. The change-of-basis matrix obtained by crossing a whole cable of \mathcal{S} -walls can be interpreted as a Stokes matrix associated to the irregular singularity of ∇ at $z = \infty$.

Remark: For most of what we will do in the rest of this section, it is not strictly necessary to start with a solution of Hitchin’s equations and corresponding WKB spectral

⁶Strictly speaking, we should be considering *twisted* flat connections; we defer this annoying detail to §5.3.

network. Instead one could just start with a minimal spectral network.⁷ This spectral network induces a coordinate system on the moduli space of flat connections on the disc, decorated by flags associated to three marked points on the boundary. Much of the following discussion could be carried out in this more abstract context.

5.2 The flags $A_\bullet, B_\bullet, C_\bullet$.

From the asymptotics of ∇ as $z \rightarrow \infty$ we can define three flags $A_\bullet, B_\bullet, C_\bullet$ in \mathcal{E} , associated with the three cables a, b, c , as follows.

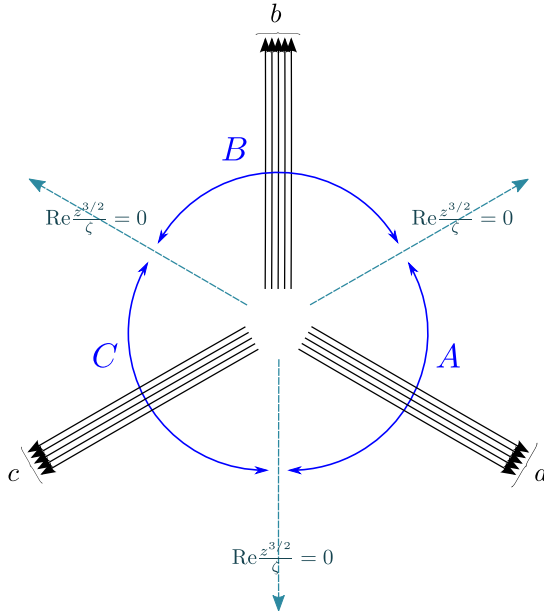


Figure 4. Regions defined by the $z \rightarrow \infty$ asymptotics of the Higgs field, in the level K lift of the AD_1 Hitchin system. In this figure ζ has argument $-\frac{\pi}{4}$. If we vary the argument of ζ by α then the regions rotate by an angle $\frac{2}{3}\alpha$. The a, b, c cables of a minimal WKB spectral network are also depicted. The position of the cables depends on ϑ ; the situation shown here is $\vartheta = \arg \zeta$. If we vary ϑ by α then the cables rotate by $\frac{2}{3}\alpha$.

Having trivialized the cover $\Sigma \rightarrow C$ on the complement of the cuts (which we will fix more precisely below), we have an unambiguous labeling of the sheets $\lambda_1, \dots, \lambda_K$. We consider z to be in the region near ∞ , so that we may approximate the roots of the level K spectral curve simply by

$$\lambda_i \approx (K + 1 - 2i)\sqrt{z} dz \quad i = 1, \dots, K \quad (5.2)$$

and hence, for any z_0 and $|z| \gg |z_0|$, we may approximate

$$\int_{z_0}^z \lambda_i \approx \frac{2}{3}(K + 1 - 2i)z^{3/2} + \text{const.} \quad (5.3)$$

⁷Here we would use the definition of “spectral network” in §9.1 of [1]; to match that definition precisely, one should cut out a small neighborhood of infinity, so that we view the spectral network as drawn on the disc, and then perturb the \mathcal{S} -walls slightly so that each \mathcal{S} -wall ends on one of three marked points on the boundary (one marked point for each cable).

In the region at large $|z|$ there are three rays where $\operatorname{Re} \zeta^{-1} z^{3/2} = 0$, and in the three regions separated by these lines the $z \rightarrow \infty$ asymptotics are different. We define the B -region to be the one in which

$$\operatorname{Re} \int_{z_0}^z \frac{1}{\zeta} \lambda_1 \ll \operatorname{Re} \int_{z_0}^z \frac{1}{\zeta} \lambda_2 \ll \cdots \ll \operatorname{Re} \int_{z_0}^z \frac{1}{\zeta} \lambda_K. \quad (5.4)$$

Then the A -region is the region clockwise from the B -region and has

$$\operatorname{Re} \int_{z_0}^z \frac{1}{\zeta} \lambda_1 \gg \operatorname{Re} \int_{z_0}^z \frac{1}{\zeta} \lambda_2 \gg \cdots \gg \operatorname{Re} \int_{z_0}^z \frac{1}{\zeta} \lambda_K, \quad (5.5)$$

while the C -region is the region counterclockwise from the B -region and also has

$$\operatorname{Re} \int_{z_0}^z \frac{1}{\zeta} \lambda_1 \gg \operatorname{Re} \int_{z_0}^z \frac{1}{\zeta} \lambda_2 \gg \cdots \gg \operatorname{Re} \int_{z_0}^z \frac{1}{\zeta} \lambda_K. \quad (5.6)$$

We have taken all of the branch cuts to be asymptotic to the ray separating the A - and C -regions. Crossing all of these cuts implements the permutation $w_0^{(K)}$ on the sheets; this is important for understanding how the three systems of inequalities (5.4), (5.5), (5.6) can be consistent.

Let us now relate these regions to those defined by the spectral network. According to [1], an \mathcal{S} -wall of type ij emerging from a branch point \mathfrak{b} in a WKB spectral network is defined by the equation

$$\int_{\mathfrak{b}}^z e^{-i\vartheta} (\lambda_i - \lambda_j) > 0, \quad (5.7)$$

and is naturally oriented outwards, so that the LHS of (5.7) increases to $+\infty$ as $z \rightarrow \infty$ along the \mathcal{S} -wall. Comparing with (5.2) we see that the a, b, c -cables lie in the A, B, C -regions, as shown in Figure 4, so long as

$$\arg \zeta - \frac{\pi}{2} < \vartheta < \arg \zeta + \frac{\pi}{2}. \quad (5.8)$$

We now define three filtrations A_{\bullet} , B_{\bullet} and C_{\bullet} of the vector space \mathcal{E} of flat sections. For $z \rightarrow \infty$ along a path asymptoting to the b -cable, the condition⁸

$$\lim_{z \rightarrow \infty} \exp \left[2 \operatorname{Re} \int_{z_0}^z \frac{R}{\zeta} \lambda_n \right] s(z) < \infty \quad (5.9)$$

defines a $(K + 1 - n)$ -dimensional subspace $B_{K+1-n} \subset \mathcal{E}$. For example, suppose we take $n = K$; λ_K gives the largest real part for the integral in the B -region at large $|z|$, and this integral overwhelms all but the smallest flat section $s(z)$; the condition (5.9) with $n = K$ thus singles out a line spanned by $s(z)$. For $n = K - 1$ there is a 2-dimensional space spanned by the smallest and next-smallest flat sections, and so forth. In a similar way we can define the other two filtrations A_{\bullet} , C_{\bullet} .

Thus, in summary:

$$\lim_{z \rightarrow \infty} \exp \left[2 \operatorname{Re} \int_{z_0}^z \frac{R}{\zeta} \lambda_n \right] s(z) < \infty \Leftrightarrow s \in A_n \quad (5.10)$$

⁸The meaning of “ $< \infty$ ” in this equation is that the limit exists.

for $z \rightarrow \infty$ along the a -cable, where A_n is n -dimensional,

$$\lim_{z \rightarrow \infty} \exp \left[2 \operatorname{Re} \int_{z_0}^z \frac{R}{\zeta} \lambda_n \right] s(z) < \infty \Leftrightarrow s \in B_{K+1-n} \quad (5.11)$$

for $z \rightarrow \infty$ along the b -cable, where B_{K+1-n} is $(K+1-n)$ -dimensional, and

$$\lim_{z \rightarrow \infty} \exp \left[2 \operatorname{Re} \int_{z_0}^z \frac{R}{\zeta} \lambda_n \right] s(z) < \infty \Leftrightarrow s \in C_n \quad (5.12)$$

for $z \rightarrow \infty$ along the c -cable, where C_n is n -dimensional.

For generic ∇ , the three flags A_\bullet , B_\bullet , C_\bullet are in general position. We can therefore apply the linear algebra of Appendix A. In particular, we define $A^n := A_{K-n}$, etc., and a set of $\frac{1}{2}(K+1)K$ lines

$$\mathfrak{L}^{x,y,z} := A^x \cap B^y \cap C^z, \quad x + y + z = K - 1, \quad (5.13)$$

where (x, y, z) is a lattice point in a $(K-1)$ -triangle. Similarly, we define $\frac{1}{2}K(K-1)$ planes

$$\mathfrak{P}^{x,y,z} := A^x \cap B^y \cap C^z, \quad x + y + z = K - 2, \quad (5.14)$$

associated to points in a $(K-2)$ -triangle, and $\frac{1}{2}(K-1)(K-2)$ spaces

$$\mathfrak{V}^{x,y,z} := A^x \cap B^y \cap C^z, \quad x + y + z = K - 3, \quad (5.15)$$

associated to points in a $(K-3)$ -triangle. These will play an important role in the following discussion.

5.3 Twistings

Now let us confront a detail we have hidden up until now (this section might reasonably be skipped on a first reading.) The construction of [1] really involves *twisted* connections over C and Σ , not ordinary ones. What this means is that they are really connections over the bundles of tangent directions \tilde{C} and $\tilde{\Sigma}$, with holonomy -1 around each fiber. Because of this holonomy it is strictly speaking nonsense to speak of the space of global flat sections of ∇ — there are no global flat sections!

There are various ways of dealing with this twisting, so as to reduce to ordinary connections; each choice leads to annoying minus signs appearing in a slightly different place. For our limited purposes in this paper, the following prescription will suffice. Fix any global nonvanishing vector field ν on the plane; this gives a global section \hat{C} of $\tilde{C} \rightarrow C$. Pulling back ∇ from \tilde{C} to C , we obtain a flat connection (not a twisted flat connection) over C ; by abuse of notation we will also call this flat connection ∇ . After so doing, we may define \mathcal{E} to be the vector space of global ∇ -flat sections over C .

Strictly speaking, different choices of nonvanishing vector field ν give different vector spaces $\mathcal{E}(\nu)$. A homotopy from ν to ν' gives an isomorphism $\mathcal{E}(\nu) \simeq \mathcal{E}(\nu')$, and any ν and ν' are indeed homotopic, so we do have isomorphisms between the different $\mathcal{E}(\nu)$; however, any ν , ν' can be related by distinct homotopies, and so we do not get *canonical* isomorphisms between the different $\mathcal{E}(\nu)$. (One can easily see this by considering a homotopy from ν to

itself which winds once around the circle; this corresponds to the automorphism of $\mathcal{E}(\nu)$ given by $s \mapsto -s$.) Speaking loosely, we may say that the space \mathcal{E} is determined only “up to multiplication by -1 .” On the other hand, the spaces $\text{End } \mathcal{E}(\nu)$ are all canonically isomorphic (since conjugation by -1 gives the identity automorphism), so $\text{End } \mathcal{E}$ is really canonically defined. Most of our considerations in this paper ultimately involve only $\text{End } \mathcal{E}$, not \mathcal{E} itself; for this reason the choice of ν will not play much role in what follows.

The vector field ν also induces a section $\hat{\Sigma}$ of $\tilde{\Sigma} \rightarrow \Sigma$, defined on the complement of the ramification locus R , and with 1 unit of winding around each point of R . Thus, given a twisted flat connection ∇^{ab} over Σ , pulling back from $\hat{\Sigma}$ gives a flat connection (not a twisted flat connection) over $\Sigma \setminus R$. This flat connection has holonomy -1 around each point of R . By abuse of notation we will also call this connection ∇^{ab} .

5.4 Line decompositions from the nonabelianization map

In [1, 6], given a spectral network \mathcal{W} , we defined a nonabelianization map $\Psi_{\mathcal{W}}$: given a twisted flat connection ∇^{ab} on a complex line bundle $L \rightarrow \Sigma$, this map produces a twisted flat connection $\nabla = \Psi_{\mathcal{W}}(\nabla^{\text{ab}})$ on a complex rank K bundle $\hat{E} \rightarrow C$. We conjectured that $\Psi_{\mathcal{W}}$ provides a coordinate system on an open patch of the moduli space of flat rank K connections over C with fixed singularity and flag structure. We will verify that conjecture here, in the case of the moduli space corresponding to the level K lift of the AD_1 theory, when we take \mathcal{W} to be a minimal spectral network. Indeed, supposing that $\nabla = \Psi_{\mathcal{W}}(\nabla^{\text{ab}})$, we will identify the holonomies of ∇^{ab} around an appropriate set of cycles with the Fock-Goncharov triangle coordinates of ∇ .

Three notes on notation. First, for simplicity we denote \hat{E} simply by E . Second, we use the notation $F(\varphi)$ for the ∇ -parallel transport along the path φ (not for the formal generating function which appeared in [1]). Third, our convention for composition of linear transformations is backward from the usual one: in particular, linear transformations act on vectors from the right, and $F(\varphi_1)F(\varphi_2) = F(\varphi_1\varphi_2)$. (See Appendix C of [1].)

A minimal spectral network divides the complex plane into several connected components. Let us focus on the $\frac{1}{2}K(K-1) + 1$ regions at infinity which abut the b -cable. Each such region is separated from its neighbor to the left by an \mathcal{S} -wall emanating from a branch point $\mathfrak{b}^{x,y,z}$ in the $(K-2)$ -triangle of branch points. We label these regions as \mathcal{R}^{α} , $\alpha = 0, \dots, \frac{1}{2}K(K-1)$. Note that $\mathcal{R}^0 = \mathcal{R}_{ab}$ and $\mathcal{R}^{\frac{1}{2}K(K-1)} = \mathcal{R}_{bc}$. There are similar regions around the a - and c -cables. If we need to distinguish these we write $\mathcal{R}^{\alpha,a}$ etc.

Suppose we have trivialized the K -fold cover $\Sigma \rightarrow C$ over $C \setminus (\text{cuts})$ as above. Then in each region \mathcal{R} we have an isomorphism

$$E|_{\mathcal{R}} \cong \pi_* L = \bigoplus_{i=1}^K L_i, \quad (5.16)$$

where L_i is the line bundle $L \rightarrow \Sigma$ restricted to the i^{th} sheet. Now we can define lines

$$\mathfrak{L}_i^{\mathcal{R}} := \{\psi \in \mathcal{E} \mid \psi(z) \in L_i|_z \ \forall z \in \mathcal{R}\} \subset \mathcal{E}. \quad (5.17)$$

We stress that $\mathfrak{L}_i^{\mathcal{R}}$ is a line in a fixed K -dimensional vector space \mathcal{E} , and is not to be confused with the fiber of any bundle on C . Thus, to each region \mathcal{R}^α there is an associated decomposition of \mathcal{E} into a direct sum of lines.

In the interest of clarity we will be somewhat pedantic and introduce two maps, the restriction map $\rho(z)$ and the extension map $\varepsilon(z)$. The restriction (or evaluation) map $\rho(z) : \mathcal{E} \rightarrow E_z$ simply evaluates a section at z . The extension map $\varepsilon(z) : E_z \rightarrow \mathcal{E}$ takes a vector in the fiber at z and extends it by parallel transport with respect to (5.1) to a flat section throughout C .⁹ We have trivial identities $\varepsilon(z)\rho(z) = 1$, $\rho(z)\varepsilon(z) = 1$, and $\varepsilon(z_1)\rho(z_2) = F(\wp(z_1, z_2))$. (Remember that we write composition of operators from left to right, i.e. subsequent operations are written to the right.) Thus,

$$\rho(z_1)F(\wp(z_1, z_2))\varepsilon(z_2) = 1 \quad (5.18)$$

is the identity transformation of \mathcal{E} . For all $z \in \mathcal{R}$ we also have by (5.17)

$$\rho(z) : \mathfrak{L}_i^{\mathcal{R}} \rightarrow L_i|_z, \quad \varepsilon(z) : L_i|_z \rightarrow \mathfrak{L}_i^{\mathcal{R}}. \quad (5.19)$$

because ∇^{ab} preserves the direct sum decomposition (5.16). Note that (5.19) is in general false if $z \notin \mathcal{R}$.

5.5 Transformation of line decompositions across \mathcal{S} -walls

Suppose that two regions $\mathcal{R}_1, \mathcal{R}_2$ of C are separated by an \mathcal{S} -wall of type ij . Let $\wp = \wp(z_1, z_2)$ be a short path from $z_1 \in \mathcal{R}_1$ to $z_2 \in \mathcal{R}_2$, crossing the \mathcal{S} -wall at z . Assume moreover that there is only one soliton charge γ_{ij} supported on the \mathcal{S} -wall, with $\mu(\gamma_{ij}) \neq 0$; this is the case for any nondegenerate spectral network and in particular for the minimal spectral networks to which we specialize below. Then according to [1] (see particularly (10.4)-(10.6)), the ∇ -parallel transport along \wp is given by

$$F(\wp) = \mathcal{D}(\wp) + \mu(\gamma_{ij})\mathcal{Y}_{\gamma_{ij}(z_1, z_2)}. \quad (5.20)$$

Here as in [1] we let \mathcal{Y}_a denote the ∇^{ab} -parallel transport along a path a , $\mathcal{D}(\wp) = \sum_{i=1}^K \mathcal{Y}_{\wp^{(i)}}$, and $\gamma_{ij}(z_1, z_2)$ denotes the “detour” path which travels along $\wp^{(i)}$ from $z_1^{(i)}$ to $z^{(i)}$, then follows the chain γ_{ij} from $z^{(i)}$ to $z^{(j)}$, and finally travels along $\wp^{(j)}$ from $z^{(j)}$ to $z_2^{(j)}$.¹⁰

The first term $\mathcal{D}(\wp)$ in (5.20) preserves the direct sum decomposition $E \simeq \bigoplus L_i$ globally on $C \setminus (\text{cuts})$. In contrast, the second term of (5.20) involves the non-diagonal $\mathcal{Y}_{\gamma_{ij}(z_1, z_2)} \in \text{Hom}(L_i|_{z_1}, L_j|_{z_2})$ (extended to $\text{Hom}(E|_{z_1}, E|_{z_2})$ by defining it to be zero on the other summands.)

In this situation we have the following three properties:

⁹In the present case, with $C = \mathbb{CP}^1$ and only a single irregular singular point, there is no monodromy and $\varepsilon(z)$ can be defined for all $z \in \mathbb{C}$. In more general situations one would choose a system of cuts and only define $\varepsilon(z)$ for z in the complement of the cuts.

¹⁰To be careful about signs we should remember that, as explained in §5.3, the sign of the parallel transport $\mathcal{Y}_{\gamma_{ij}}$ depends on how we lift γ_{ij} from $H_1(\Sigma, \mathbb{Z})$ to $H_1(\Sigma \setminus R, \mathbb{Z})$. From the discussion in [1] it follows that there is a canonical way of defining the combination $\mu(\gamma_{ij})\mathcal{Y}_{\gamma_{ij}(z_1, z_2)}$, and this is what we are using in (5.20).

1. $\mathfrak{L}_s^{\mathcal{R}_1} = \mathfrak{L}_s^{\mathcal{R}_2}$ for $s \neq i$.
2. $\mathfrak{L}_i^{\mathcal{R}_1} \neq \mathfrak{L}_i^{\mathcal{R}_2}$.
3. The plane spanned by $\mathfrak{L}_i^{\mathcal{R}_1}$ and $\mathfrak{L}_i^{\mathcal{R}_2}$ contains $\mathfrak{L}_j^{\mathcal{R}_1} = \mathfrak{L}_j^{\mathcal{R}_2}$.

Let us give a careful proof of the third, absolutely crucial, statement. We apply (5.18) and the definition (5.20) of the parallel transport to an element $s \in \mathfrak{L}_i^{\mathcal{R}_1}$, to conclude

$$s = s(z_1)\mathcal{D}(\varphi)\varepsilon(z_2) + \mu(\gamma_{ij})s(z_1)\mathcal{Y}_{\gamma_{ij}(z_1, z_2)}\varepsilon(z_2). \quad (5.21)$$

Now, $s(z_1)\mathcal{D}(\varphi) \in L_i|_{z_2}$, so the extension $s(z_1)\mathcal{D}(\varphi)\varepsilon(z_2) \in \mathfrak{L}_i^{\mathcal{R}_2}$. Similarly, $s(z_1)\mathcal{Y}_{\gamma_{ij}(z_1, z_2)} \in L_j|_{z_2}$, so $s(z_1)\mathcal{Y}_{\gamma_{ij}(z_1, z_2)}\varepsilon(z_2) \in \mathfrak{L}_j^{\mathcal{R}_2}$. Thus, (5.21) is an equation of the form

$$s_i^{\mathcal{R}_1} = s_i^{\mathcal{R}_2} + s_j^{\mathcal{R}_2}, \quad (5.22)$$

where $s_i^{\mathcal{R}_1} \in \mathfrak{L}_i^{\mathcal{R}_1}$, $s_i^{\mathcal{R}_2} \in \mathfrak{L}_i^{\mathcal{R}_2}$, and $s_j^{\mathcal{R}_2} \in \mathfrak{L}_j^{\mathcal{R}_2} = \mathfrak{L}_j^{\mathcal{R}_1}$. Thus the three lines sit in a common plane.

5.6 The plane in \mathcal{E} associated to a branch point

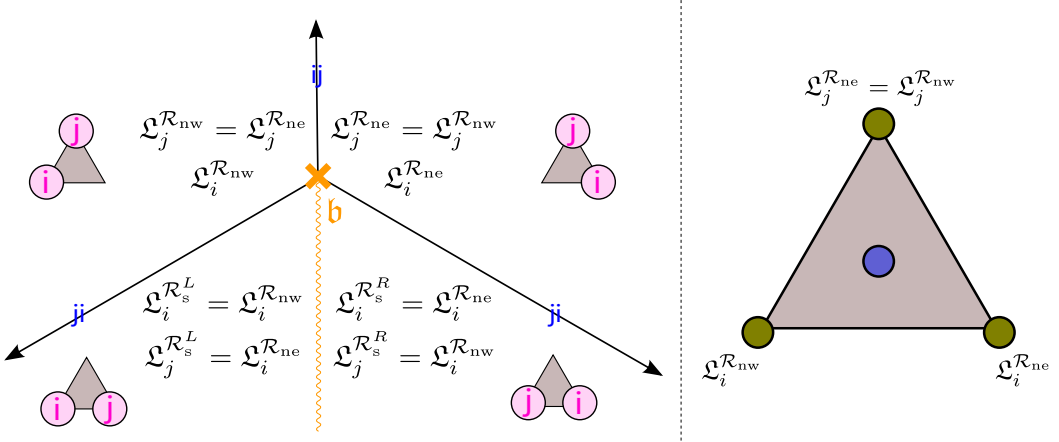


Figure 5. Left: Associated to each branch point in any spectral network there is a distinguished plane in the vector space of local flat sections, containing several distinguished lines. The relation between these lines is as indicated here. **Right:** A 1-triangle representing the plane determined by the branch point b , with the three distinguished lines at its vertices.

For later use in §11 we note a corollary of the previous discussion. We apply the transformation rules across \mathcal{S} -walls to the neighborhood of a single branch point of type (ij) , with \mathcal{S} -walls of type ij (north) and ji (southeast and southwest) and a branch cut pointing south. The branch point determines four regions $\mathcal{R}_{\text{ne}}, \mathcal{R}_{\text{nw}}, \mathcal{R}_s^L, \mathcal{R}_s^R$ as indicated in Figure 5. Our discussion above shows, first, that for $s \neq i, j$ the lines $\mathfrak{L}_s^{\mathcal{R}} \subset \mathcal{E}$ are the same in all four regions. It shows also that of the eight possible lines $\mathfrak{L}_i^{\mathcal{R}}, \mathfrak{L}_j^{\mathcal{R}}$ there are in

fact only three lines, and they are coplanar:

$$\begin{aligned}\mathfrak{L}_i^{\mathcal{R}_{\text{ne}}} &= \mathfrak{L}_i^{\mathcal{R}_s^R} = \mathfrak{L}_j^{\mathcal{R}_s^L}, \\ \mathfrak{L}_i^{\mathcal{R}_{\text{nw}}} &= \mathfrak{L}_i^{\mathcal{R}_s^L} = \mathfrak{L}_j^{\mathcal{R}_s^R}, \\ \mathfrak{L}_j^{\mathcal{R}_{\text{ne}}} &= \mathfrak{L}_j^{\mathcal{R}_{\text{nw}}}.\end{aligned}\tag{5.23}$$

To prove this, note that from the three rules above we immediately get $\mathfrak{L}_j^{\mathcal{R}_{\text{ne}}} = \mathfrak{L}_j^{\mathcal{R}_{\text{nw}}}$, $\mathfrak{L}_i^{\mathcal{R}_{\text{ne}}} = \mathfrak{L}_i^{\mathcal{R}_s^R}$, and $\mathfrak{L}_i^{\mathcal{R}_{\text{nw}}} = \mathfrak{L}_i^{\mathcal{R}_s^L}$. However, crossing the cut must exchange $\mathfrak{L}_i^{\mathcal{R}_s^L}$ for $\mathfrak{L}_j^{\mathcal{R}_s^R}$ and $\mathfrak{L}_i^{\mathcal{R}_s^R}$ for $\mathfrak{L}_j^{\mathcal{R}_s^L}$. This is enough to determine all of the lines.

We thus obtain the key result: each branch point of type (ij) is associated with a *plane* in the space of local flat sections, containing three lines of types $\mathfrak{L}_i^{\mathcal{R}}$ and $\mathfrak{L}_j^{\mathcal{R}}$. A 1-triangle representing this plane, with the three lines at its vertices, is shown on the right side of Figure 5.

5.7 Snakes and the planes

We now apply the discussion of §5.5 to a minimal spectral network of *Yin* type. From the various line decompositions which appear in the various regions \mathcal{R} we will extract a canonical $(K-1)$ -triangle of lines in the vector space \mathcal{E} . This $(K-1)$ -triangle will then be identified with one associated to the flags $A_{\bullet}, B_{\bullet}, C_{\bullet}$ by Fock and Goncharov in [2], thus making the crucial link between spectral networks and their work.

Consider a minimal spectral network of *Yin* type, with \mathcal{S} -walls arranged so that when traversing the b -cable, moving east to west, the \mathcal{S} -walls one encounters are (reading the product from right to left):

$$S_{12} \cdot (S_{23}S_{12}) \cdots (S_{K-2,K-1} \cdots S_{23}S_{12}) \cdot (S_{K-1,K} \cdots S_{23}S_{12}).\tag{5.24}$$

Let us describe how the lines $\mathfrak{L}_i^{\mathcal{R}^{\alpha}}$ are related to each other. When we cross the first \mathcal{S} -wall of type 12 from \mathcal{R}^{ab} into region \mathcal{R}^1 , we find $\mathfrak{L}_s^{\mathcal{R}^1} = \mathfrak{L}_s^{\mathcal{R}^{ab}}$ for $s = 2, \dots, K$, but $\mathfrak{L}_1^{\mathcal{R}^1} \neq \mathfrak{L}_1^{\mathcal{R}^{ab}}$. Rather $\mathfrak{L}_1^{\mathcal{R}^1}, \mathfrak{L}_1^{\mathcal{R}^{ab}}, \mathfrak{L}_2^{\mathcal{R}^{ab}}$ are all coplanar. Moving further across a wall of type 23 from \mathcal{R}^1 into \mathcal{R}^2 , we have a similar story: $\mathfrak{L}_s^{\mathcal{R}^2} = \mathfrak{L}_s^{\mathcal{R}^1}$ for $s \neq 2$, but $\mathfrak{L}_2^{\mathcal{R}^1} \neq \mathfrak{L}_2^{\mathcal{R}^2}$ and $\mathfrak{L}_2^{\mathcal{R}^1}, \mathfrak{L}_2^{\mathcal{R}^2}$ and $\mathfrak{L}_3^{\mathcal{R}^1}$ are all coplanar. We can continue in this fashion, reading off the \mathcal{S} -wall types from (5.24).

Note that near the b -cable the line $\mathfrak{L}_1^{\mathcal{R}^{ab}}$ is spanned by the *largest* section as $z \rightarrow \infty$, while $\mathfrak{L}_2^{\mathcal{R}^{ab}}$ is spanned by the next largest. In the next region to the left the largest section has changed by adding a *smaller* section. This is the standard pattern in Stokes theory: our basis of sections jumps when we cross a Stokes line, but the asymptotics of this basis does not jump.

Now we assign the lines $\mathfrak{L}_i^{\mathcal{R}^{\alpha}}$ to vertices of a $(K-1)$ -triangle, as follows. We begin by assigning the lines $\mathfrak{L}_i^{\mathcal{R}^{ab}}$, $i = 1, \dots, K$, to points on the right side of the $(K-1)$ -triangle: the vertex $(K-1, 0, 0)$ corresponds to $\mathfrak{L}_1^{\mathcal{R}^{ab}}$, and we go up the right side of the triangle from there, assigning $\mathfrak{L}_i^{\mathcal{R}^{ab}}$ to $(K-i, i-1, 0)$. Thus the line decomposition in \mathcal{R}_{ab} corresponds to that associated to the snake from the B vertex to the A vertex. We next fill in the triangle, assigning lines $\mathfrak{L}_i^{\mathcal{R}^{\alpha}}$ to vertices, so that the change of line decompositions as we

step to the left from \mathcal{R}^α to $\mathcal{R}^{\alpha+1}$ corresponds to a step in the canonical path of snakes. We can do this precisely because the moves in the canonical path of snakes match the ordering of \mathcal{S} -wall types given in (5.24).

For example, crossing into \mathcal{R}^1 we have seen that the line $\mathcal{L}_1^{\mathcal{R}_{ab}}$ is changed to $\mathcal{L}_1^{\mathcal{R}^1}$; hence we assign $\mathcal{L}_1^{\mathcal{R}^1}$ to the position $(K-2, 0, 1)$ in the $(K-1)$ -triangle. Next we assign $\mathcal{L}_2^{\mathcal{R}^2}$ to the position $(K-3, 1, 1)$. We continue this process using the pattern of \mathcal{S} -walls (5.24). See Figure 6.

The resulting $(K-1)$ -triangle of lines in \mathcal{E} has the following properties:

1. All shaded up-triangles have vertices corresponding to coplanar lines.
2. The set of lines associated to any region $\mathcal{R}^{\alpha,b}$ constitutes a snake from the B -vertex to the B -side in the $(K-1)$ -triangle.
3. The sequence of regions \mathcal{R}^α corresponds to the canonical path of snakes from \mathcal{SN}_{BA} to \mathcal{SN}_{BC} described below (A.50). In particular, the change of snake from \mathcal{R}^α to $\mathcal{R}^{\alpha+1}$ is given by a Fock-Goncharov elementary move of type I or type II, as described in Appendix A.

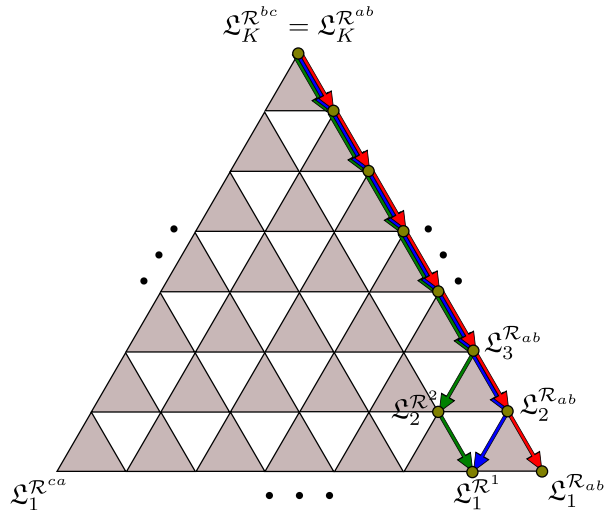


Figure 6. The first two moves in the canonical path of snakes associated to the b -cable, which we use for construction of a $(K-1)$ -triangle of lines. The red arrows indicate the snake \mathcal{SN}_{BA} which is associated to the region \mathcal{R}_{ab} . The blue arrows indicate the snake associated to region \mathcal{R}^1 , which differs from \mathcal{SN}_{BA} by a type I move. The green arrows indicate the snake associated to region \mathcal{R}^2 . Note that for crossing the a -cable we would use instead the initial snake \mathcal{SN}_{AB} , obtained by reversing all the red arrows.

Of course, a similar procedure can be applied to the other two cables. For example, consider crossing the a -cable from \mathcal{R}_{ab} to \mathcal{R}_{ca}^R . We first cross an \mathcal{S} -wall of type $K, K-1$ to enter region \mathcal{R}^1 . Thus $\mathcal{L}_s^{\mathcal{R}_{ab}} = \mathcal{L}_s^{\mathcal{R}^1}$ for $s = 1, \dots, K-1$, but $\mathcal{L}_K^{\mathcal{R}_{ab}} \neq \mathcal{L}_K^{\mathcal{R}^1}$. On the $(K-1)$ -triangle of lines we have constructed, this corresponds to a type I move between two snakes running from the A vertex to the A side. The snake corresponding to \mathcal{R}_{ab} is

the northeast side of the triangle (but oriented oppositely to the orientation we used when crossing the b -cable.) Continuing in this way, following the pattern of \mathcal{S} -walls given in (4.7), we obtain the canonical path of snakes from \mathcal{SN}_{AB} to \mathcal{SN}_{AC} . Similarly, crossing the c -cable from \mathcal{R}_{bc} to \mathcal{R}_{ca}^L , we begin with a snake from the C vertex to the B vertex (the line decomposition in \mathcal{R}_{bc}), and then proceed with the canonical path of snakes until we reach a snake from the C vertex to the A vertex. Note that the lines in \mathcal{R}_{ca}^L and \mathcal{R}_{ca}^R are related across the cuts by the permutation $w_0^{(K)}$.

One might worry that the triangles of lines constructed by the above procedure crossing the a -, b -, and c -cables might be different, but in fact they are all the same. This follows from the fact that they can all be identified with the triangle of lines considered by Fock-Goncharov, as we show in the next section.

5.8 Identifying our triangle with Fock-Goncharov's

We now claim that the $(K-1)$ -triangle of lines we have just constructed is identical to the $(K-1)$ -triangle of lines associated by Fock and Goncharov's construction to the triple of flags $A_\bullet, B_\bullet, C_\bullet$ of §5.2.

To prove this, first consider the region \mathcal{R}_{ab} . Applying the WKB approximation to the flat connection ∇ as $z \rightarrow \infty$, we expect that the sections s_i in the line $\mathfrak{L}_i^{\mathcal{R}_{ab}}$ behave asymptotically as

$$s_i(z) \sim s_i(z_0) \exp \left[-2\text{Re} \int_{z_0}^z \frac{R\lambda_i}{\zeta} \right] \quad (5.25)$$

throughout the region \mathcal{R}_{ab} . If we take $z \rightarrow \infty$ along the b -cable, comparing with the definition (5.11) we find the limit exists for $n \leq i$ and therefore s_i is in $B_{K+1-i} = B^{i-1}$. Similarly, taking $z \rightarrow \infty$ along the a -cable and comparing with (5.10) reveals that the limit exists for $n \geq i$ and hence s_i is also in $A_i = A^{K-i}$. Therefore,

$$\mathfrak{L}_i^{\mathcal{R}_{ab}} = A^{K-i} \cap B^{i-1} = \mathfrak{L}^{K-i, i-1, 0}. \quad (5.26)$$

Thus we have shown that the lines $\mathfrak{L}_i^{\mathcal{R}_{ab}}$, which by definition make up the northeast side of our triangle of lines, agree with the lines $\mathfrak{L}^{K-i, i-1, 0}$ which make up the northeast side of Fock-Goncharov's triangle of lines. Similarly, considering the behavior in \mathcal{R}_{bc} we see that the lines on the northwest side of our triangle are given by

$$\mathfrak{L}_i^{\mathcal{R}_{bc}} = C^{K-i} \cap B^{i-1} = \mathfrak{L}^{0, i-1, K-i}. \quad (5.27)$$

Thus we have found that the northeast and northwest sides of our $(K-1)$ -triangle match with the same two sides of Fock and Goncharov's triangle. Moreover, as we have already shown, our triangle obeys *coplanarity relations*: the three vertices of each small shaded up-triangle correspond to three coplanar lines. Fock and Goncharov's triangle also obeys these relations. As we now show, these properties are actually enough to *characterize* Fock and Goncharov's triangle, and thus prove that the two triangles are the same.

Indeed, an easy induction from the coplanarity relations shows that given any upward-pointing subtriangle inside the $(K-1)$ -triangle, the line at any vertex of the subtriangle is contained in the sum of the lines along the opposite side of the subtriangle. Now consider

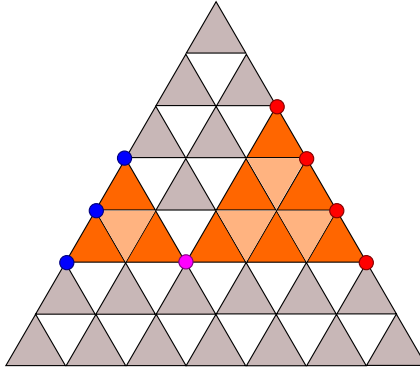


Figure 7. Two subtriangles inside a $(K-1)$ -triangle of lines, with a common vertex x, y, z (purple dot). The line $\mathcal{L}^{x,y,z}$ is contained in the direct sum of the lines marked by the blue dots, and also in the direct sum of the lines marked by the red dots; these two facts together suffice to determine $\mathcal{L}^{x,y,z}$.

a pair of subtriangles, one flush with the northeast side of the $(K-1)$ -triangle and one flush with the northwest side, with one vertex x, y, z in common, as shown in Figure 7. The right subtriangle then implies that the line $\mathcal{L}^{x,y,z} \subset A^x \cap B^y$, while the left subtriangle implies that $\mathcal{L}^{x,y,z} \subset C^z \cap B^y$. Combining the two we obtain $\mathcal{L}^{x,y,z} \subset A^x \cap B^y \cap C^z$, but the latter space is 1-dimensional, so in fact $\mathcal{L}^{x,y,z} = A^x \cap B^y \cap C^z$, as desired.

5.9 Identifying Darboux sections with canonical homs

Now that we have identified our triangle of lines with the Fock-Goncharov triangle of lines, we invoke some more of the linear algebra reviewed in Appendix A. In particular, as explained there, given an oriented edge E in the triangle, with source and target $s(E)$ and $t(E)$ respectively, and given also an orientation of the triangle, there is a canonical hom $x_E \in \text{Hom}(\mathcal{L}^{s(E)}, \mathcal{L}^{t(E)})$. We are going to identify these canonical homs with our ‘‘Darboux sections,’’ by finding chains $\gamma_{ij}(z_1, z_2)$ such that

$$x_E = \rho(z_1) \mathcal{Y}_{\gamma_{ij}(z_1, z_2)} \varepsilon(z_2), \quad (5.28)$$

where z_1 and z_2 are points on opposite sides of the wall. To summarize this in a pithier way we can take the limit where z_1 and z_2 both approach a common point z on the wall, and define

$$\hat{\mathcal{Y}}_{\gamma_{ij}(z)} = \lim_{z_1, z_2 \rightarrow z} \rho(z_1) \mathcal{Y}_{\gamma_{ij}(z_1, z_2)} \varepsilon(z_2). \quad (5.29)$$

Then our result becomes simply

$$x_E = \hat{\mathcal{Y}}_{\gamma_{ij}(z)}. \quad (5.30)$$

Implicit in (5.30) is the fact that the right side does not depend on the chosen point z on the wall. Indeed, more is true: we can even push z away from the wall without changing $\hat{\mathcal{Y}}_{\gamma_{ij}(z)}$, as long as z does not cross any \mathcal{S} -walls of type ki or jk for any k . This extra freedom will be important for us below.

Identifying precisely the correct chains $\gamma_{ij}(z)$ takes a bit of care. We now do this.

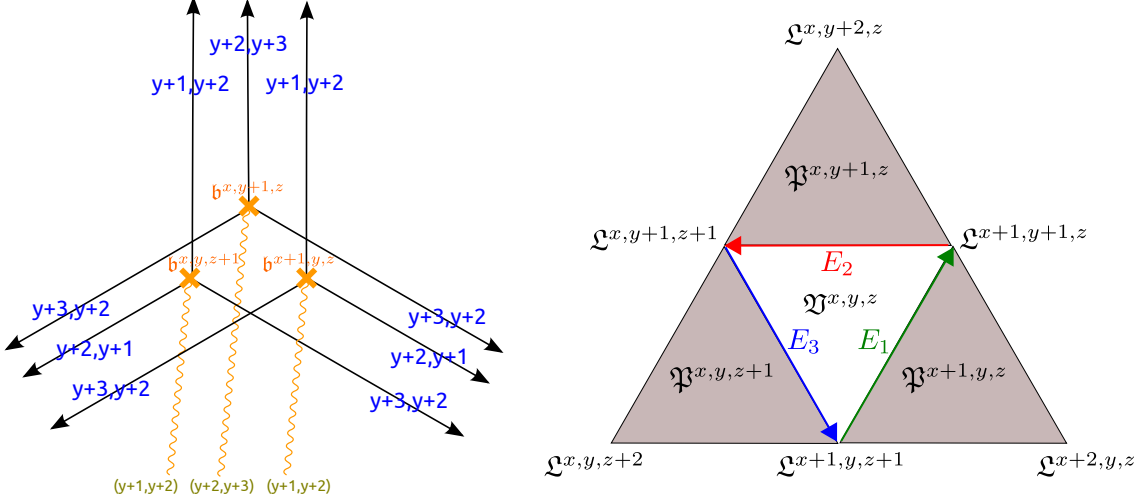


Figure 8. Left: In a minimal spectral network there are local clusters of 3 branch points labeled by points (x, y, z) in a $(K - 3)$ -triangle. We show here one such cluster, in a minimal spectral network of *Yin* type. We have, roughly, a “mini” AD_2 theory here. **Right:** The associated 2-triangle of lines, with three edges E_i marked, for which we will compute the canonical homs x_{E_i} below.

For later convenience, we will consider three canonical homs at once. Thus let us consider three adjacent branch points $b^{x,y,z+1}$, $b^{x+1,y,z}$, $b^{x,y+1,z}$ with $(x, y, z) \in T(K - 3)$. Associated to this triple is a 2-subtriangle of the triangle of lines; see Figure 8.

Consider a short path φ crossing the b -cable \mathcal{S} -wall emanating from $b^{x+1,y,z}$, say from $\mathcal{R}^{\alpha,b}$ to $\mathcal{R}^{\alpha+1,b}$. This crossing will be related to the canonical hom associated with the green internal edge

$$E_1 : (x + 1, y, z + 1) \rightarrow (x + 1, y + 1, z) \quad (5.31)$$

in Figure 8. Indeed, fix some $s_{y+1}^\alpha \in \mathfrak{L}^{x+2,y,z} = \mathfrak{L}^{\mathcal{R}^\alpha}_{y+1}$, and suppose $s_{y+1}^{\alpha+1} \in \mathfrak{L}^{x+1,y,z+1} = \mathfrak{L}^{\mathcal{R}^{\alpha+1}}_{y+1}$ is related to it by ∇^{ab} -parallel transport,

$$s_{y+1}^{\alpha+1} = s_{y+1}^\alpha(z_1) \mathcal{D}(\varphi) \varepsilon(z_2). \quad (5.32)$$

Now we consider the definition (5.20) of the ∇ -parallel transport along φ . For this particular \mathcal{S} -wall, the product $\mu(\gamma_{ij}) \mathcal{Y}_{\gamma_{ij}}$ which appears in (5.20) can be described concretely: one has simply $\mu(\gamma_{ij}) = 1$ and $\gamma_{ij} = \gamma_{y+1,y+2}^{b^{x+1,y,z},b}(z_1, z_2)$. (To be really precise, as noted in §5.3, we have to specify how the chain $\gamma_{y+1,y+2}^{b^{x+1,y,z},b}(z_1, z_2)$ is lifted from $H_1(\Sigma, \mathbb{Z})$ to $H_1(\Sigma \setminus R, \mathbb{Z})$. The answer is that $\gamma_{y+1,y+2}^{b^{x+1,y,z},b}(z_1, z_2)$ should be represented by a path which goes clockwise around the ramification point covering $b^{x+1,y,z}$, as in Figure 9.¹¹) Applying (5.20) to s_{y+1}^α ,

¹¹This answer can be checked in laborious fashion beginning with the rules of [1] and §5.3, but there is also a shortcut. The rules determining $F(\varphi)$ in [1] were essentially determined by the constraint that the connection ∇ should be flat even at the branch points. In particular $F(\varphi)$ should be the same as $F(\varphi')$, where φ' is a path which takes a detour around the branch point, thus avoiding this \mathcal{S} -wall. The term involving $\mathcal{Y}_{\gamma_{y+1,y+2}^{b^{x+1,y,z},b}(z_1, z_2)}$ in $F(\varphi)$ should thus be identified with a term in $F(\varphi')$, which in fact comes from $\mathcal{D}(\varphi')$. In other words this term should simply be parallel transport along a lift of φ' to Σ . This is enough to fix which way $\mathcal{Y}_{\gamma_{y+1,y+2}^{b^{x+1,y,z},b}(z_1, z_2)}$ should wind around the branch point.

we thus obtain

$$s_{y+1}^\alpha = s_{y+1}^{\alpha+1} + s_{y+1}^\alpha(z_1) \mathcal{Y}_{\gamma_{y+1,y+2}^{b^{x+1},y,z,b}(z_1,z_2)} \varepsilon(z_2). \quad (5.33)$$

Taking the limit $z_1, z_2 \rightarrow z_b$ this equation becomes

$$s_{y+1}^\alpha = s_{y+1}^{\alpha+1} + s_{y+1}^\alpha \hat{\mathcal{Y}}_{\gamma_{y+1,y+2}^{b^{x+1},y,z,b}(z_b)}, \quad (5.34)$$

and using the fact that $\hat{\mathcal{Y}}_{\gamma_{y+1,y+2}^{b^{x+1},y,z,b}(z_b)}^2 = 0$ we can also rewrite this as

$$s_{y+1}^\alpha = s_{y+1}^{\alpha+1} + s_{y+1}^{\alpha+1} \hat{\mathcal{Y}}_{\gamma_{y+1,y+2}^{b^{x+1},y,z,b}(z_b)}. \quad (5.35)$$

Comparing this with the definition of the canonical hom x_{E_1} in (A.8), we see that

$$x_{E_1} = \hat{\mathcal{Y}}_{\gamma_{y+1,y+2}^{b^{x+1},y,z,b}(z_b)}. \quad (5.36)$$

Similarly, the canonical hom x_{E_2} associated with the red oriented edge

$$E_2 : (x+1, y+1, z) \rightarrow (x, y+1, z+1) \quad (5.37)$$

arises in crossing the c -cable and has

$$x_{E_2} = \hat{\mathcal{Y}}_{\gamma_{y+2,y+3}^{b^x,y+1,z,c}(z_c)}. \quad (5.38)$$

Finally, the canonical hom x_{E_3} associated with the blue edge

$$E_3 : (x, y+1, z+1) \rightarrow (x+1, y, z+1) \quad (5.39)$$

arises in crossing the a -cable and has

$$x_{E_3} = \hat{\mathcal{Y}}_{\gamma_{y+2,y+1}^{b^x,y,z+1,a}(z_a)}. \quad (5.40)$$

Note that in these equations z_a, z_b, z_c lie on the corresponding \mathcal{S} -walls and are close to the relevant branch points, in particular not separated from the branch points by any cuts.

5.10 Identifying Fock-Goncharov triangle coordinates with Darboux coordinates

Now consider a point (x, y, z) in a $(K-3)$ -triangle. To this point we can associate a triplet of planes $\mathfrak{P}^{x+1,y,z}$, $\mathfrak{P}^{x,y+1,z}$, $\mathfrak{P}^{x,y,z+1}$, and a sextuplet of lines as in Figure 8. On the one hand, we can consider the composition of canonical homs counterclockwise around the internal downward pointing triangle of the $(K-1)$ -triangle of lines as in (A.20). This gives the Fock-Goncharov coordinate $r^{x,y,z}$ associated with the triplet of flags in \mathcal{E} . On the other hand, we have just seen that these three canonical homs correspond to operators $\hat{\mathcal{Y}}_{\gamma_{ij}}$, where γ_{ij} runs over the three relative homology classes

$$\gamma_{y+1,y+2}^{b^{x+1},y,z,b}(z_b), \quad \gamma_{y+3,y+2}^{b^x,y+1,z,c}(z_c), \quad \gamma_{y+2,y+1}^{b^x,y,z+1,a}(z_a), \quad (5.41)$$

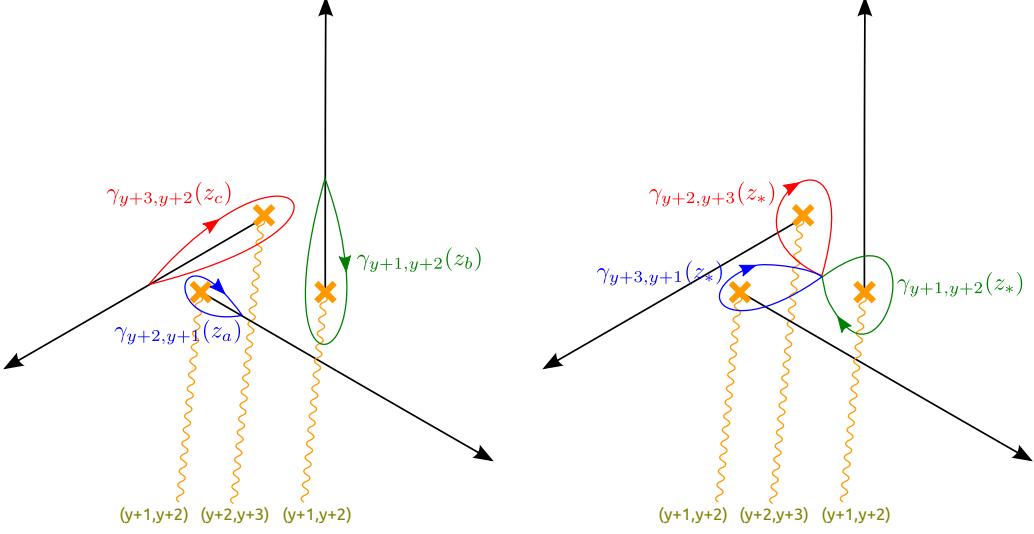


Figure 9. Left: The three canonical homs x_{E_k} are identified with the three operators $\hat{\mathcal{Y}}_{\gamma_{ij}}$ associated with the three chains γ_{ij} on Σ shown here. **Right:** By moving their basepoints, these three chains can be deformed so that they combine into a closed cycle γ^v on Σ .

shown on the left of Figure 9.

As we have commented, these three operators $\hat{\mathcal{Y}}_{\gamma_{ij}(z)}$ do not change as we continue z_a , z_b , z_c to the common point z_* shown on the right of Figure 9. Note that in doing so we move z_a and z_c across a cut of type $(y+2, y+3)$, so the indices ij of the chains have to be relabeled appropriately. These three chains can now be combined into a single closed cycle on Σ ,

$$\gamma^v = \text{cl} \left(\gamma_{y+2,y+3}^{b^{x,y+1,z},c}(z_*) + \gamma_{y+3,y+1}^{b^{x,y,z+1},a}(z_*) + \gamma_{y+1,y+2}^{b^{x+1,y,z},b}(z_*) \right). \quad (5.42)$$

The composition of the abelian parallel transports around these three open paths gives the abelian parallel transport along the closed cycle γ^v . Thus we finally arrive at one of the main results of this paper:

$$\mathcal{Y}_{\gamma^v} = r^{x,y,z}. \quad (5.43)$$

Let us summarize our result. The minimal spectral network of the level K lift of the AD_1 theory provides a Darboux coordinate system on the moduli space of flat $SL(K, \mathbb{C})$ connections on the disc with three fixed flags. What we have shown is that these Darboux coordinates coincide with the Fock-Goncharov coordinates on the same moduli space.

5.11 Another viewpoint on the Darboux coordinates

There is another point of view on the $\mathcal{Y}_{\gamma_{ij}}$ and the \mathcal{Y}_γ , used heavily in [2] and [7, 12]: one can construct them directly as combinations of flat sections determined by flags around singular points. (For example, in [2, 7], the \mathcal{Y}_γ in case $K = 2$ are defined using cross-ratios of 4-tuples of distinguished ‘‘small’’ flat sections associated to 4 singular points.) We will not make much use of the generalization of these formulas to the higher rank case in this paper, but we note here how they could in principle be obtained.

The essential remark is that we can interpret (5.22) as a transformation from a basis for the plane P using flat sections $s_a^{\mathcal{R}_1}$, $a = i, j$, associated to region \mathcal{R}_1 , to a basis using flat sections $s_a^{\mathcal{R}_2}$, $a = i, j$, associated to region \mathcal{R}_2 :

$$\begin{aligned} s_i^{\mathcal{R}_2} &= s_i^{\mathcal{R}_1} - s_j^{\mathcal{R}_1}, \\ s_j^{\mathcal{R}_2} &= s_j^{\mathcal{R}_1}. \end{aligned} \quad (5.44)$$

This may be written as

$$s_a^{\mathcal{R}_2} = s_a^{\mathcal{R}_1} \mathcal{O}^{\mathcal{R}_1 \rightarrow \mathcal{R}_2} \quad (5.45)$$

where

$$\mathcal{O}^{\mathcal{R}_1 \rightarrow \mathcal{R}_2} = 1 - \left(\frac{\cdot \wedge s_j^{\mathcal{R}_1}}{s_i^{\mathcal{R}_1} \wedge s_j^{\mathcal{R}_1}} \right) \otimes s_j^{\mathcal{R}_1} \cdot \left(\frac{s_i^{\mathcal{R}_2} \wedge s_i^{\mathcal{R}_1}}{s_i^{\mathcal{R}_2} \wedge s_j^{\mathcal{R}_1}} \right). \quad (5.46)$$

Here we have focused on a plane \mathfrak{P} of flat sections in the K -dimensional space \mathcal{E} , so these wedge products are valued in the line $\wedge^2 \mathfrak{P}$, and hence their ratios are scalars. From this starting point, one can write an expression for $\mathcal{Y}_{\gamma_{ij}}$ in terms of flat sections. In turn the \mathcal{Y}_γ can be obtained by composition of appropriate choices of $\mathcal{Y}_{\gamma_{ij}}$.

It can be useful to rewrite the ratios of elements of $\wedge^2 \mathfrak{P}$ in a way that does not distinguish \mathfrak{P} . To do this one chooses a complementary basis of sections s_t , $t = 1, \dots, K-2$, and interprets

$$\frac{s_i^{\mathcal{R}_2} \wedge s_i^{\mathcal{R}_1}}{s_i^{\mathcal{R}_2} \wedge s_j^{\mathcal{R}_1}} = \frac{s_i^{\mathcal{R}_2} \wedge s_i^{\mathcal{R}_1} \wedge s_1 \wedge \dots \wedge s_{K-2}}{s_i^{\mathcal{R}_2} \wedge s_j^{\mathcal{R}_1} \wedge s_1 \wedge \dots \wedge s_{K-2}} \quad (5.47)$$

as a ratio of elements of the line $\wedge^K \mathcal{E}$. The choice of basis sections s_t does not matter.

5.12 Compact regions

Thus far we have focused on the noncompact regions cut out by a minimal spectral network. For $K > 2$, there are of course also compact regions in $C \setminus \mathcal{W}$. The nonabelianization map again gives a decomposition of \mathcal{E} into lines associated with these regions, and the transformations across \mathcal{S} -walls are again governed by the discussion of Section §5.5. Indeed, one can show that the decomposition into lines associated with an internal region \mathcal{R} is again given by a family of K lines each of which is of the type $\mathfrak{L}^{x,y,z}$. However, these K lines need not lie along a snake. In Figure 10 we indicate these decompositions in the case $K = 3$.

5.13 WKB asymptotics

Let us briefly comment on another important feature of our line decompositions of \mathcal{E} : as explained in §10.9 of [1], if our spectral network is a WKB spectral network \mathcal{W}_ϑ , these decompositions are naturally related to the WKB asymptotics of the flat sections as $\zeta \rightarrow 0$. Indeed, in each region of $C \setminus \mathcal{W}_\vartheta$, our line decomposition of \mathcal{E} consists of flat sections with simple asymptotics (schematically $s_i \sim s_i(z_0) \exp(-R/\zeta \int_{z_0}^z \lambda_i)$) as $\zeta \rightarrow 0$ in the half-plane \mathbb{H}_ϑ . When we cross the \mathcal{S} -walls, the lines of asymptotically larger sections get modified by the addition of asymptotically smaller sections. This discussion applies equally well to the compact and non-compact regions.

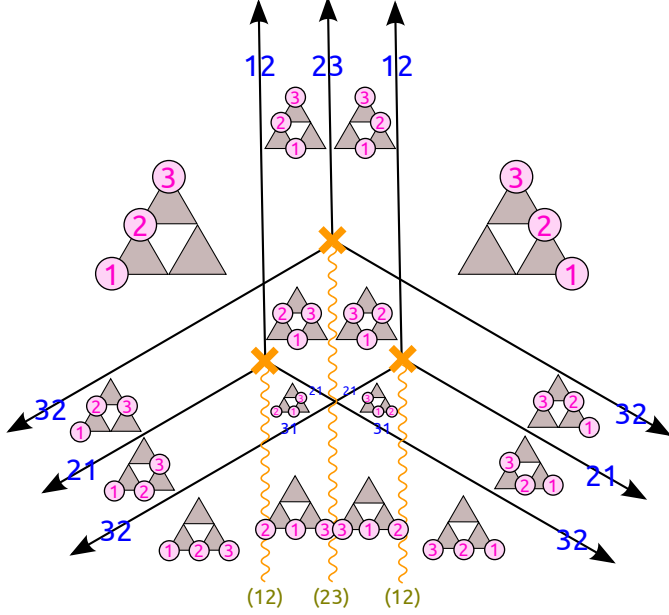


Figure 10. The line decompositions of \mathcal{E} in the various regions of the complement of a minimal spectral network, with $K = 3$. In each region we display the canonical 2-triangle of lines, and mark the three lines which occur in the line decomposition. (Decompositions separated by a branch cut are essentially the same, differing only in the numbering of the lines.) In all of the asymptotic regions the line decompositions correspond to snakes, while in the hexagonal interior region the line decompositions do not correspond to any snake.

5.14 Formal monodromy

As we remarked at the beginning of this section, the change-of-basis matrix obtained by crossing a whole cable of \mathcal{S} -walls can be interpreted as a Stokes matrix associated to the irregular singularity of ∇ at $z = \infty$. So we have three such Stokes matrices $T_{a\text{-cable}}$, $T_{b\text{-cable}}$, $T_{c\text{-cable}}$. Each one is further decomposed into \mathcal{S} -wall matrices according to (4.5)-(4.9). Some concrete examples of these matrices appear in Appendix A.4.1.

In general the product of all the Stokes matrices around an irregular singularity gives the formal monodromy. In particular, if the mass parameters are all set to 1, then the formal monodromy is just W_0 , so the decomposition of the cables gives a solution to the equation (3.24):

$$T_{c\text{-cable}} T_{b\text{-cable}} T_{a\text{-cable}} = W_0, \quad (5.48)$$

where W_0 is the antidiagonal matrix defined in (3.21).

5.15 The Yang case

So far in this section we have exclusively considered a minimal spectral network of *Yin* type. If we consider instead a minimal spectral network of *Yang* type, the story is slightly different. Each region still corresponds to a line decomposition of \mathcal{E} , but the lines which occur in these decompositions are not the ones in the Fock-Goncharov triangle associated to the three flags A_\bullet , B_\bullet , C_\bullet in \mathcal{E} . To describe the decompositions which we do get, first

observe that a line decomposition of \mathcal{E} induces a dual line decomposition of \mathcal{E}^* . Hence in each region we have a line decomposition of \mathcal{E}^* . In the *Yang* case it is these dual decompositions which turn out to have a simple description: they are the ones in the Fock-Goncharov triangle associated to the three flags \check{A}_\bullet , \check{B}_\bullet , \check{C}_\bullet in \mathcal{E}^* .

In order to check this, it is convenient to use a volume form to identify \mathcal{E}^* as $\wedge^{K-1}\mathcal{E}$, and then realize the Fock-Goncharov triangle of lines in \mathcal{E}^* as

$$\begin{aligned}\hat{\mathcal{L}}_K^{\mathcal{R}} &= \mathcal{L}_1^{\mathcal{R}} \wedge \cdots \wedge \mathcal{L}_{K-1}^{\mathcal{R}} \\ \hat{\mathcal{L}}_{K-1}^{\mathcal{R}} &= \mathcal{L}_1^{\mathcal{R}} \wedge \cdots \wedge \mathcal{L}_{K-2}^{\mathcal{R}} \wedge \mathcal{L}_K^{\mathcal{R}} \\ \hat{\mathcal{L}}_{K-2}^{\mathcal{R}} &= \mathcal{L}_1^{\mathcal{R}} \wedge \cdots \wedge \mathcal{L}_{K-3}^{\mathcal{R}} \wedge \mathcal{L}_{K-1}^{\mathcal{R}} \wedge \mathcal{L}_K^{\mathcal{R}} \\ &\vdots & \vdots \\ \hat{\mathcal{L}}_1^{\mathcal{R}} &= \mathcal{L}_2^{\mathcal{R}} \wedge \cdots \wedge \mathcal{L}_K^{\mathcal{R}}.\end{aligned}\tag{5.49}$$

Using this representation one can check directly that the canonical path of snakes in \mathcal{E}^* is obtained by crossing the b -cable of the *Yang* network.

6 Example: \mathcal{S} -walls and coordinates for the level 3 lift of AD_1

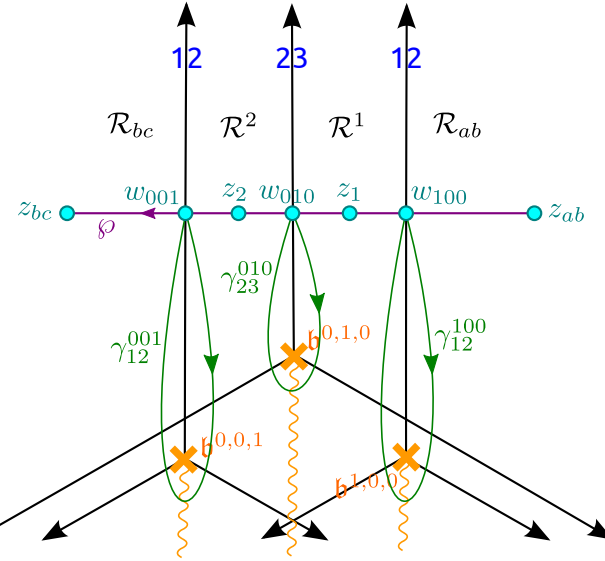


Figure 11. Parallel transport of sections in the $K = 3$ lift of AD_1 .

In this section we illustrate some of the general claims of Section 5 above in the case of $K = 3$. We will focus on the changes of basis which one meets in crossing the b -cable, using parallel transport across the path φ illustrated in Figure 11. The various snakes which we will use on the 2-triangle of lines are illustrated in Figure 12.

We begin by choosing three vectors

$$s_i^{\mathcal{R}_{ab}}(z_{ab}) \in L_i|_{z_{ab}}.\tag{6.1}$$

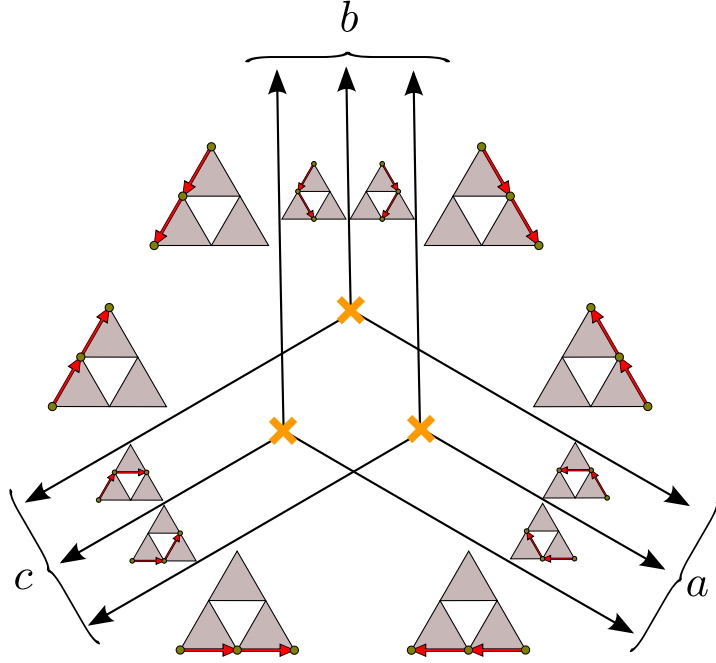


Figure 12. The snakes which are used in our construction of the triangle of lines for $K = 3$. Note that in the regions \mathcal{R}_{ab} , \mathcal{R}_{bc} and \mathcal{R}_{ca} we use two different orientations for the snakes, the choice depending on which cable we choose to cross. The outer transitions are type I, but the transition across the inner wall in each cable is type II and introduces the Darboux coordinate \mathcal{Y}_{γ^0} into the Stokes matrix.

We have made a choice of three scale factors here. We then extend these three vectors to flat sections $s_i^{\mathcal{R}_{ab}} \in \mathcal{E}$. More formally, we apply the extension map: $s_i^{\mathcal{R}_{ab}} = s_i^{\mathcal{R}_{ab}}(z_{ab})\varepsilon(z_{ab})$.

Next we define three vectors in $L_i|_{z_1}$ by

$$s_i^{\mathcal{R}^1}(z_1) := s_i^{\mathcal{R}_{ab}}(z_{ab})\mathcal{Y}_{\wp^{(i)}(z_{ab}, z_1)} \in L_i|_{z_1}. \quad (6.2)$$

We stress that (6.2) is merely a definition of reference sections in the lines above z_1 , not parallel transport with respect to the flat nonabelian connection ∇ . Parallel transport with respect to ∇ of course preserves flat sections:

$$s_i^{\mathcal{R}_{ab}}(z_f) = s_i^{\mathcal{R}_{ab}}(z_i)F(\wp'(z_i, z_f)) \quad (6.3)$$

for parallel transport along *any* path $\wp'(z_i, z_f)$ from z_i to z_f . In particular,

$$s_i^{\mathcal{R}_{ab}}(z_1) = s_i^{\mathcal{R}_{ab}}(z_{ab})F(\wp(z_{ab}, z_1)). \quad (6.4)$$

Combining (6.2) and (6.4) and writing out the definition of $F(\wp)$, we arrive at

$$\begin{aligned} s_3^{\mathcal{R}_{ab}}(z_1) &= s_3^{\mathcal{R}_{ab}}(z_{ab})\mathcal{Y}_{\wp^{(3)}(z_{ab}, z_1)} = s_3^{\mathcal{R}^1}(z_1), \\ s_2^{\mathcal{R}_{ab}}(z_1) &= s_2^{\mathcal{R}_{ab}}(z_{ab})\mathcal{Y}_{\wp^{(2)}(z_{ab}, z_1)} = s_2^{\mathcal{R}^1}(z_1), \\ s_1^{\mathcal{R}_{ab}}(z_1) &= s_1^{\mathcal{R}_{ab}}(z_{ab})\mathcal{Y}_{\wp^{(1)}(z_{ab}, z_1)} \\ &\quad + s_1^{\mathcal{R}_{ab}}(z_{ab})\mathcal{Y}_{\wp^{(1)}(z_{ab}, w^{100})}\mathcal{Y}_{\gamma_{12}^{100}(w^{100})}\mathcal{Y}_{\wp^{(2)}(w^{100}, z_1)}. \end{aligned} \quad (6.5)$$

Now we can simplify the last line of (6.5), by noting that there must be a constant $\kappa_1 \in \mathbb{C}^\times$ such that

$$s_1^{\mathcal{R}_{ab}}(z_{ab})\mathcal{Y}_{\wp^{(1)}(z_{ab}, w^{100})}\mathcal{Y}_{\gamma_{12}^{100}(w^{100})}\mathcal{Y}_{\wp^{(2)}(w^{100}, z_1)} = \kappa_1 s_2^{\mathcal{R}_{ab}}(z_{ab})\mathcal{Y}_{\wp^{(2)}(z_{ab}, z_1)}. \quad (6.6)$$

Applying the extension map $\varepsilon(z_1)$ to the definitions (6.2) we define sections $s_i^{\mathcal{R}^1} \in \mathcal{E}$. It follows from (6.5) and (6.6) that we have the linear relations:

$$\begin{aligned} s_1^{\mathcal{R}^1} &= s_1^{\mathcal{R}_{ab}} - \kappa_1 s_2^{\mathcal{R}_{ab}}, \\ s_2^{\mathcal{R}^1} &= s_2^{\mathcal{R}_{ab}}, \\ s_3^{\mathcal{R}^1} &= s_3^{\mathcal{R}_{ab}}. \end{aligned} \quad (6.7)$$

Now we describe the change of basis from \mathcal{R}^1 to \mathcal{R}^2 in an entirely analogous way. We begin by defining

$$s_i^{\mathcal{R}^2}(z_2) := s_i^{\mathcal{R}^1}(z_1)\mathcal{Y}_{\wp^{(i)}(z_1, z_2)}. \quad (6.8)$$

On the other hand, since $s_i^{\mathcal{R}^1}$ are flat sections we have

$$s_i^{\mathcal{R}^1}(z_2) = s_i^{\mathcal{R}^1}(z_1)F(\wp(z_1, z_2)). \quad (6.9)$$

Writing this out using the definition of F , we arrive at equations completely analogous to (6.5). In analogy to (6.6), we define $\kappa_2 \in \mathbb{C}^\times$ by

$$s_2^{\mathcal{R}^1}(z_1)\mathcal{Y}_{\wp^{(2)}(z_1, w^{010})}\mathcal{Y}_{\gamma_{23}^{010}(w^{010})}\mathcal{Y}_{\wp^{(3)}(w^{010}, z_2)} = \kappa_2 s_3^{\mathcal{R}^1}(z_1)\mathcal{Y}_{\wp^{(3)}(z_1, z_2)}. \quad (6.10)$$

This leads to the analog of (6.7):

$$\begin{aligned} s_1^{\mathcal{R}^2} &= s_1^{\mathcal{R}^1}, \\ s_2^{\mathcal{R}^2} &= s_2^{\mathcal{R}^1} - \kappa_2 s_3^{\mathcal{R}^1}, \\ s_3^{\mathcal{R}^2} &= s_3^{\mathcal{R}^1}. \end{aligned} \quad (6.11)$$

Finally, proceeding from \mathcal{R}^2 to \mathcal{R}_{bc} , we introduce a third constant $\kappa_3 \in \mathbb{C}^\times$ in the equation

$$s_1^{\mathcal{R}^2}(z_2)\mathcal{Y}_{\wp^{(1)}(z_2, w^{001})}\mathcal{Y}_{\gamma_{12}^{001}(w^{001})}\mathcal{Y}_{\wp^{(2)}(w^{001}, z_{bc})} = \kappa_3 s_2^{\mathcal{R}^2}(z_2)\mathcal{Y}_{\wp^{(2)}(z_2, z_{bc})}, \quad (6.12)$$

leading to the change of basis

$$\begin{aligned} s_1^{\mathcal{R}_{bc}} &= s_1^{\mathcal{R}^2} - \kappa_3 s_2^{\mathcal{R}^2}, \\ s_2^{\mathcal{R}_{bc}} &= s_2^{\mathcal{R}^2}, \\ s_3^{\mathcal{R}_{bc}} &= s_3^{\mathcal{R}^2}. \end{aligned} \quad (6.13)$$

Combining these linear transformations, we have altogether

$$\begin{aligned} s_1^{\mathcal{R}_{bc}} &= s_1^{\mathcal{R}_{ab}} - (\kappa_1 + \kappa_3)s_2^{\mathcal{R}_{ab}} + \kappa_2\kappa_3 s_3^{\mathcal{R}_{ab}}, \\ s_2^{\mathcal{R}_{bc}} &= s_2^{\mathcal{R}_{ab}} - \kappa_2 s_3^{\mathcal{R}_{ab}}, \\ s_3^{\mathcal{R}_{bc}} &= s_3^{\mathcal{R}_{ab}}. \end{aligned} \quad (6.14)$$

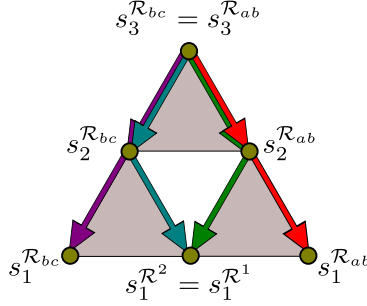


Figure 13. The canonical 2-triangle of lines in the $K = 3$ lift of the AD_1 theory. We also indicate basis sections in the various lines, and the snakes in the canonical path.

Now, we consider the canonical 2-triangle of lines, illustrated in Figure 13. We choose normalizations so that the basis in \mathcal{R}_{ab} and \mathcal{R}_{bc} coincide with those determined by the snakes indicated in Figure 13. For $s_1^{\mathcal{R}_{ab}}$ to be obtained from $s_2^{\mathcal{R}_{ab}}$ by the canonical hom, a glance at (6.7) shows we must choose $\kappa_1 = -1$. Similarly, for $s_2^{\mathcal{R}_{ab}}$ to be obtained from $s_3^{\mathcal{R}_{ab}}$ by the canonical hom, (6.14) shows that we must choose $\kappa_2 = -1$.

At this point we have fixed the normalization of $s_2^{\mathcal{R}_{ab}}$ and $s_3^{\mathcal{R}_{ab}}$ relative to $s_1^{\mathcal{R}_{ab}}$, as expected. The remaining constant κ_3 is therefore invariant.

We are now in a position to show that the coordinate κ_3 is related to the coordinate Fock and Goncharov associate to a triple of flags in a three-dimensional vector space. See (A.12). In the present case we have three flags:

$$A_\bullet : \quad s_1^{\mathcal{R}_{ab}} \mathbb{C} \subset s_1^{\mathcal{R}_{ab}} \mathbb{C} \oplus s_2^{\mathcal{R}_{ab}} \mathbb{C} \subset \mathcal{E}, \quad (6.15)$$

$$B_\bullet : \quad s_3^{\mathcal{R}_{ab}} \mathbb{C} \subset s_3^{\mathcal{R}_{ab}} \mathbb{C} \oplus s_2^{\mathcal{R}_{ab}} \mathbb{C} \subset \mathcal{E}, \quad (6.16)$$

$$C_\bullet : \quad s_1^{\mathcal{R}_{bc}} \mathbb{C} \subset s_1^{\mathcal{R}_{bc}} \mathbb{C} \oplus s_2^{\mathcal{R}_{bc}} \mathbb{C} \subset \mathcal{E}. \quad (6.17)$$

Using the change of basis (6.14) and the definition (A.12), or, more elegantly, using equations (6.7), (6.11), (6.13), and (A.19), we find that the triple ratio for these three flags is

$$r(A_\bullet, B_\bullet, C_\bullet) = \kappa_3^{-1}. \quad (6.18)$$

On the other hand, comparing (6.6) with (6.12), then using the definitions (6.2) and (6.8), we can deduce

$$\begin{aligned} s_1^{\mathcal{R}_{ab}}(z_{ab}) \mathcal{Y}_{\wp^{(1)}(z_{ab}, w^{001})} \mathcal{Y}_{\gamma_{12}^{001}(w^{001})} \mathcal{Y}_{\wp^{(2)}(w^{001}, z_{bc})} = \\ \kappa_3 s_1^{\mathcal{R}_{ab}}(z_{ab}) \mathcal{Y}_{\wp^{(1)}(z_{ab}, w^{100})} \mathcal{Y}_{\gamma_{12}^{100}(w^{100})} \mathcal{Y}_{\wp^{(2)}(w^{100}, z_{bc})}. \end{aligned} \quad (6.19)$$

The two sides here are parallel transport of the same section around two different paths, differing by γ^{000} ; from this we learn

$$\kappa_3 = \mathcal{Y}_{\gamma^{000}}^{-1}. \quad (6.20)$$

Combining this with equation (6.18) we confirm our main result,

$$r(A_\bullet, B_\bullet, C_\bullet) = \mathcal{Y}_{\gamma^{000}}. \quad (6.21)$$

7 How to find the BPS spectrum of the level K lift of AD_1

In this section we will give a recipe for determining the BPS spectra of level K lifts of AD_1 .

7.1 The spectrum generator

We first recall that the general formalism of wall-crossing in $\mathcal{N} = 2$ theories [12–18] implies that the BPS spectrum of any $\mathcal{N} = 2$ theory can be organized into a single natural object, the *spectrum generator* \mathbb{S} . Abstractly speaking, \mathbb{S} is simply the birational transformation which relates the quantities \mathcal{Y}_γ computed at a phase ϑ to the \mathcal{Y}_γ at phase $\vartheta + \pi$ (we will see below what this means concretely in theories of class S). \mathbb{S} is a wall-crossing invariant (up to conjugation), but one can extract from it all of the BPS degeneracies $\Omega(\gamma)$. The idea is that after fixing a point of the Coulomb branch and hence in particular an ordering of the “BPS phases” $\arg -Z_\gamma$, \mathbb{S} admits a unique factorization into a product of the form

$$\mathbb{S} = \prod_{\gamma: \vartheta \leq \arg -Z_\gamma < \vartheta + \pi} \mathcal{K}_\gamma^{\Omega(\gamma)}, \quad (7.1)$$

where the product is taken in order of increasing $\arg -Z_\gamma$, and \mathcal{K}_γ denotes a transformation of the form¹²

$$\mathcal{K}_\gamma : \mathcal{Y}_{\gamma'} \rightarrow \mathcal{Y}_{\gamma'} (1 - \sigma(\gamma) \mathcal{Y}_\gamma)^{\langle \gamma', \gamma \rangle}. \quad (7.2)$$

Different chambers of the Coulomb branch correspond to different orderings of the $\arg Z_\gamma$ and thus to different factorizations of \mathbb{S} ; this is why the $\Omega(\gamma)$ can undergo wall-crossing even while \mathbb{S} is invariant. Indeed, because it is more invariant, in some sense \mathbb{S} is superior to the $\Omega(\gamma)$ as a way of packaging the BPS particle content of the theory.

It was pointed out in [7] that the spectrum generator \mathbb{S} can sometimes be computed directly without prior knowledge of the BPS spectrum (hence the name). In particular an algorithm based on spectral networks (actually, on their dual WKB triangulations) was given for A_1 theories in [7].¹³ Below we will determine \mathbb{S} for level K lifts of AD_1 . We will first consider the case $K = 3$ where we will read off the individual factors $\mathcal{K}_\gamma^{\Omega(\gamma)}$ directly by looking at the WKB spectral networks (indeed, it will turn out that in this case there is just a single factor \mathcal{K}_γ). We will then turn to general K where we will use a more powerful approach, which gives \mathbb{S} directly rather than its factorization.

7.2 Morphisms of WKB spectral networks for the level 3 lift of AD_1

We begin with the simple case $K = 3$.

¹²The term $\sigma(\gamma) \mathcal{Y}_\gamma$ appearing in (7.2) needs a little explanation: \mathcal{Y}_γ is the holonomy of the twisted connection ∇^{ab} along the canonical lift of γ to $H_1(\tilde{\Sigma}, \mathbb{Z})$, and $\sigma(\gamma) = \pm 1$ is a tricky sign, conjecturally a canonical quadratic refinement of the mod 2 intersection pairing in Γ (this conjecture is true at least for $K = 2$).

¹³A nice application of this description of \mathbb{S} appeared recently in [19]: there it was noted that while the TBA-like integral equations of [14] depend on knowing the $\Omega(\gamma)$, there is a variant of those equations which depends directly on \mathbb{S} , and this variant can be easier to use in the application to moduli of Hitchin systems. This could be further extended to produce solutions of Hitchin equations themselves, using the extended 2d-4d integral equations in [6] and the extended 2d-4d spectrum generator for A_1 theories given in [20].

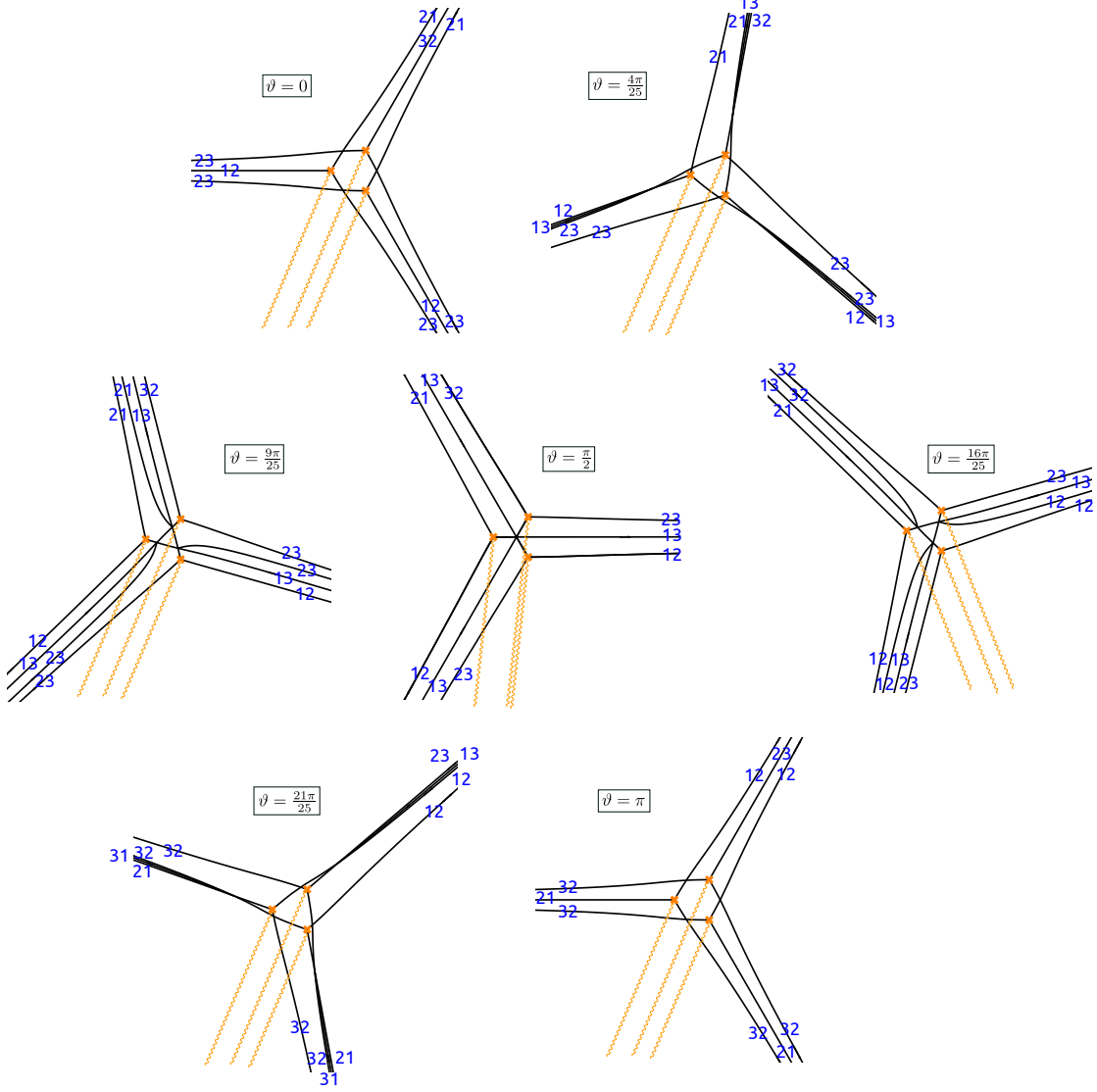


Figure 14. WKB spectral networks \mathcal{W}_ϑ in the $K = 3$ lift of the AD_1 theory, at the point of the Coulomb branch with spectral curve $\lambda^3 + (4zdz^2)\lambda + dz^3 = 0$ at seven values of ϑ . Note the three-pronged web which appears in the middle of the figure at $\vartheta = \pi/2$, and the topology change as we cross this critical phase.

In Figure 14 we depict the variation of the WKB spectral network \mathcal{W}_ϑ with ϑ in the $K = 3$ lift of the AD_1 theory, at the point of the Coulomb branch with spectral curve

$$\lambda^3 + (4zdz^2)\lambda + dz^3 = 0. \quad (7.3)$$

(Compare the unperturbed equation (2.7).) At $\vartheta = 0$ we have a *Yang* type minimal network, while at $\vartheta = \pi$ we have a *Yin* type minimal network.

On the top line of Figure 14 we see the evolution from $\vartheta = 0$ to $\vartheta = \frac{4\pi}{25}$. At $\vartheta = 0$ the network is truly minimal, while at $\vartheta = \frac{4\pi}{25}$ it is only essentially minimal, i.e. equivalent to a minimal network, in the sense of §9 of [1]. For example, in evolving from $\vartheta = 0$ to

$\vartheta = \frac{4\pi}{25}$, in the cable pointing to the north, an \mathcal{S} -wall of type 12 and one of type 23 have crossed one another, producing a new joint from which an \mathcal{S} -wall of type 13 emerges. For our present purposes, though, the distinction between minimal and essentially minimal is of little consequence. What we are really interested in is the phases where \mathcal{W}_ϑ jumps in a way that is *not* an equivalence.

The latter phenomenon happens in the middle row of Figure 14. Focusing on this row, we observe that there is an internal triangle, first visible at $\vartheta = \frac{9\pi}{25}$, which shrinks as ϑ increases and collapses completely at the critical phase $\vartheta_c = \frac{\pi}{2}$. At this critical phase the spectral network degenerates to include a three-pronged string web. This string web lifts to the cycle $\gamma = \gamma^{000}$ associated to the triangle of branch points in §4.3 above.

Such degenerations of spectral networks were studied in §6 of [1]. As explained there, the parallel transport operators $F(\vartheta)$ jump discontinuously whenever ϑ crosses a critical phase. Writing $F(\vartheta, \vartheta)$ for the parallel transport induced by the spectral network \mathcal{W}_ϑ and a fixed abelian connection ∇^{ab} , we have

$$F(\vartheta, \vartheta^+) = \mathcal{K}F(\vartheta, \vartheta^-), \quad (7.4)$$

for a particular transformation \mathcal{K} which contains the information of the 4d BPS degeneracies for particles with BPS phase ϑ . \mathcal{K} can be determined from the degenerate network \mathcal{W}_ϑ at the critical phase. The specific type of degenerate network we see at $\vartheta = \frac{\pi}{2}$ in Figure 14 was considered in §7.3 of [1], where we found that \mathcal{K} is given by

$$\mathcal{K} = \mathcal{K}_{\gamma^{000}} : \mathcal{Y}_{\gamma'} \rightarrow \mathcal{Y}_{\gamma'}(1 + \mathcal{Y}_{\gamma^{000}})^{\langle \gamma', \gamma^{000} \rangle}. \quad (7.5)$$

Comparing this with the general story reviewed in §7.1, we see that this corresponds to the BPS degeneracy $\Omega(\gamma^{000}) = 1$, i.e. to a single BPS hypermultiplet of charge γ^{000} (with $\sigma(\gamma^{000}) = -1$).

This kind of analysis by looking directly at the evolution of the WKB spectral network rapidly becomes cumbersome as we increase K . In the next section we turn to a more efficient algebraic method.

7.3 Determining the spectrum generator

We now describe a scheme which allows one to write the spectrum generator \mathbb{S} explicitly for all level K lifts of the AD_1 theory. We also exhibit the answers for $K = 3, 4, 5$.

We consider some phase ϑ and point of the Coulomb branch such that the WKB spectral network \mathcal{W}_ϑ is an essentially minimal spectral network of *Yin* type. For any flat connection ∇ over C , there is a flat abelian connection ∇_ϑ^{ab} over Σ such that

$$\Psi_{\mathcal{W}_\vartheta}(\nabla_\vartheta^{ab}) = \nabla. \quad (7.6)$$

As we have described in §5, for each $\mathfrak{v} \in T(K-3)$, the holonomy $\mathcal{Y}_{\gamma^\mathfrak{v}}$ of ∇_ϑ^{ab} is equal to the coordinate $r^\mathfrak{v}$ associated with the flags $A_\bullet, B_\bullet, C_\bullet$ determined by ∇ . There is another abelian connection $\nabla_{\vartheta+\pi}^{ab}$ such that

$$\Psi_{\mathcal{W}_{\vartheta+\pi}}(\nabla_{\vartheta+\pi}^{ab}) = \nabla. \quad (7.7)$$

The spectrum generator \mathbb{S} is the birational transformation which takes the holonomies \mathcal{Y}_γ of $\nabla_\vartheta^{\text{ab}}$ to the holonomies $\hat{\mathcal{Y}}_\gamma$ of $\nabla_{\vartheta+\pi}^{\text{ab}}$.

Combining (7.7) with (10.16) of [1], we obtain

$$\Psi_{\mathcal{W}_\vartheta}((\nabla_{\vartheta+\pi}^{\text{ab}})^*) = \nabla^*. \quad (7.8)$$

It follows that the holonomies of $(\nabla_{\vartheta+\pi}^{\text{ab}})^*$ are the coordinates $\check{r}^{\mathfrak{v}}$ associated to the flags determined by ∇^* , i.e. to the dual flags $\check{A}_\bullet, \check{B}_\bullet, \check{C}_\bullet$. The desired $\check{\mathcal{Y}}_\gamma$ are the holonomies of $\nabla_{\vartheta+\pi}^{\text{ab}}$, which are thus given by $\check{\mathcal{Y}}_{\gamma^{\mathfrak{v}}} = 1/\check{r}^{\mathfrak{v}}$.

Thus, the problem of determining the spectrum generator \mathbb{S} is really a question of linear algebra: how are the coordinates of a triple of flags related to those of the dual triple? We answer this question in Appendix A.5: the formula (A.74) gives an explicit way to compute $\check{r}^{\mathfrak{v}}$ as functions of the $r^{\mathfrak{v}}$.

7.3.1 Example: $K = 3$

As a simple example we first consider $K = 3$. As we work out in Appendix B.1, in this case the relation between r and \hat{r} is particularly simple:

$$\hat{r}^{000} = 1/r^{000}. \quad (7.9)$$

Therefore

$$\hat{\mathcal{Y}}_{\gamma^{000}} = \mathcal{Y}_{\gamma^{000}}. \quad (7.10)$$

This is just as expected: the charge lattice contains only the single charge γ^{000} , which is pure flavor, so that the transformation $\mathcal{K}_{\gamma^{000}}$ induced by the BPS state of charge γ^{000} acts trivially on $\mathcal{Y}_{\gamma^{000}}$.

7.3.2 Example: $K = 4$

The next example is $K = 4$. In Appendix B.2 we show that in this case

$$\begin{aligned} \hat{r}^{100} &= \frac{1 + r^{100} + r^{100}r^{010}}{r^{010}(1 + r^{001} + r^{001}r^{100})}, \\ \hat{r}^{010} &= \frac{1 + r^{010} + r^{010}r^{001}}{r^{001}(1 + r^{100} + r^{100}r^{010})}, \\ \hat{r}^{001} &= \frac{1 + r^{001} + r^{001}r^{100}}{r^{100}(1 + r^{010} + r^{010}r^{001})}. \end{aligned} \quad (7.11)$$

This exactly matches the result for the AD_4 theory discussed in [7], equations (11.45)-(11.47). (This is not a coincidence: upon writing $\lambda = y dz$ one finds that the spectral curves in this theory are related to those of the AD_4 theory by the exchange $y \leftrightarrow z$. In the language of [21], the theory we are studying here is the (A_3, A_1) theory while the AD_4 theory is the (A_1, A_3) theory.) We can therefore borrow some results from [7]. In particular, as explained in §11.3 of [7], the factorization of this spectrum generator shows that there are four BPS states. These consist of three states carrying the three charges $\gamma^{\mathfrak{v}}$, together with a fourth state which is a bound state of two of the original three. Which two of the three form a bound state depends on which region of the Coulomb branch we are in.

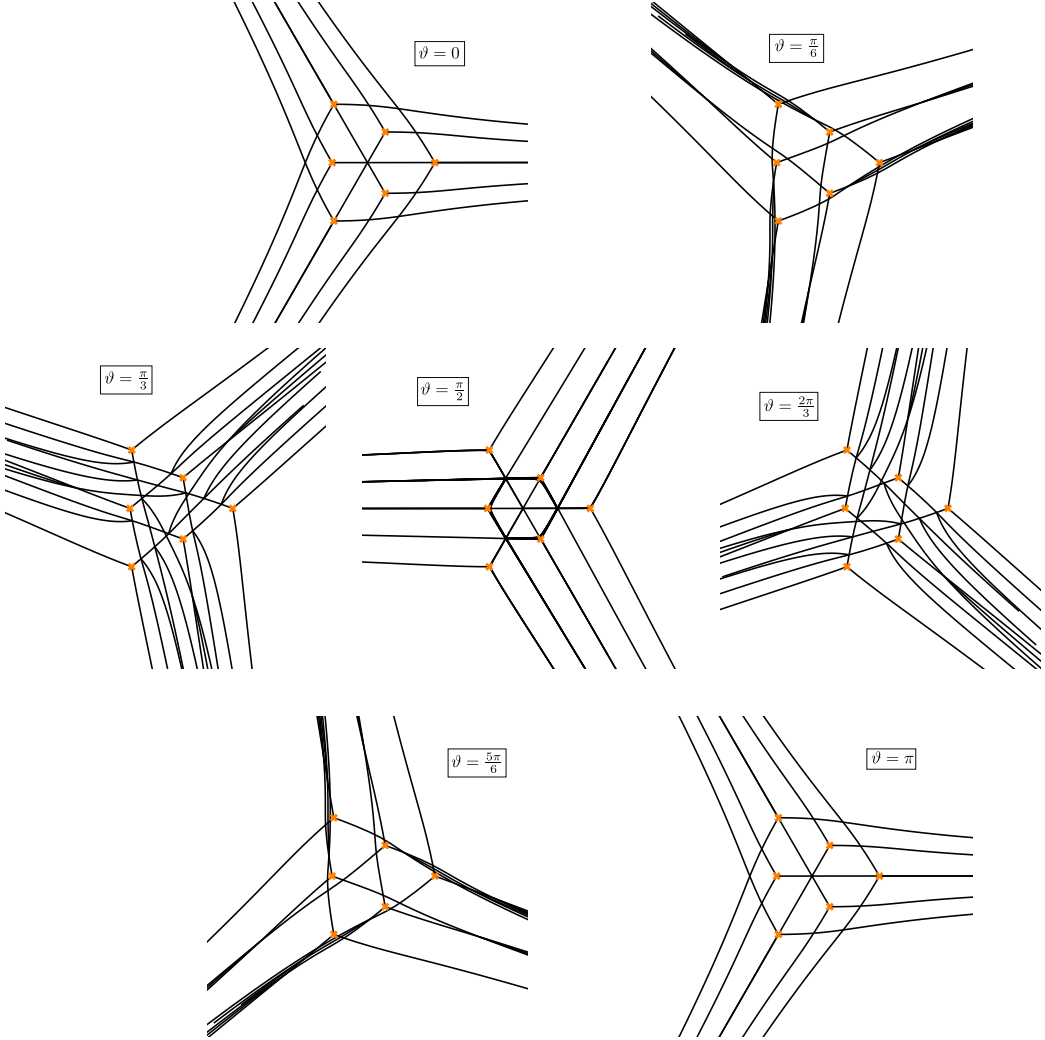


Figure 15. WKB spectral networks for the spectral curve $\lambda^4 - 10z(dz)^2\lambda^2 + 4(dz)^3\lambda + 9z^2(dz)^4 = 0$, as ϑ varies from 0 to π . There is a nontrivial jump at $\vartheta = \frac{\pi}{2}$.

In Figure 15 we show the variation of the spectral network \mathcal{W}_ϑ as ϑ varies from 0 to π , at a point of the Coulomb branch where the spectral curve is

$$\lambda^4 - 10z(dz)^2\lambda^2 + 4(dz)^3\lambda + 9z^2(dz)^4 = 0. \quad (7.12)$$

(Compare (2.7) for the unperturbed equation.) The variation is by equivalences except for a nontrivial jump at $\vartheta = \pi/2$.

In Figure 16 we zoom in on the behavior near this critical phase. Note that this behavior looks more complicated than the BPS states we have encountered to this point: at $\vartheta \rightarrow \pi/2$ an infinite number of winding \mathcal{S} -walls coalesce onto the hexagon visible in Figure 15. This behavior is still treatable using the methods of [1] (in particular it is somewhat similar to what happens in the example of §7.2 of that paper), but it is rather subtle. Part of the reason for this difficulty is that at the point of the Coulomb branch we have chosen to consider there is an exact \mathbb{Z}_3 symmetry (the spectral curve Σ is invariant

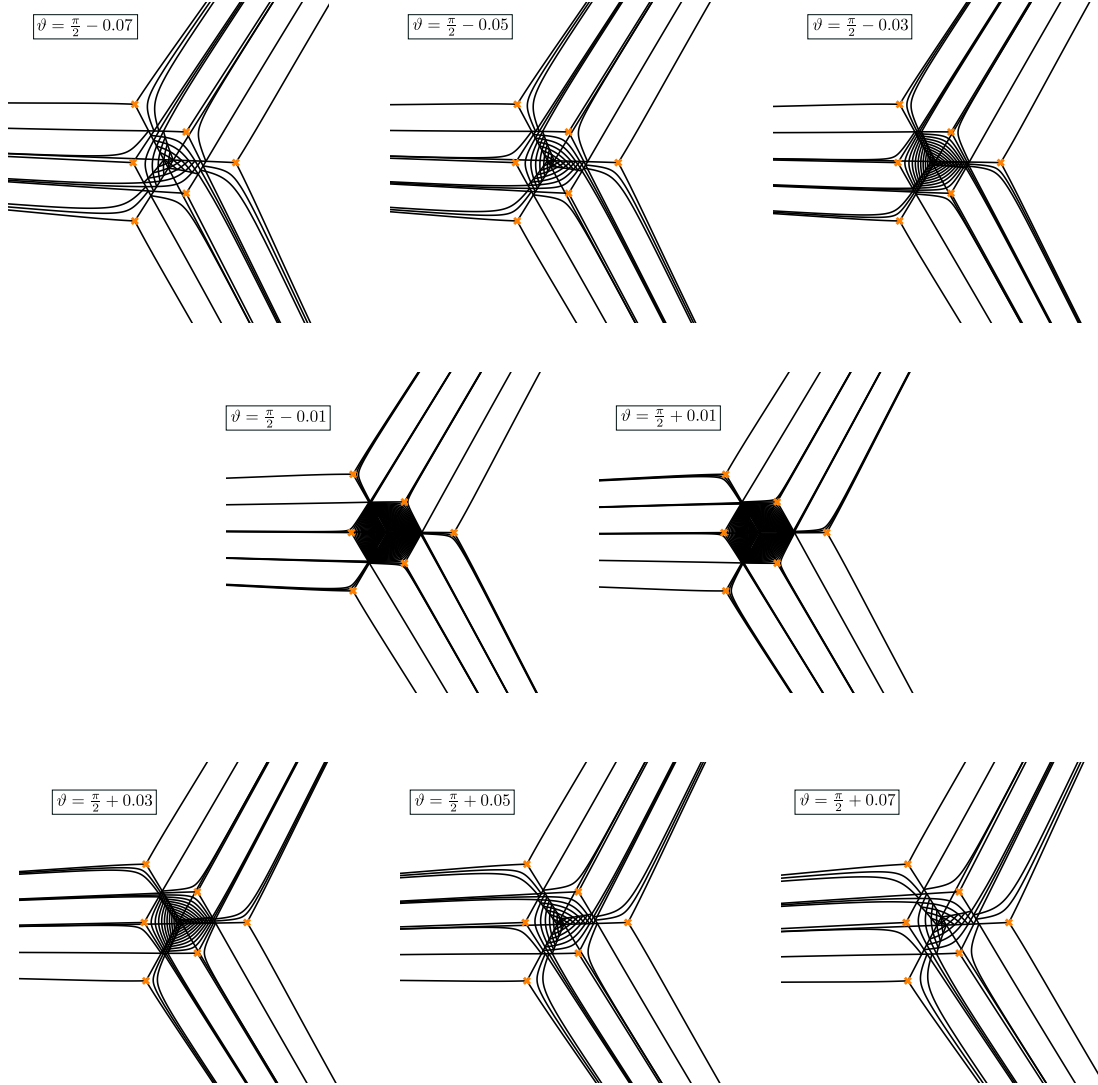


Figure 16. WKB spectral networks for the spectral curve $\lambda^4 - 10z(dz)^2\lambda^2 + 4(dz)^3\lambda + 9z^2(dz)^4 = 0$, as ϑ varies from $\frac{\pi}{2} - 0.07$ to $\frac{\pi}{2} + 0.07$.

under $(z, \lambda) \mapsto (e^{2\pi i/3}z, \lambda)$), and in particular all three of the Z_{γ^0} have the same phase. Since the γ^0 are mutually non-local charges and all support BPS states, this means we are sitting on a wall of marginal stability, where we may expect that the picture becomes more intricate. Perturbing slightly to move off the wall, we should expect to find the four states predicted in the previous paragraph. Indeed, we have confirmed experimentally that this is the case.

7.3.3 Example: $K = 5$

Just for the record, we also give the spectrum generator for $K = 5$. The new coordinates at the vertices of the 2-triangle of spaces are given by a fairly simple formula:

$$\begin{aligned}\hat{r}^{200} &= \frac{(1 + r^{110} + r^{020}r^{110} + r^{101}r^{110} + r^{020}r^{101}r^{110} + r^{011}r^{020}r^{101}r^{110})}{r^{020}(1 + r^{011} + r^{002}r^{011} + r^{011}r^{110} + r^{002}r^{011}r^{110} + r^{002}r^{011}r^{101}r^{110})}, \\ \hat{r}^{020} &= \frac{(1 + r^{011} + r^{002}r^{011} + r^{011}r^{110} + r^{002}r^{011}r^{110} + r^{002}r^{011}r^{101}r^{110})}{r^{002}(1 + r^{101} + r^{011}r^{101} + r^{101}r^{200} + r^{011}r^{101}r^{200} + r^{011}r^{101}r^{110}r^{200})}, \\ \hat{r}^{002} &= \frac{(1 + r^{101} + r^{011}r^{101} + r^{101}r^{200} + r^{011}r^{101}r^{200} + r^{011}r^{101}r^{110}r^{200})}{r^{200}(1 + r^{110} + r^{020}r^{110} + r^{101}r^{110} + r^{020}r^{101}r^{110} + r^{011}r^{020}r^{101}r^{110})},\end{aligned}\quad (7.13)$$

while the transformation laws for the intermediate coordinates are a bit more intricate:

$$\begin{aligned}\hat{r}^{110} &= \frac{A^{110}B^{110}}{r^{011}C^{110}D^{110}}, \\ A^{110} &= (1 + r^{101} + r^{011}r^{101} + r^{101}r^{200} + r^{011}r^{101}r^{200} + r^{011}r^{101}r^{110}r^{200}), \\ B^{110} &= (1 + r^{020} + r^{011}r^{020} + r^{002}r^{011}r^{020}), \\ C^{110} &= (1 + r^{110} + r^{020}r^{110} + r^{101}r^{110} + r^{020}r^{101}r^{110} + r^{011}r^{020}r^{101}r^{110}), \\ D^{110} &= (1 + r^{002} + r^{002}r^{101} + r^{002}r^{101}r^{200}),\end{aligned}\quad (7.14)$$

$$\begin{aligned}\hat{r}^{101} &= \frac{A^{101}B^{101}}{r^{110}C^{101}D^{101}}, \\ A^{101} &= (1 + r^{011} + r^{002}r^{011} + r^{011}r^{110} + r^{002}r^{011}r^{110} + r^{002}r^{011}r^{101}r^{110}), \\ B^{101} &= (1 + r^{200} + r^{110}r^{200} + r^{020}r^{110}r^{200}), \\ C^{101} &= (1 + r^{101} + r^{011}r^{101} + r^{101}r^{200} + r^{011}r^{101}r^{200} + r^{011}r^{101}r^{110}r^{200}), \\ D^{101} &= (1 + r^{020} + r^{011}r^{020} + r^{002}r^{011}r^{020}),\end{aligned}\quad (7.15)$$

$$\begin{aligned}\hat{r}^{011} &= \frac{A^{011}B^{011}}{r^{101}C^{011}D^{011}}, \\ A^{011} &= (1 + r^{110} + r^{020}r^{110} + r^{101}r^{110} + r^{020}r^{101}r^{110} + r^{011}r^{020}r^{101}r^{110}), \\ B^{011} &= (1 + r^{002} + r^{002}r^{101} + r^{002}r^{101}r^{200}), \\ C^{011} &= (1 + r^{011} + r^{002}r^{011} + r^{011}r^{110} + r^{002}r^{011}r^{110} + r^{002}r^{011}r^{101}r^{110}), \\ D^{011} &= (1 + r^{200} + r^{110}r^{200} + r^{020}r^{110}r^{200}).\end{aligned}\quad (7.16)$$

It appears likely that these formulas can be written in terms of trees on the triangle of spaces, and thereby generalized to arbitrary K . We leave a detailed discussion of that for another occasion.

8 Gluing of triangles, amalgamation, and identifying Fock-Goncharov edge coordinates with Darboux coordinates

Let us now consider level K lifts of more general theories $S[\mathfrak{g}, C, D]$ with $\mathfrak{g} = A_1$. Choosing ϑ and a point in the Coulomb branch, we obtain a WKB spectral network, which is roughly dual to a decorated ideal triangulation $T_{\text{WKB}}(\vartheta)$ of C . (This triangulation is described at

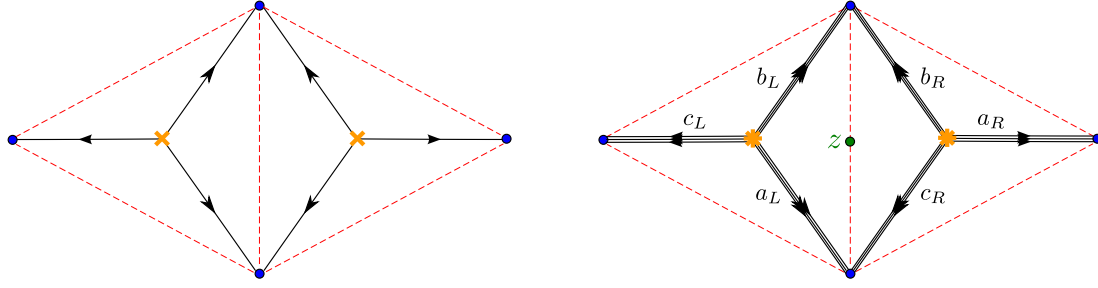


Figure 17. Left: An idealized picture of a quadrilateral formed by two adjacent triangles in a WKB triangulation $T_{\text{WKB}}(\vartheta)$ of C . The \mathcal{S} -walls of the corresponding WKB spectral network are shown in black. The edges of the WKB triangulation are shown in dashed red; they run between singular points, shown in blue. **Right:** An idealized picture of the level K lift of the picture at left, at a point of the Coulomb branch near the lift locus. Each triangle now contains a spectral network for the level K lift of the AD_1 theory. Each branch point has been fattened into a cluster of branch points, and the \mathcal{S} -walls of the original theory have been thickened into cables. We also mark a ‘‘pinning point’’ z for later use.

length in [7], and its relation to the $K = 2$ WKB spectral network is explained in [1].) A local picture of this triangulation is shown on the left side of Figure 17;¹⁴ this picture can be considered as part of a larger triangulation, or as a triangulation associated to the theory AD_2 .

Now consider making a small perturbation away from the lift locus of the level K lifted theory. Each branch point \mathfrak{b} then splits into $\frac{1}{2}K(K-1)$ branch points $\mathfrak{b}^{x,y,z}$ with $(x,y,z) \in T(K-2)$. Each of the \mathcal{S} -walls shown on the left of Figure 17 splits into a cable of \mathcal{S} -walls in the perturbed lift. Topologically speaking, each triangle contains a spectral network for the lifted AD_1 theory. The idealized picture is shown on the right side of Figure 17, while Figure 18 is an actual realization of this picture by WKB spectral networks, in the case $K = 3$.

In general, the WKB spectral networks which appear in the various triangles of the lifted theory need not be minimal. We will assume, however, that there exist regions of the Coulomb branch of the lifted theory for which the WKB spectral network in each triangle is essentially minimal. (It is not strictly necessary to use WKB spectral networks at all: we could work with more general spectral networks as defined in §9 of [1]. In this case we could simply declare that we are going to study the case where the network is minimal in each triangle. The only disadvantage of doing this is that then we cannot relate our results directly to BPS states at a particular point of the Coulomb branch of the lifted theory.)

The spectral network now provides Darboux coordinates on the moduli space of flat connections associated to the lifted theory. Our object is to relate these coordinates to the Fock-Goncharov coordinates of [2].

Some of the Darboux coordinates are easy to identify with Fock-Goncharov coordinates: indeed, in each triangle we have a collection of cycles $\gamma^{\mathfrak{v}}$, and the Darboux coor-

¹⁴In Figure 17 we have shown only the simplest situation; in general one also has to consider degenerate triangles, obtained as quotients of Figure 17 where some of the singular points are identified.

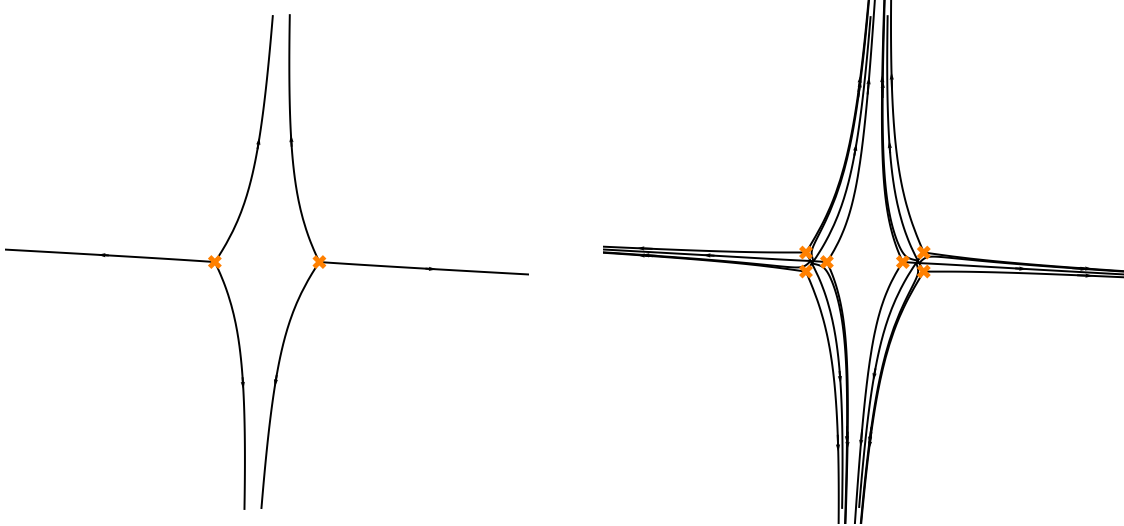


Figure 18. **Left:** a WKB spectral network \mathcal{W}_ϑ in the AD_2 theory, at the point of the Coulomb branch with $\phi_2 = 4(z^2 - 1)dz^2$, with $\vartheta = \frac{7\pi}{15}$. **Right:** a WKB spectral network \mathcal{W}_ϑ in the level $K = 3$ lift of the AD_2 theory, at the point of the Coulomb branch with $\phi_2 = 4(z^2 - 1)dz^2$, $\phi_3 = dz^3$, with $\vartheta = \frac{7\pi}{15}$. This is a small perturbation of the lift of the original theory on the left. Each branch point on the left has split into 3 branch points on the right, and the \mathcal{S} -walls on the left have thickened into cables on the right.

ordinates $\mathcal{Y}_{\gamma^\flat}$ will be identified with corresponding Fock-Goncharov “triangle coordinates” just as in §5.10. What is new here is that, when we have more than one triangle, we also get coordinates associated with the internal edges of the triangulation.

To understand these “edge coordinates,” let us return to the local picture in Figure 17. The spectral network in each of the two triangles shown will be either of *Yin* or *Yang* type. There are therefore four cases we should consider, but it suffices to consider just the cases (*Yin, Yin*) and (*Yin, Yang*).

First consider the (*Yin, Yin*) type lift. Because there is a common region $\mathcal{R}_{a_L b_L} = \mathcal{R}_{b_R c_R}$ there is a common edge in the corresponding triangles of lines, as shown in Figure 19. There are $(K - 1)$ edge segments along this common edge, which we call

$$E_j^L : \mathcal{L}_{K+1-j}^{\mathcal{R}_{a_L b_L}} \rightarrow \mathcal{L}_{K-j}^{\mathcal{R}_{a_L b_L}}, \quad E_j^R : \mathcal{L}_j^{\mathcal{R}_{b_R c_R}} \rightarrow \mathcal{L}_{j+1}^{\mathcal{R}_{b_R c_R}}. \quad (8.1)$$

Here $j = 1, \dots, K - 1$, and we have labeled the edges so that E_{K-j}^L and E_j^R are the same edge, but oppositely oriented. Therefore, if we compose the canonical homs attached to these edges (defined in (A.8)), we get a scalar:

$$r_{E_{K-j}^L} = r_{E_j^R} := x_{E_j^R} x_{E_{K-j}^L}. \quad (8.2)$$

These scalars are the Fock-Goncharov edge coordinates.

Next, we relate the Fock-Goncharov coordinates $r_{E_{K-j}^L}$ to Darboux coordinates \mathcal{Y}_γ for appropriate γ . Choose a “pinning point” z as indicated in Figure 17. As in §5.9, the canonical homs can then be identified with the Darboux sections for chains $\gamma_{ij}^R(z), \gamma_{ji}^L(z) \in$

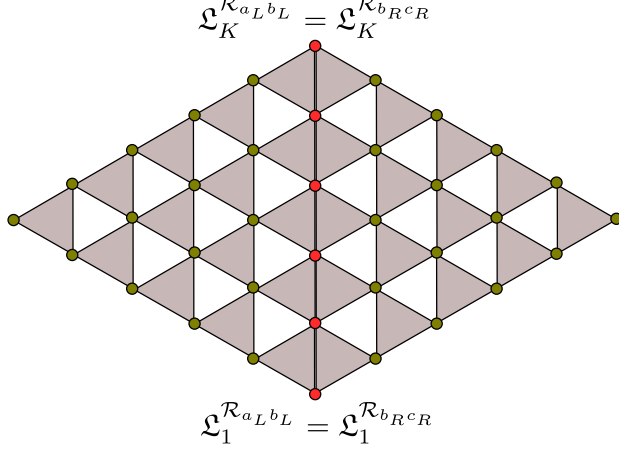


Figure 19. Each of the two minimal spectral networks in Figure 17 is associated to a triangle of lines. Since there is a common region $\mathcal{R}_{a_L b_L} = \mathcal{R}_{b_R c_R}$, the two triangles of lines can be considered to share a common edge, as depicted here. The lines along the common edge are highlighted.

$\Gamma(z, z)$:

$$x_{E_j^R} = \mathcal{Y}_{\gamma_{ij}^R(z)}, \quad x_{E_{K-j}^L} = \mathcal{Y}_{\gamma_{ji}^L(z)}. \quad (8.3)$$

Here $\gamma_{ij}^R(z)$ is an open chain which begins on sheet i above z , circles the branch point $\mathfrak{b}_R^{0, K-1-j, j-1}$ in the triangle $t(\mathfrak{b}_R)$ and returns to sheet j above z . There is a similar description for $\gamma_{ji}^L(z)$, which meets the branch point $\mathfrak{b}_L^{j-1, K-1-j, 0}$. Concatenating these chains gives a closed cycle $\gamma = \text{cl}(\gamma_{ij}^R(z) + \gamma_{ji}^L(z))$. Now using (8.2) and (8.3) we obtain

$$r_{E_{K-j}^L} = r_{E_j^R} = \mathcal{Y}_\gamma. \quad (8.4)$$

In other words, we have identified the $(K-1)$ Darboux coordinates \mathcal{Y}_γ associated with these closed curves with the $(K-1)$ Fock-Goncharov edge coordinates.

If we have two neighboring triangles of type (*Yin*, *Yang*), then along the common edge of the triangle of lines we pair the lines $\mathfrak{L}_j^{\mathcal{R}_{a_L b_L}}$ with the dual lines $\hat{\mathfrak{L}}_j^{\mathcal{R}_{b_R c_R}}$. Under this dual pairing $\mathfrak{L}_i^{\mathcal{R}_{a_L b_L}}$ is orthogonal to $\hat{\mathfrak{L}}_j^{\mathcal{R}_{b_R c_R}}$ for $i \neq j$ and has a nondegenerate pairing for $i = j$. The analog of (8.2) is that we choose arbitrary nonzero vectors $v_j \in \mathfrak{L}_j^{\mathcal{R}_{a_L b_L}}$ and $\hat{v}_j \in \hat{\mathfrak{L}}_j^{\mathcal{R}_{a_L b_L}}$ and consider

$$r = \frac{x_E(v_j) \cdot \hat{x}_E(\hat{v}_j)}{v_j \cdot \hat{v}_j}. \quad (8.5)$$

As before, r is the composition of Darboux sections for open paths $\mathcal{Y}_{\gamma_{ij}(z)}$, and the ratio in (8.5) is \mathcal{Y}_γ , for γ a cycle encircling an ji branch point $\mathfrak{b}_L^{j-1, K-1-j, 0}$ in the left triangle and an ij branch point $\mathfrak{b}_R^{0, j-1, K-1-j}$ in the right triangle.

The above concatenation procedures have a nice algebraic interpretation. In [8] Fock and Goncharov introduced a notion of *amalgamation* of cluster algebras and cluster varieties. The procedure we have outlined above appears to fit naturally into that framework, as follows. Each triangle corresponds to a seed. This seed includes some “unfrozen” or “active” variables corresponding to the Darboux coordinates $\mathcal{Y}_{\gamma^\flat}$; it also includes “frozen

variables,” corresponding to the Darboux sections $\mathcal{Y}_{\gamma_{ij}(z)}$ associated with the $(K - 1)$ edge segments on each edge of the triangle. One can now amalgamate the seeds corresponding to the various triangles of some triangulation, to make a seed in a bigger cluster algebra. This bigger algebra has unfrozen variables which are built as products of the frozen variables from the smaller seeds: this corresponds to concatenating the open paths $\gamma_{ij}(z)$ along common edges of the triangles to make closed paths, as we have described above.

In this section we have not taken careful account of the twistings discussed in §5.3. We leave a proper discussion of that detail to the future.

9 BPS spectra of level K lifts

In this section we give a description of some (perhaps all) of the BPS states of the level K lift of a general A_1 theory $S[A_1, C, D]$, in special regions of the Coulomb branch near the lift locus.

So, fix an A_1 theory $S[A_1, C, D]$, and fix a point u of its Coulomb branch. We assume that at u the A_1 theory has only BPS hypermultiplets, not vectormultiplets. (For example, for gauge theories with gauge group $SU(2)$ and $N_f \leq 4$, this condition is satisfied when u lies in a strong coupling region.) Let ϑ_α denote the phases of the central charges of these BPS hypermultiplets, with α running over the hypermultiplets. As we vary ϑ , the WKB spectral network $\mathcal{W}_\vartheta(u)$ undergoes a flip at each critical phase ϑ_α .

Now, we are going to consider the level K lift of our original A_1 theory. In the Coulomb branch of the lifted theory, there is a point of the lift locus corresponding to u . At this point there are a lot of massless BPS charges, so rather than working exactly at this point, we will study the lifted theory at a point u' slightly perturbed from the lift of u . At u' , for generic ϑ , the relation between the WKB spectral networks $\mathcal{W}_\vartheta(u')$ and the original $\mathcal{W}_\vartheta(u)$ is as indicated in Figure 17. In particular, $\mathcal{W}_\vartheta(u')$ is naturally divided into subnetworks embedding into triangles on C , and each of these subnetworks looks like a spectral network for the level K lift of AD_1 . Now, we make an important assumption: we assume that for most phases ϑ the restriction of $\mathcal{W}_\vartheta(u')$ to each triangle is essentially minimal, and that all the triangle states in each triangle occur in a narrow range of phases. The minimality is then violated only in this narrow range; for phases on one side of this critical range the triangle is of *Yin* type, for phases on the other side it is *Yang*.

Under this assumption, we now describe three different types of BPS states in the lifted theory, which we call *triangle states*, *lifted dyons*, and *lifted flavor states*.

We first consider the triangle states. As we have discussed, each branch point \mathfrak{b} of the A_1 theory splits into $\frac{1}{2}K(K - 1)$ branch points $\mathfrak{b}^{x,y,z}$, $(x, y, z) \in T(K - 2)$, in the lifted theory. The triangle states are the BPS states associated with the level K lift of the “local AD_1 ” theory associated with \mathfrak{b} . As we have seen in examples in §7, among the triangle states there are $\frac{1}{2}(K - 1)(K - 2)$ “elementary” hypermultiplets carrying charges $\gamma^\mathfrak{v}$, with $\mathfrak{v} \in T(K - 3)$, and in general there are also additional bound states of these hypermultiplets. Also as discussed in §7, the triangle states for any given triangle can be enumerated by considering the spectrum generator \mathbb{S} determined by (A.74), and decomposing \mathbb{S} into an ordered product of elementary \mathcal{K} -transformations as in (7.1). This decomposition depends

on the phases of the central charges Z_{γ^0} , hence depends on u' . We have such a collection of triangle states for each of the triangles of the A_1 theory.

Next we consider the lifted dyons. Consider a BPS hypermultiplet of the A_1 theory, with central charge of phase ϑ_α . At the phase ϑ_α , the WKB spectral network $\mathcal{W}_\vartheta(u)$ of the A_1 theory undergoes a flip. This flip involves two triangles which we call T_L, T_R , containing two branch points which we call $\mathfrak{b}_L, \mathfrak{b}_R$. At phases ϑ near ϑ_α , restricting the network $\mathcal{W}_\vartheta(u')$ of the lifted theory to these two triangles gives two essentially minimal spectral networks. When the phase ϑ crosses ϑ_α , in the original A_1 theory, one of the \mathcal{S} -walls emerging from \mathfrak{b}_L sweeps across one of the \mathcal{S} -walls emerging from \mathfrak{b}_R . In the lifted theory, this means that one of the cables emerging from the left triangle T_L sweeps across one of the cables emerging from the right triangle T_R . In this process, an \mathcal{S} -wall of type ij in the left cable can collide head-on with an \mathcal{S} -wall of type ji in the right cable; each time this happens we get a BPS hypermultiplet in the lifted theory, which we call a lifted gauge state.

The precise counting of these lifted dyons depends on the type of minimal spectral networks we have in the two triangles T_L, T_R at phases near ϑ_α . There are 4 cases: (Yin, Yin) , $(Yin, Yang)$, $(Yang, Yin)$, or $(Yang, Yang)$ types.

In the (Yin, Yin) or $(Yang, Yang)$ case, each of the $(K - i)$ \mathcal{S} -walls coming from T_L of type $(i, i + 1)$ can meet each of the i \mathcal{S} -walls of type $(i + 1, i)$ coming from T_R . Thus we obtain a total of

$$\sum_{i=1}^{K-1} i(K - i) = \frac{1}{6} K(K^2 - 1) \quad (9.1)$$

lifted gauge hypermultiplets. All of these hypermultiplets have phase close to ϑ_α .

On the other hand, in the $(Yin, Yang)$ or $(Yang, Yin)$ case, each of the i \mathcal{S} -walls from T_L of type $(i + 1, i)$ can meet each of the i \mathcal{S} -walls of type $(i, i + 1)$ from T_R . Thus there will be a total of

$$\sum_1^{K-1} i^2 = \frac{1}{6} K(K - 1)(2K - 1) \quad (9.2)$$

lifted gauge hypermultiplets, again all with phases close to ϑ_α . In Figure 20 we show an example: the single BPS hypermultiplet in the AD_2 theory lifts to 5 BPS hypermultiplets in the $K = 3$ lift of AD_2 .

Finally, we come to the *lifted flavor states*. In an A_1 theory, we say a “pure flavor state” arises when at a critical phase we have a closed \mathcal{S} -wall, beginning and ending on the same branch point \mathfrak{b} , and encircling a single singular point.¹⁵ In the level K lifted theory, when we sweep through the critical phase, two cables emerging from the same triangle will sweep across one another. In the process we will encounter \mathcal{S} -walls which begin and end at the same branch point; these correspond to pure flavor states of the lifted theory.

¹⁵These pure flavor states have a special status as they play no role in the four-dimensional Kontsevich-Soibelman wall-crossing-formula, since their charges are in the annihilator of the antisymmetric product on Γ . Nevertheless, since we can construct them using strings in the $(2, 0)$ theory, or membranes in M-theory, they are full-fledged members of the BPS spectrum with all the rights, privileges, and responsibilities pertaining thereunto. For example, they are visible in the 2d4d wall-crossing formula [6].

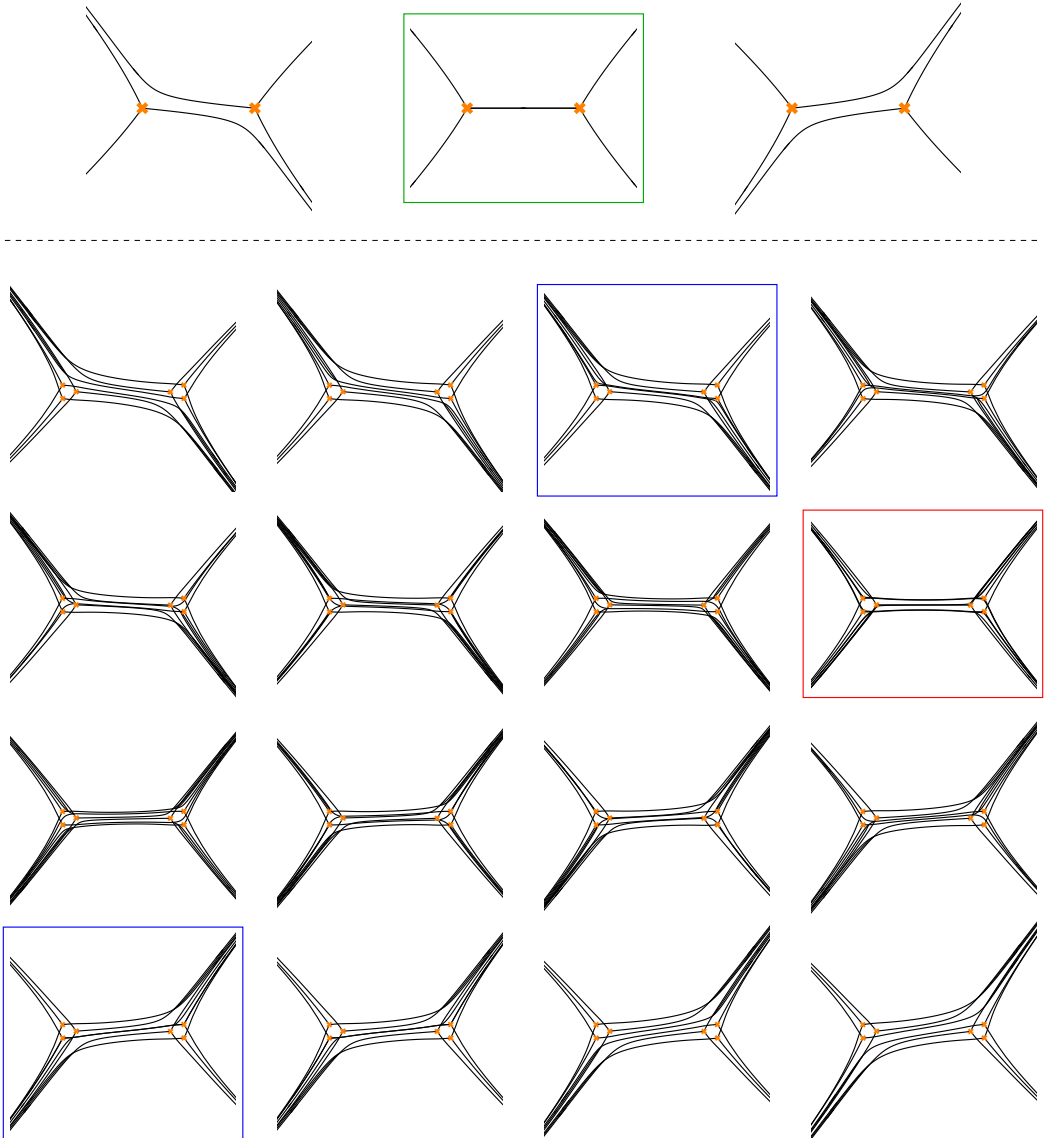


Figure 20. Top: Evolution of \mathcal{W}_ϑ in the AD_2 theory, with $\phi_2 = 4(z^2 - 1)dz^2$, for $\vartheta = \frac{-7\pi}{150}, 0, \frac{7\pi}{150}$. $\vartheta = 0$ is a critical phase at which \mathcal{W}_ϑ jumps; this frame is boxed (green). In this frame we see a single \mathcal{S} -wall connecting two branch points, representing a single BPS hypermultiplet. **Bottom:** Evolution of \mathcal{W}_ϑ in the level $K = 3$ lift of the AD_2 theory, with $\phi_2 = 4(z^2 - 1)dz^2$ and $\phi_3 = (\frac{1}{2} + \frac{i}{100})dz^3$, for phases ϑ running from $\frac{-8\pi}{150}$ to $\frac{7\pi}{150}$ in steps of $\frac{\pi}{150}$. The two minimal spectral networks shown are in a (*Yin*, *Yang*) configuration. There are 3 critical phases at which \mathcal{W}_ϑ jumps; the frames closest to these phases are boxed. At 2 of these phases (blue boxes) we see a single \mathcal{S} -wall which very nearly connects two branch points, while at 1 of them (red box) there are three such \mathcal{S} -walls at once. Each of these saddle connections corresponds to a BPS hypermultiplet. Altogether we have 5 such hypermultiplets: these are the “lifted dyons” associated to the single BPS hypermultiplet of the AD_2 theory. An animated version of this figure, along with its *Yin* counterpart, can be found at [22].

More interestingly, we will also encounter \mathcal{S} -walls which connect distinct branch points from the same cluster; these correspond to states of the lifted theory carrying nontrivial gauge charge. The number of such hypermultiplets is

$$\sum_{i=1}^{K-1} i^2 - i = \frac{1}{3} K(K-1)(K-2) \quad (9.3)$$

for each original flavor state. The reason is that there are i branch points of type $(K-i, K-i+1)$, and there are $i(i-1)$ *ordered* pairs of distinct branch points. We must use ordered pairs because the strings in the string web are oriented.

As an example, we apply this to the trinion theories $\mathcal{T}(K)$ of [23]. The theory $\mathcal{T}(2)$ is an A_1 theory, with $C = \mathbb{CP}^1$ and 3 defects. In this theory the generic WKB triangulation involves two triangles, each containing a single branch point. This theory has four charged hypermultiplets (associated with paths connecting the two distinct branch points)¹⁶ and three pure flavor particles (associated with paths connecting branch points to themselves after looping around a defect). The level K lift of $\mathcal{T}(2)$ is the theory $\mathcal{T}(K)$. Thus in theory $\mathcal{T}(K)$ we will have BPS states of all the three types described above: triangle states for each of the two triangles, lifted dyons for each of the four hypermultiplets, and lifted flavor states for each of the three flavor states.

In particular, let us consider the case $K = 3$. In this case each triangle contains a single elementary triangle state, and there is no possibility of any bound triangle states. Thus we get a total of 2 triangle states. Suppose that each of the 4 hypermultiplets arises from a quadrilateral of (Yin, Yin) type; in this case each lifts to 4 more BPS states. Finally, each of the 3 flavor states lifts to 2 BPS states with gauge charge. Thus we conclude that if our assumptions are all satisfied, the theory $\mathcal{T}(3)$ has at least $2 + 4 \times 4 + 3 \times 2 = 24$ BPS states in some region near the lift locus. It is interesting to note that this 24 matches the total number of BPS states found in some region of the Coulomb branch in [24, 25]; so if the region studied there is the same as the region we are studying, we would expect that the 24 states just described exhaust the whole BPS spectrum there. In principle this could be settled by looking at the spectral networks \mathcal{W}_ϑ as ϑ evolves through an interval of length π .

10 Lifting wall-crossing identities

Combining the above picture of BPS states of the lifted theory with the Kontsevich-Soibelman formula [13], which is known to govern the wall-crossing behavior of the BPS spectrum in $\mathcal{N} = 2$ theories [12, 14–18], leads to a number of identities on the Kontsevich-Soibelman symplectomorphisms \mathcal{K}_γ . In this section we briefly sketch how a few of these identities arise.

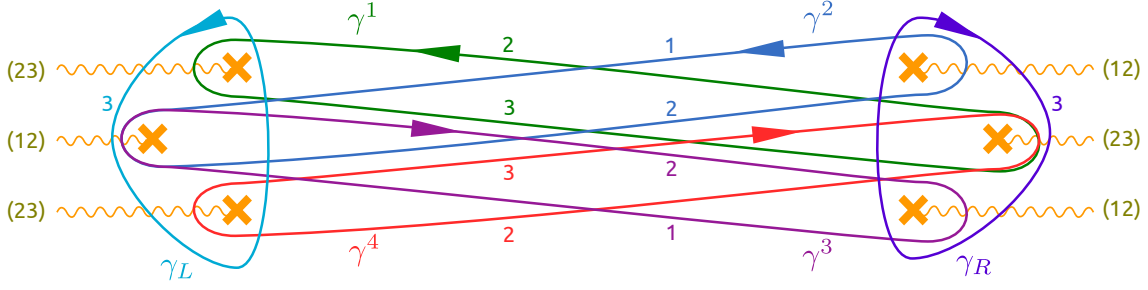


Figure 21. Cycles representing charges of BPS states which appear in a (*Yin, Yin*) configuration with $K = 3$ (4 lifted dyons and 2 triangle states). The small numbers next to the paths indicate which sheet of Σ they lie on.

10.1 Conjugating (*Yin, Yin*) to (*Yin, Yang*)

Consider a (*Yin, Yin*) quadrilateral in a level $K = 3$ lift. The charges of the associated BPS states are shown in Figure 21. Each triangle has a single associated BPS triangle state; we label their charges γ_L and γ_R . There are also 4 charges γ^i for the 4 lifted dyons.

Now, imagine varying Coulomb branch parameters so that the central charge Z_{γ_L} sweeps past the central charges Z_{γ^i} . After so doing we should reach a (*Yang, Yin*) quadrilateral. This is nicely reflected in the behavior of the KS transformations. Recall the basic pentagon identity [13],

$$\mathcal{K}_{\gamma_2} \mathcal{K}_{\gamma_2 + \gamma_1} \mathcal{K}_{\gamma_1} = \mathcal{K}_{\gamma_1} \mathcal{K}_{\gamma_2} \quad \text{for } \langle \gamma_2, \gamma_1 \rangle = +1. \quad (10.1)$$

Using this identity, together with $\langle \gamma_L, \gamma^1 \rangle = +1$ and $\gamma^4 = \gamma^1 + \gamma_L$, we can write

$$\mathcal{K}_{\gamma_L} \mathcal{K}_{\gamma^4} \mathcal{K}_{\gamma^1} \mathcal{K}_{\gamma^2} \mathcal{K}_{\gamma^3} = \mathcal{K}_{\gamma^1} \mathcal{K}_{\gamma_L} \mathcal{K}_{\gamma^2} \mathcal{K}_{\gamma^3}, \quad (10.2)$$

and then using $\langle \gamma_L, \gamma^2 \rangle = \langle \gamma_L, \gamma^3 \rangle = -1$, we obtain

$$\mathcal{K}_{\gamma_L} \mathcal{K}_{\gamma^4} \mathcal{K}_{\gamma^1} \mathcal{K}_{\gamma^2} \mathcal{K}_{\gamma^3} = \mathcal{K}_{\gamma^1} \mathcal{K}_{\gamma^2} \mathcal{K}_{\gamma^2 + \gamma_L} \mathcal{K}_{\gamma^3} \mathcal{K}_{\gamma^3 + \gamma_L} \mathcal{K}_{\gamma_L}. \quad (10.3)$$

Thus, with an appropriate ordering of the 4 BPS states of the (*Yin, Yin*) quadrilateral, conjugation by \mathcal{K}_{γ_L} can bring the product of 4 symplectomorphisms representing these 4 states to the product of 5 symplectomorphisms representing the 5 BPS states of the (*Yang, Yin*) quadrilateral.

10.2 Level 3 lift of the pentagon identity

Consistency of our picture of the BPS spectrum of the lifted theory implies in particular that there should be higher- K lifts of the basic ‘‘pentagon’’ and ‘‘juggle’’ identities which guarantee consistency of the spectra of A_1 theories. In this section we consider the $K = 3$ lift of the pentagon identity (10.1). The generalizations to higher K and to lifts of the juggle identity are left as open problems.

¹⁶This is the expected number, because we have half-hypermultiplets in the $(2, 2, 2)$ of the flavor $su(2) \oplus su(2) \oplus su(2)$ symmetry; alternatively this prediction can be verified directly, e.g. by plotting the spectral network by hand.

We consider three triangles in the $K = 3$ lift, or equivalently we consider the $K = 3$ lift of the AD_3 theory. Recall that in the AD_3 theory there is a wall of marginal stability: on one side of the wall there are 2 BPS hypermultiplets, on the other side there are 3, and the consistency of the spectrum follows from the pentagon identity (10.1). We would like to see how the consistency is maintained in the $K = 3$ lift.

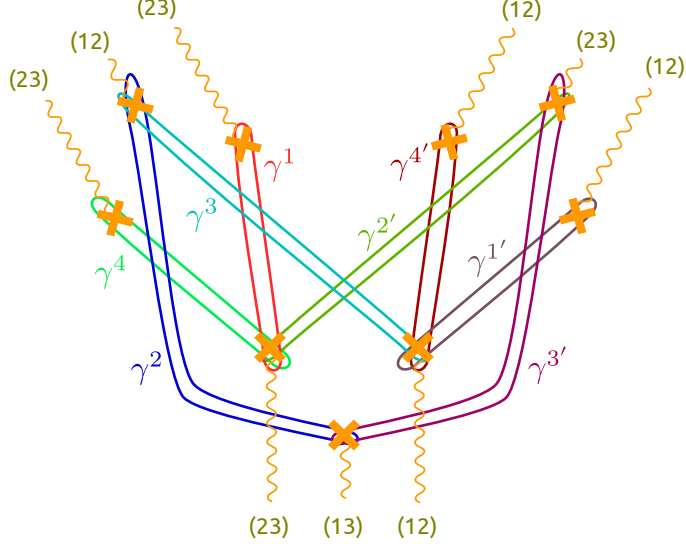


Figure 22. Cycles used in the $K = 3$ lift of the pentagon identity. These cycles represent the charges of 8 hypermultiplets obtained by lifting 2 hypermultiplets of the AD_3 theory.

Consider for simplicity the case where all of the quadrilaterals are of (Yin, Yin) type. Then in the $K = 3$ lift, each of the hypermultiplets of AD_3 gets lifted to 4 hypermultiplets. The charges of the lifts of 2 hypermultiplets of AD_3 are shown in Figure 22. One can show (just using the pentagon identity, the intersection numbers, and linear relations among the various cycles) that one has

$$\begin{aligned} & (\mathcal{K}_{\gamma_1} \mathcal{K}_{\gamma_2} \mathcal{K}_{\gamma_3} \mathcal{K}_{\gamma_4}) (\mathcal{K}_{\gamma_1} \mathcal{K}_{\gamma_2} \mathcal{K}_{\gamma_3} \mathcal{K}_{\gamma_4}) = \\ & (\mathcal{K}_{\gamma_1} \mathcal{K}_{\gamma_2} \mathcal{K}_{\gamma_3} \mathcal{K}_{\gamma_4}) (\mathcal{K}_{\gamma_1 + \gamma_2} \mathcal{K}_{\gamma_3 + \gamma_1} \mathcal{K}_{\gamma_4 + \gamma_2} \mathcal{K}_{\gamma_3 + \gamma_4}) (\mathcal{K}_{\gamma_1} \mathcal{K}_{\gamma_2} \mathcal{K}_{\gamma_3} \mathcal{K}_{\gamma_4}). \end{aligned} \quad (10.4)$$

This is the needed lift of the pentagon identity, which ensures consistency of the spectrum in the lifted theory.

10.3 Flips and Darboux coordinates

Finally, let us briefly consider one more natural question.

We have seen that each spectral network of an A_1 theory, i.e. each ideal triangulation of C , can be naturally lifted to a spectral network of the level K lifted theory. When the lifted network has Yin type in each triangle, the coordinates \mathcal{Y}_γ in the lifted theory match those defined by Fock-Goncharov in [2]. We may now ask: how do these coordinates transform when we flip the underlying ideal triangulation?

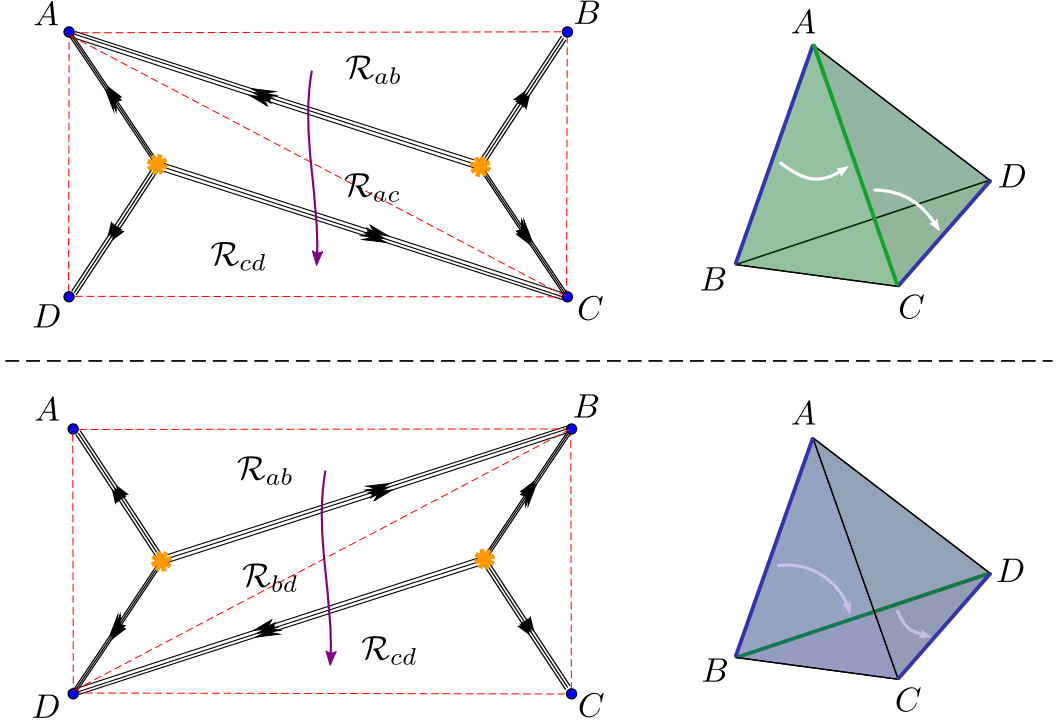


Figure 23. **Top left:** A schematic picture of a spectral network in the level K lift of AD_3 , and a path connecting three asymptotic regions, $\mathcal{R}_{ab} \rightarrow \mathcal{R}_{ac} \rightarrow \mathcal{R}_{cd}$. **Top right:** The canonical tetrahedron of lines in \mathcal{E} , with the snakes \mathcal{SN}_{AB} , \mathcal{SN}_{AC} , \mathcal{SN}_{CD} marked; our path corresponds to a path of snakes interpolating between these three, involving snakes sweeping across the faces ABC and ACD (the front faces, shaded green). **Bottom left:** Another spectral network in the same theory, related by a flip to the one at top left. The region \mathcal{R}_{ac} has disappeared and been replaced by \mathcal{R}_{bd} , so our path now connects $\mathcal{R}_{ab} \rightarrow \mathcal{R}_{bd} \rightarrow \mathcal{R}_{cd}$. **Bottom right:** The canonical tetrahedron of lines in \mathcal{E} , with the snakes \mathcal{SN}_{AB} , \mathcal{SN}_{BD} , \mathcal{SN}_{CD} marked; our path corresponds to a path of snakes interpolating between these three, involving snakes sweeping across the faces ABD and BCD (the rear faces, shaded green). The two paths of snakes on the right are related by a kind of discrete homotopy across the interior of the tetrahedron; the steps in this homotopy (not pictured here) correspond to the elementary jumps of the spectral network, whose composition makes up the flip.

This transformation was worked out in §10, p. 153, of [2]: when we flip the triangulation, the coordinates transform by a certain sequence of elementary symplectomorphisms. In the context of the lifted spectral network, these elementary symplectomorphisms have a natural interpretation. As we have discussed in §9, the flip decomposes into a sequence of more elementary transformations of the spectral networks, each one corresponding to a single “lifted gauge state.” Indeed, there is a 1-1 correspondence between the lifted dyons we found in the (Yin, Yin) case and the elementary symplectomorphisms which appeared in [2]. Moreover, using the results of [1], we know already that these lifted gauge states indeed induce symplectomorphisms of the right form (corresponding to single “mutations” in the language of [2]). This is a useful consistency check of our story.

We believe there is more to say here. Indeed, the analysis of this transformation in [2] involves a beautiful generalization of the combinatorics of m -triangles to “ m -simplices” of

higher dimension, which should also have an interpretation in terms of spectral networks. To be concrete, consider a spectral network in the level K lift of the AD_2 theory, with 4 cables of lines asymptoting to 4 singular points, and 4 associated flags $A_\bullet, B_\bullet, C_\bullet, D_\bullet$. See Figure 23.

If the 4 flags are in general position, then we can construct a corresponding “ $(K - 1)$ -tetrahedron” of lines in \mathcal{E} :

$$\mathcal{L}^{x,y,z,w} = A^x \cap B^y \cap C^z \cap D^w, \quad x + y + z + w = K - 1. \quad (10.5)$$

Now consider the two regions \mathcal{R}_{ab} and \mathcal{R}_{cd} . These regions correspond to snakes \mathcal{SN}_{AB} , \mathcal{SN}_{CD} drawn on edges of the tetrahedron. Other regions correspond to other snakes, and in particular a path from \mathcal{R}_{ab} to \mathcal{R}_{cd} corresponds to a particular path of snakes. The path shown in Figure 23 corresponds before the flip to the composition of the two canonical paths $\mathcal{SN}_{AB} \rightarrow \mathcal{SN}_{AC} \rightarrow \mathcal{SN}_{CD}$, and after the flip to the composition of the two canonical paths $\mathcal{SN}_{AB} \rightarrow \mathcal{SN}_{BD} \rightarrow \mathcal{SN}_{CD}$. These two compositions can be homotoped into one another across the $(K - 1)$ -tetrahedron. Indeed, the variation of the spectral network during the flip should give an explicit homotopy between them, with the intermediate spectral networks corresponding to intermediate paths of snakes from \mathcal{SN}_{AB} to \mathcal{SN}_{CD} .

By studying the projective bases associated to these snakes, we would expect to find an equation of the form

$$T^{AB \rightarrow AC}(\mathcal{Y}_\gamma) T^{AC \rightarrow DC}(\mathcal{Y}_\gamma) = \left(\prod_\alpha \mathcal{K}_{\gamma_\alpha} \right) \cdot T^{AB \rightarrow BD}(\mathcal{Y}_\gamma) T^{BD \rightarrow DC}(\mathcal{Y}_\gamma), \quad (10.6)$$

where the γ_α are the charges of the lifted dyons and the $T(\mathcal{Y}_\gamma)$ are the Stokes matrices for crossing cables. When we consider a spectral network with more than 2 triangles, we will get various equations of this sort; the mutual consistency of the resulting system should be guaranteed by identities following from lifts of pentagon identities, involving homotopies of homotopies, related to 5-simplices, and so on. We leave this to the future.

11 Open problems and future directions

The present paper is (deliberately) left somewhat sketchy and leaves much work to be done. Some of the more obvious directions in which this work could be continued are the following:

1. In §4.2 we describe how to perturb the level K lift of the AD_1 theory to produce spectral networks which are “essentially minimal” in the sense of §4.1. We showed by example that this could be done for small K but gave no systematic procedure for doing it for all K . We believe such a procedure exists and it would be nice to fill in this gap. We hasten to add that finding such a procedure is not logically necessary for the validity of the subsequent discussion of coordinates at arbitrary K .
2. In §7 we determined the spectrum generator for the level K lift of the AD_1 theory, in the region of the Coulomb branch admitting minimal spectral networks. The spectra

of these theories are essential building blocks in describing the BPS spectra of all level K lifts, as follows from the amalgamation procedure described in §8 below. We believe there should be elegant formulae for the general transformation of coordinates $r^\mathbf{v} \rightarrow \hat{r}^\mathbf{v}$ in terms of some simple algorithm involving trees on the $(K - 3)$ -triangle of spaces. Moreover, to read off the BPS spectrum from the spectrum generator requires one to factorize the spectrum generator into elementary \mathcal{K} -transformations (given a point of the Coulomb branch and hence an ordering of the phases of the periods). One such factorization has been found in [26]; it would be very interesting to know whether this factorization corresponds to the BPS spectrum at some point of the Coulomb branch.

3. Our discussion in the final three sections of the paper — the relation to cluster algebra amalgamation, the BPS spectrum of level K lifts of A_1 theories, and the spin lifts of wall-crossing identities — is especially sketchy. Much more remains to be done here. Among many open questions we mention just one: The physical interpretation of the amalgamation procedure in terms of four-dimensional quantum field theory might be very interesting. In the ultraviolet theory an analogous gluing statement described in [23, 27–31] is extremely powerful and deep. The amalgamation procedure should be some kind of infrared version of that statement. The inverse of amalgamation involves an RG flow, which decouples some degrees of freedom. Thus a physical interpretation of amalgamation might involve BPS domain walls between theories, such as the RG domain walls in [32, 33].
4. In §9 we described a general scenario for constructing the BPS spectrum of any lifted A_1 theory of class S. We did not show that there really do exist regions in the Coulomb branch where the spectral network is an essentially minimal network of, say, Yin type in all the triangles of the A_1 theory. We also did not show that the BPS states we exhibited exhaust all the BPS states in such regions of the Coulomb branch. Of course, for any given theory completeness can in principle be established by varying \mathcal{W}_θ and applying the algorithm of [1], but it would be nice to have a general argument.
5. It would be interesting to use these methods to compare in detail our results with the results of [24, 25, 34, 35] on the BPS spectra of higher rank $\mathcal{N} = 2, d = 4$ theories. We have not done so, but we conjecture that the BPS quiver for the level K lift of the AD_1 theory is the following: associate one node to each vector $\mathbf{v} \in T(K - 3)$ with charge $\gamma^\mathbf{v}$ and then determine the edges from equation (4.12). Similar remarks apply to lifts of AD_n theories.
6. While this paper focuses on some very special spectral networks, we can apply some of the constructions and lessons learned here to more general spectral networks. We think it could be very fruitful to investigate these constructions at the more general level. In particular, in this paper we show — in our special examples — explicitly how to express the “monodromy data” (here, Stokes matrices) in terms of

the “Darboux coordinates” \mathcal{Y}_γ on the moduli space of flat connections. But some of the key constructions of §5 apply more generally. A general spectral network provides a “nonabelianization map” from abelian flat connections on the Seiberg-Witten curve Σ (also known as the spectral curve, or the infrared curve) to non-abelian flat connections on the ultraviolet curve C . Quite generally, the construction of [1] produces three extra pieces of data:

- A collection of K lines $\mathcal{L}_i^{\mathcal{R}}$ of flat sections associated to each connected component \mathcal{R} of the complement of the spectral network on C .
- A collection of “coplanarity relations” associated to the \mathcal{S} -walls of the spectral network. Indeed, the discussion of §5.5 and §5.6 applies quite generally to show that if an \mathcal{S} -wall of type ij separates two regions \mathcal{R}_1 and \mathcal{R}_2 then the $(K-1)$ lines $\mathcal{L}_s^{\mathcal{R}}$ with $s \neq i$ are the same in the two regions, while $\mathcal{L}_i^{\mathcal{R}_1}$, $\mathcal{L}_i^{\mathcal{R}_2}$, and $\mathcal{L}_j^{\mathcal{R}_1} = \mathcal{L}_j^{\mathcal{R}_2}$ lie in a common plane.
- A collection of incidence relations determining how the lines are related to each other in terms of flags attached to the punctures of C .

For the minimal spectral networks of this paper, the Darboux coordinates are derived in two steps. First, one builds the collection of lines associated to a non-abelian flat connection. Next, the coplanarity relations on lines associated with \mathcal{S} -walls allow one to define canonical homs between certain lines, discussed in §5.5 and §A.2.1. Third, composition of these canonical homs associated with collections of lines forming a closed loop can be used to form coordinates, as in (5.43).

We conjecture that the three-step procedure described in the previous paragraph can be generalized to arbitrary spectral networks. Interestingly, the above procedure naturally lends itself to a description in terms of a *bipartite graph*, where lines are represented by white dots, coplanarity relations are represented by black dots, and white dots are connected to black dots if they sit in the relevant plane. We believe this observation might provide a useful link to the recent work of Goncharov [36] and Goncharov and Kontsevich [37]. It might also be a link to upcoming work of Arkani-Hamed et al. on scattering amplitudes in $\mathcal{N} = 4$ supersymmetric Yang-Mills theory [38].

Acknowledgements

We thank Sasha Goncharov for important discussions on his work with Fock on defining cluster coordinates for moduli spaces of flat connections with rank greater than 1. We also thank N. Arkani-Hamed for discussions and P. Longhi for some suggestions on the draft.

GM and AN would like to thank the KITP, where some of this work was done, for hospitality. The work of GM is supported by the DOE under grant DE-FG02-96ER40959. GM also gratefully acknowledges partial support from the Institute for Advanced Study and the Ambrose Monell Foundation. The work of AN is supported by the NSF under grant numbers DMS-1006046 and DMS-1151693. The research of DG was supported in

part by the NSF grant PHY-0503584. The research of DG was supported in part by the Roger Dashen membership in the Institute for Advanced Study. The research of DG was supported by the Perimeter Institute for Theoretical Physics. Research at Perimeter Institute is supported by the Government of Canada through Industry Canada and by the Province of Ontario through the Ministry of Economic Development and Innovation.

A Linear algebra of three flags in general position

Now we will review some constructions from Fock and Goncharov [2], concerning three flags $A_\bullet, B_\bullet, C_\bullet$ in general position in a K -dimensional vector space.

In our main application, these three flags will be determined by the $z \rightarrow \infty$ asymptotics in three regions of the level K lift of the AD_1 theory.

A.1 m -triangles

The m -triangle is a triangulation of the triangle in \mathbb{R}^3 with vertices $(m, 0, 0)$, $(0, m, 0)$ and $(0, 0, m)$. The vertices of the m -triangle are all lattice points in the interior, i.e. all triples (x, y, z) of nonnegative integers satisfying

$$x + y + z = m. \quad (\text{A.1})$$

We sometimes denote the set of vertices in the m -triangle by $T(m)$.

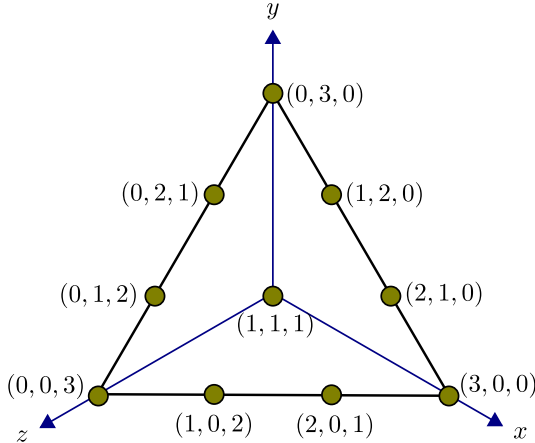


Figure 24. The lattice points of the m -triangle with $m = 3$, embedded in \mathbb{R}^3 .

The m -triangle lies on a plane orthogonal to the vector $(1, 1, 1)$. The lines with constant x , y or z are diagonals cutting through the triangle as indicated in Figure 25. Let us note a few properties:

1. Each edge of an m -triangle contains $m + 1$ lattice points. Altogether, an m -triangle contains $\frac{1}{2}(m + 1)(m + 2)$ lattice points.
2. The small upwards-pointing subtriangles of the m -triangle, shown shaded in Figure 25 are in 1-1 correspondence with the lattice points in the $(m - 1)$ -triangle. The

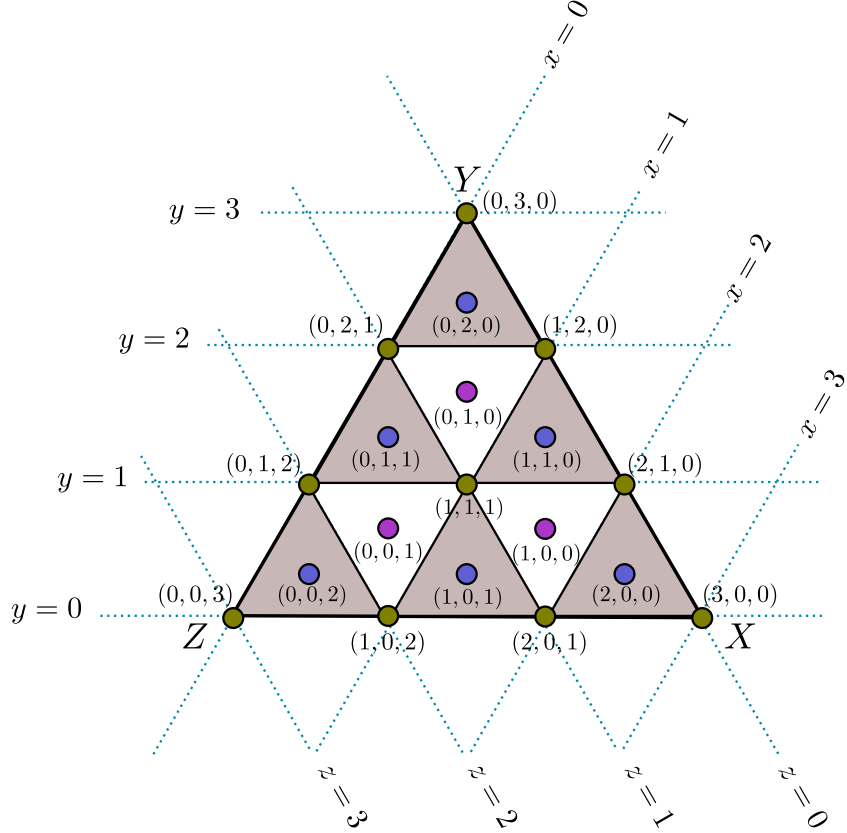


Figure 25. The m -triangle with $m = 3$, projected onto a plane along the $(1, 1, 1)$ axis. The shaded upwards-pointing subtriangles are labeled by the lattice points of the 2-triangle (blue). The unshaded downwards-pointing subtriangles are labeled by the lattice points of the 1-triangle (purple).

correspondence is induced by projecting both the m -triangle and the $(m-1)$ -triangle from \mathbb{R}^3 to \mathbb{R}^2 along the $(1, 1, 1)$ -axis. The lattice points of the $(m-1)$ -triangle then sit naturally at the center of the shaded up-triangles in the m -triangle.

3. The unshaded downwards-pointing triangles in the m -triangle are in 1-1 correspondence with the vertices of the $(m-2)$ -triangle. Again, the correspondence is realized geometrically by projecting along the $(1, 1, 1)$ axis.
4. The lattice points of the $(m-3)$ triangle are in 1-1 correspondence with the *interior* lattice points of the m -triangle. A simple way to see this is that if (x, y, z) are nonnegative and $x + y + z = m - 3$ then $(x + 1, y + 1, z + 1)$ is an interior lattice point of an m -triangle. As before, this correspondence can be realized geometrically by projecting along the $(1, 1, 1)$ axis.
5. Label the vertex $(m, 0, 0)$ in the m -triangle by X and call the opposite side the X -side. Do the same for y and z . Then the (x, y, z) coordinates of a point P in the m -triangle can be easily computed by the following observation: consider any path from P in the triangulation to the X -side, always traveling toward the X -side (no

backtracking.) Then the x -coordinate of P is the number of steps taken by the path. Analogous statements hold for the y, z coordinates. We often refer to the X, Y, Z vertices as the A, B, C vertices, respectively.

A.2 m -triangles associated with three flags

Let us suppose we have a vector space V of dimension K and three flags $A_\bullet, B_\bullet, C_\bullet$ in general position. In this section we define a distinguished set of lines in V labeled by lattice points of the $(K - 1)$ -triangle, planes in V labeled by lattice points of the $(K - 2)$ -triangle, and spaces in V labeled by lattice points of the $(K - 3)$ -triangle.¹⁷ The relations among the lattice points of the $(K - 1)$, $(K - 2)$, $(K - 3)$ -triangles reflect the incidence relations among their attached lines, planes and spaces.

Our convention for a flag is that A_n is an n -dimensional subspace of V , so

$$\{0\} = A_0 \subset A_1 \subset A_2 \subset \cdots \subset A_{K-1} \subset A_K = V. \quad (\text{A.2})$$

It is very convenient to introduce a notation that emphasizes the *codimension*, so we define

$$A^x := A_{K-x} \quad (\text{A.3})$$

and so forth, so that

$$\{0\} = A^K \subset A^{K-1} \subset A^{K-2} \subset \cdots \subset A^2 \subset A^1 \subset A^0 = V. \quad (\text{A.4})$$

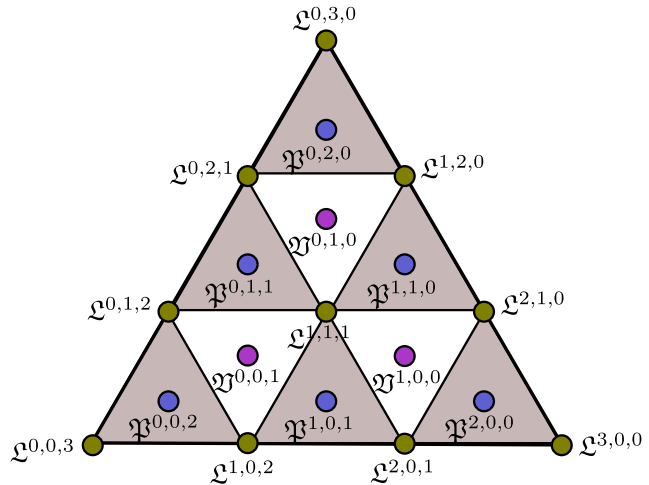


Figure 26. Incidence relations among the lines $\mathfrak{L}^{x,y,z}$, planes $\mathfrak{P}^{x,y,z}$ and spaces $\mathfrak{V}^{x,y,z}$ in the case $K = 4$. The vertices of the 3-triangle correspond to lines \mathfrak{L} . The shaded upwards pointing triangles correspond to planes \mathfrak{P} , and the three corners of a shaded triangle are three lines contained in the plane. The unshaded downwards pointing triangles correspond to spaces \mathfrak{V} , and the three shaded triangles abutting an unshaded triangle correspond to three planes \mathfrak{P} contained in the space \mathfrak{V} .

¹⁷By *space* in this subsection we mean a three-dimensional vector space. Living as we do in spacetime with only four macroscopic dimensions, our language has not evolved a convenient term to distinguish “space” of three dimensions from “space” of higher dimensions.

The lines we consider are simply

$$\mathfrak{L}^{x,y,z} := A^x \cap B^y \cap C^z, \quad x + y + z = K - 1. \quad (\text{A.5})$$

Here (x, y, z) is a point in the $(K - 1)$ -triangle. See Figure 26 for the case $K = 4$. For flags in general position, $\mathfrak{L}^{x,y,z}$ is a one-dimensional subspace of V . In an analogous way we define planes

$$\mathfrak{P}^{x,y,z} := A^x \cap B^y \cap C^z, \quad x + y + z = K - 2, \quad (\text{A.6})$$

labeled by points in the $(K - 2)$ -triangle, and spaces

$$\mathfrak{V}^{x,y,z} := A^x \cap B^y \cap C^z, \quad x + y + z = K - 3, \quad (\text{A.7})$$

labeled by points of the $(K - 3)$ -triangle. In particular, there are $\frac{1}{2}(K + 1)K$ different lines, $\frac{1}{2}K(K - 1)$ different planes, and $\frac{1}{2}(K - 1)(K - 2)$ different spaces.

The relations between points of the $m, m - 1, m - 2$ triangles we observed above have an elegant interpretation in terms of incidence relations among the lines $\mathfrak{L}^{x,y,z}$, planes $\mathfrak{P}^{x,y,z}$ and spaces $\mathfrak{V}^{x,y,z}$. We shade the small upwards-pointing subtriangles of the $(K - 1)$ -triangle. Then the shaded subtriangles are in 1-1 correspondence with vertices of the $(K - 2)$ -triangle. The plane $\mathfrak{P}^{x,y,z}$ corresponding to each shaded subtriangle contains the three lines $\mathfrak{L}^{x+1,y,z}, \mathfrak{L}^{x,y+1,z}$, and $\mathfrak{L}^{x,y,z+1}$ at its three vertices. Generically, these are the only such incidence relations we expect. That is, generically, we do not expect other triples of lines $\mathfrak{L}^{x',y',z'}$ to sit in any plane, let alone one of the special planes $\mathfrak{P}^{x,y,z}$. Similarly, the unshaded subtriangles are in 1-1 correspondence with the vertices of a $(K - 3)$ -triangle, and with the spaces $\mathfrak{V}^{x,y,z}$. Each unshaded triangle is abutted by 3 shaded triangles. This corresponds to the fact that $\mathfrak{V}^{x,y,z}$ contains the three planes $\mathfrak{P}^{x+1,y,z}, \mathfrak{P}^{x,y+1,z}$, and $\mathfrak{P}^{x,y,z+1}$. Generically, these are the only such incidence relations we expect. That is, generically, we do not expect any other planes of type $\mathfrak{P}^{x',y',z'}$ to sit in the space $\mathfrak{V}^{x,y,z}$.

A.2.1 Canonical homs

An edge E oriented from a line \mathfrak{L}_1 to a line \mathfrak{L}_2 determines an element $x_E \in \text{Hom}(\mathfrak{L}_1, \mathfrak{L}_2)$ as follows. E is a side of a unique shaded triangle, and hence E determines three lines $\mathfrak{L}_1, \mathfrak{L}_2, \mathfrak{L}_3$, the vertices of that shaded triangle. Given $v_1 \in \mathfrak{L}_1$ we define $x_E(v_1)$ to be the unique vector $v_2 \in \mathfrak{L}_2$ such that

$$\begin{cases} v_1 + v_2 \in \mathfrak{L}_3 & \text{clockwise} \\ v_1 - v_2 \in \mathfrak{L}_3 & \text{counterclockwise} \end{cases} \quad (\text{A.8})$$

where the cases refer to whether E is oriented clockwise or counterclockwise around the shaded triangle.

Note that if \bar{E} is the orientation reversal of E then $x_E x_{\bar{E}} = -1$ and $x_{\bar{E}} x_E = -1$. Similarly, if E_1, E_2, E_3 are three consecutive edges going around a shaded up-triangle, then $x_{E_1} x_{E_2} x_{E_3} = -1$ if they are oriented counterclockwise and $x_{E_1} x_{E_2} x_{E_3} = 1$ if oriented clockwise.

A.3 Fock and Goncharov's triple ratio

The space of flags in a K -dimensional complex vector space V is G/B , where $G = GL(K, \mathbb{C})$ and B is the Borel subgroup of upper-triangular matrices. It thus has dimension $K^2 - \frac{1}{2}K(K+1) = \frac{1}{2}K(K-1)$. We want to study the quotient of the space of triples of flags by the G -action:

$$\mathcal{C}_3 = G \setminus (G/B)^3. \quad (\text{A.9})$$

Since only $SL(K, \mathbb{C})$ acts effectively, \mathcal{C}_3 has dimension

$$\dim \mathcal{C}_3 = \frac{1}{2}(K-1)(K-2). \quad (\text{A.10})$$

In [2] Fock and Goncharov introduced a nice set of coordinates on this space. The coordinates are in 1-1 correspondence with points in the $(K-3)$ -triangle of spaces in V .

Let us begin with the case $K = 3$, in which case \mathcal{C}_3 is 1-dimensional. We fix the three flags:

$$\begin{aligned} A_\bullet &= a_1 \mathbb{C} \subset a_1 \mathbb{C} \oplus a_2 \mathbb{C} \subset V, \\ B_\bullet &= b_1 \mathbb{C} \subset b_1 \mathbb{C} \oplus b_2 \mathbb{C} \subset V, \\ C_\bullet &= c_1 \mathbb{C} \subset c_1 \mathbb{C} \oplus c_2 \mathbb{C} \subset V. \end{aligned} \quad (\text{A.11})$$

where a_i, b_i, c_i are vectors in V . Then in [2], p. 135, Section 4, Fock and Goncharov introduce the triple ratio:

$$r(A_\bullet, B_\bullet, C_\bullet) := \frac{(a_1 \wedge a_2 \wedge b_1)}{(a_1 \wedge a_2 \wedge c_1)} \frac{(b_1 \wedge b_2 \wedge c_1)}{(b_1 \wedge b_2 \wedge a_1)} \frac{(c_1 \wedge c_2 \wedge a_1)}{(c_1 \wedge c_2 \wedge b_1)}. \quad (\text{A.12})$$

The triple ratio r only depends on the three flags, not on the choice of basis vectors. To check this note first that the scales cancel out, and second that if we shift x_2 by a multiple of x_1 , where x is one of a, b, c , then r does not change. Note that

$$r(A_\bullet, B_\bullet, C_\bullet) = \frac{1}{r(B_\bullet, A_\bullet, C_\bullet)}, \quad r(A_\bullet, B_\bullet, C_\bullet) = r(B_\bullet, C_\bullet, A_\bullet). \quad (\text{A.13})$$

A.3.1 Three alternative formulations of the triple ratio

There are three useful ways to think about the triple ratio $r(A_\bullet, B_\bullet, C_\bullet)$, which we now describe.

First, consider the 2-triangle of lines defined by the three flags $A_\bullet, B_\bullet, C_\bullet$. Let us attempt to choose basis vectors $v^{x,y,z} \in \mathcal{L}^{x,y,z}$ so that the canonical homs associated to edges are as simple as possible. See Figure 27. First we choose $v^{0,2,0}, v^{0,1,1}$ and $v^{1,1,0}$ such that

$$v^{0,2,0} + v^{0,1,1} + v^{1,1,0} = 0. \quad (\text{A.14})$$

Having chosen $v^{1,1,0}$, we are still at liberty to choose $v^{1,0,1}$ and $v^{2,0,0}$ so that

$$v^{1,1,0} + v^{1,0,1} + v^{2,0,0} = 0. \quad (\text{A.15})$$

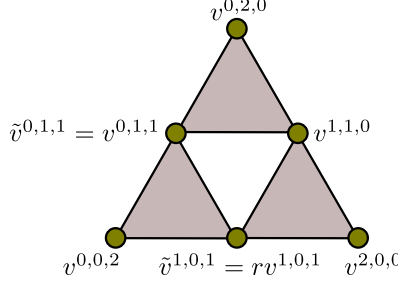


Figure 27. Basis vectors in the 2-triangle of lines in a 3-dimensional vector space, making the canonical homs as simple as possible.

However, for the third triangle we are now stuck. We have already chosen two of the relevant basis vectors $v^{0,1,1}$ and $v^{1,0,1}$. There is of course a triplet of basis vectors $\tilde{v}^{0,1,1}$, $\tilde{v}^{1,0,1}$, $v^{0,0,2}$ such that

$$\tilde{v}^{0,1,1} + \tilde{v}^{1,0,1} + v^{0,0,2} = 0. \quad (\text{A.16})$$

Such a triplet is unique up to overall scale. Now we fix this scale by choosing $\tilde{v}^{0,1,1} = v^{0,1,1}$. Then $\tilde{v}^{1,0,1} = rv^{1,0,1}$ for some $r \in \mathbb{C}^\times$. Now with

$$\begin{aligned} A_\bullet &= \mathfrak{L}^{2,0,0} \subset \mathfrak{P}^{1,0,0} \subset V, \\ B_\bullet &= \mathfrak{L}^{0,2,0} \subset \mathfrak{P}^{0,1,0} \subset V, \\ C_\bullet &= \mathfrak{L}^{0,0,2} \subset \mathfrak{P}^{0,0,1} \subset V, \end{aligned} \quad (\text{A.17})$$

a small computation shows that

$$r(A_\bullet, B_\bullet, C_\bullet) = r. \quad (\text{A.18})$$

A second way to understand r is to consider the canonical homs associated with the edges shown in Figure 29 below. An easy computation using the above basis vectors reveals that

$$x_{\tilde{E}_1} x_{\tilde{E}_2} = r x_{E_1} x_{E_2}. \quad (\text{A.19})$$

A third, rather elegant, way to view the invariant r associated with a 2-triangle of lines is to consider the composition of the canonical homs associated to the three internal edges bounding the downward pointing unshaded triangle in Figure 27. If we compose the three canonical homs going around the triangle counterclockwise,

$$\text{Hom}(\mathfrak{L}^{0,1,1}, \mathfrak{L}^{1,0,1}) \otimes \text{Hom}(\mathfrak{L}^{1,0,1}, \mathfrak{L}^{1,1,0}) \otimes \text{Hom}(\mathfrak{L}^{1,1,0}, \mathfrak{L}^{0,1,1}) \rightarrow \text{Hom}(\mathfrak{L}^{0,1,1}, \mathfrak{L}^{0,1,1}) \cong \mathbb{C}, \quad (\text{A.20})$$

we obtain

$$x_{E_1} x_{E_2} x_{E_3} = r. \quad (\text{A.21})$$

If we instead compose the three canonical homs going around the triangle clockwise, we obtain

$$x_{\tilde{E}_3} x_{\tilde{E}_2} x_{\tilde{E}_1} = -1/r. \quad (\text{A.22})$$

These statements are easily verified using the basis vectors in (A.14)-(A.16).

A.3.2 Fock and Goncharov's triple ratios for $K > 3$

Now let us proceed to the case where $\dim V = K > 3$. We want to assign a coordinate to each interior point (x, y, z) with $x + y + z = K - 3$. Around equation (9.10), p. 140, of [2], Fock and Goncharov observe that the three flags $A_\bullet, B_\bullet, C_\bullet$ in V induce three flags $\bar{A}_\bullet, \bar{B}_\bullet, \bar{C}_\bullet$ in the three-dimensional space $\bar{V} := V/(A_x + B_y + C_z)$, and they define their coordinate $r_{FG}^{x,y,z}$ to be the triple ratio of the induced flags in this three-dimensional space.

More precisely, by the projected flag \bar{A}_\bullet we mean the flag

$$\begin{aligned} 0 \cong (A_x + B_y + C_z)/W_{x,y,z} &\subset (A_{x+1} + B_y + C_z)/W_{x,y,z} \subset (A_{x+2} + B_y + C_z)/W_{x,y,z} \subset \\ &\subset (A_{x+3} + B_y + C_z)/W_{x,y,z} \subset \dots \end{aligned} \tag{A.23}$$

where $W_{x,y,z} = A_x + B_y + C_z$. For flags in generic position $(A_{x+3} + B_y + C_z)/W_{x,y,z} = V/W_{x,y,z}$, and thus we get a flag \bar{A}_\bullet in three dimensions. Defining similarly \bar{B}_\bullet and \bar{C}_\bullet and taking their triple ratio gives Fock and Goncharov's definition:

$$r_{FG}^{x,y,z} := r(\bar{A}_\bullet, \bar{B}_\bullet, \bar{C}_\bullet). \tag{A.24}$$

In preparation for the discussion in §A.3.4 we note that there is a dual construction which Fock and Goncharov could equally well have employed. In general if $W_1 \subset W_2 \subset V$ then there is a surjection $V/W_1 \rightarrow V/W_2$ and hence a dual injection $(V/W_2)^* \hookrightarrow (V/W_1)^*$. Therefore, we can also consider the flag $A'_\bullet \subset V^*$ of length three:

$$(V/(A_{x+2} + B_y + C_z))^* \hookrightarrow (V/(A_{x+1} + B_y + C_z))^* \hookrightarrow (V/(A_x + B_y + C_z))^*, \tag{A.25}$$

and similarly B'_\bullet and C'_\bullet . A short computation shows that the triple ratio of these flags in the common three-dimensional space $(V/(A_x + B_y + C_z))^*$ is

$$r(A'_\bullet, B'_\bullet, C'_\bullet) = 1/r_{FG}^{x,y,z}. \tag{A.26}$$

A.3.3 An alternative coordinate system for $K > 3$

For $K = 3$ we illustrated an alternative formulation of the triple ratio using equations (A.20) and (A.21). For $K > 3$ we can use the same idea to construct *different* coordinates $r^{x,y,z}$ on the moduli space \mathcal{C}_3 of triples of flags, as follows. We consider the down-triangle with vertices $\mathfrak{L}^{x+1,y+1,z}$, $\mathfrak{L}^{x,y+1,z+1}$, $\mathfrak{L}^{x+1,y,z+1}$, and take the composition of canonical homs going around this triangle counterclockwise:

$$\mathfrak{L}^{x,y+1,z+1} \rightarrow \mathfrak{L}^{x+1,y,z+1} \rightarrow \mathfrak{L}^{x+1,y+1,z} \rightarrow \mathfrak{L}^{x,y+1,z+1}. \tag{A.27}$$

The composition of these homs is multiplication by a scalar; we define $r^{x,y,z}$ to be this scalar.

Here is another construction of the same coordinate. To the interior point (x, y, z) with $x + y + z = K - 3$ we associate the three-dimensional space $\mathfrak{V}^{x,y,z}$. This space contains the three planes $\mathfrak{P}^{x+1,y,z}$, $\mathfrak{P}^{x,y+1,z}$, $\mathfrak{P}^{x,y,z+1}$, the six lines

$$\mathfrak{L}^{x+2,y,z}, \mathfrak{L}^{x,y+2,z}, \mathfrak{L}^{x,y,z+2}, \mathfrak{L}^{x+1,y+1,z}, \mathfrak{L}^{x,y+1,z+1}, \mathfrak{L}^{x+1,y,z+1}, \tag{A.28}$$

and the three associated flags:

$$\begin{aligned}\tilde{A}_\bullet : \quad 0 &\subset \mathfrak{L}^{x+2,y,z} \subset \mathfrak{P}^{x+1,y,z} \subset \mathfrak{V}^{x,y,z}, \\ \tilde{B}_\bullet : \quad 0 &\subset \mathfrak{L}^{x,y+2,z} \subset \mathfrak{P}^{x,y+1,z} \subset \mathfrak{V}^{x,y,z}, \\ \tilde{C}_\bullet : \quad 0 &\subset \mathfrak{L}^{x,y,z+2} \subset \mathfrak{P}^{x,y,z+1} \subset \mathfrak{V}^{x,y,z}.\end{aligned}\tag{A.29}$$

There is, accordingly, a triple ratio $r(\tilde{A}_\bullet, \tilde{B}_\bullet, \tilde{C}_\bullet)$, which coincides with our $r^{x,y,z}$.

A.3.4 Relation between the coordinate systems

The coordinates $r^{x,y,z}$ and $r_{FG}^{x,y,z}$ are *not* the same when $K > 3$. In this section we explain the relation between them.

To begin, recall that if W is any linear subspace of V we can define

$$W^\perp := \{\ell | \ell(w) = 0 \quad \forall w \in W\} \subset V^*. \tag{A.30}$$

Of course $(W^\perp)^\perp = W$. We can use this to construct a notion of a dual flag, as follows. If

$$W_\bullet : \quad 0 = W_0 \subset W_1 \subset \cdots \subset W_{K-1} \subset W_K = V \tag{A.31}$$

is a flag in V , with $\dim W_x = x$, then we define

$$\check{W}_x := (W_{K-x})^\perp = (W^x)^\perp. \tag{A.32}$$

Note that $\dim \check{W}_x = x$ and so

$$\check{W}_\bullet : \quad 0 = \check{W}_0 \subset \check{W}_1 \subset \cdots \subset \check{W}_{K-1} \subset \check{W}_K = V^* \tag{A.33}$$

is a flag, which we call the *dual flag*. There is an *a priori* different notion of dual flag: we could have defined

$$0 \hookrightarrow (V/W_{K-1})^* \hookrightarrow (V/W_{K-2})^* \hookrightarrow \cdots \hookrightarrow (V/W_2)^* \hookrightarrow (V/W_1)^* \hookrightarrow V^* \tag{A.34}$$

to be the dual flag. The two are in fact canonically isomorphic since there is a canonical isomorphism $(V/W)^* \cong W^\perp$.¹⁸

So, given flags $A_\bullet, B_\bullet, C_\bullet$ in V , there are dual flags $\check{A}_\bullet, \check{B}_\bullet, \check{C}_\bullet$ in V^* . We are going to show that the Fock-Goncharov coordinates of these dual flags are related to our coordinates by:

$$r_{FG}^{x,y,z}(\check{A}_\bullet, \check{B}_\bullet, \check{C}_\bullet) = 1/r^{x,y,z}(A_\bullet, B_\bullet, C_\bullet). \tag{A.35}$$

In order to prove (A.35) we first note that if W_1 and W_2 are any two subspaces of V then $(W_1 + W_2)^\perp = W_1^\perp \cap W_2^\perp$. It follows that

$$(V/(W_1 + W_2 + W_3))^* \cong W_1^\perp \cap W_2^\perp \cap W_3^\perp \subset V^*. \tag{A.36}$$

¹⁸Indeed, given $\ell \in W^\perp$, we may define $\bar{\ell} \in (V/W)^*$ by $\bar{\ell}(\bar{u}) := \ell(u)$, where u is any lift of \bar{u} . The map $\ell \mapsto \bar{\ell}$ clearly has zero kernel, and hence, by dimension counting, must be an isomorphism.

We now apply (A.36) replacing V by V^* and taking W_1, W_2, W_3 to be spaces in the dual flags, to obtain three canonical isomorphisms:

$$(V^*/(\check{A}_x + \check{B}_y + \check{C}_z))^* \cong \check{A}_x^\perp \cap \check{B}_y^\perp \cap \check{C}_z^\perp = A^x \cap B^y \cap C^z = \mathfrak{V}^{x,y,z}, \quad (\text{A.37})$$

$$(V^*/(\check{A}_{x+1} + \check{B}_y + \check{C}_z))^* \cong \check{A}_{x+1}^\perp \cap \check{B}_y^\perp \cap \check{C}_z^\perp = A^{x+1} \cap B^y \cap C^z = \mathfrak{P}^{x+1,y,z}, \quad (\text{A.38})$$

$$(V^*/(\check{A}_{x+2} + \check{B}_y + \check{C}_z))^* \cong \check{A}_{x+2}^\perp \cap \check{B}_y^\perp \cap \check{C}_z^\perp = A^{x+2} \cap B^y \cap C^z = \mathfrak{L}^{x+2,y,z}. \quad (\text{A.39})$$

Now, the Fock-Goncharov coordinate $r_{FG}^{x,y,z}(\check{A}_\bullet, \check{B}_\bullet, \check{C}_\bullet)$ is, by (A.26), the reciprocal of the triple ratio associated to the flags $\check{A}'_\bullet, \check{B}'_\bullet, \check{C}'_\bullet$ in three dimensions, defined by

$$\check{A}'_\bullet : 0 \subset (V^*/(\check{A}_{x+2} + \check{B}_y + \check{C}_z))^* \hookrightarrow (V^*/(\check{A}_{x+1} + \check{B}_y + \check{C}_z))^* \hookrightarrow (V^*/(\check{A}_x + \check{B}_y + \check{C}_z))^* \quad (\text{A.40})$$

and similarly for \check{B}'_\bullet and \check{C}'_\bullet . Applying the isomorphisms (A.37), (A.38), and (A.39) we identify \check{A}'_\bullet with the flag $\mathfrak{L}^{x+2,y,z} \subset \mathfrak{P}^{x+1,y,z} \subset \mathfrak{V}^{x,y,z}$, and similarly for \check{B}'_\bullet and \check{C}'_\bullet . Combining this with the observation (A.26) we obtain (A.35).

We close with two remarks:

1. In §A.5 below we give an algorithm for determining explicit expressions for the $r_{FG}^{x,y,z}$ as functions of the $r^{x,y,z}$. Explicit examples of such transformations are given in (7.11) and (7.13) above for $K = 4, 5$ respectively.
2. We have not demonstrated that the $r^{x,y,z}$ really do form an independent set of coordinates on \mathcal{C}_3 . One way to do this is to invoke (A.35) and the results of Fock and Goncharov. Another way to proceed is to consider the perturbation of the Stokes matrices defined in equations (A.48) and (A.49) around the point $r^{x,y,z} = 1$. It can be shown that the perturbations by the different $r^{x,y,z}$ are independent.

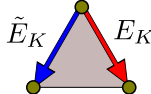


Figure 28. The type I elementary snake move of Fock-Goncharov. The bottom edge of the triangle shown is on the final destination edge of the snake.

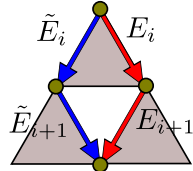


Figure 29. The type II elementary snake move of Fock-Goncharov. The triangle shown is embedded into a larger m -triangle, and we only show the i^{th} and $(i+1)^{th}$ edges of the snakes. The type II move replaces the chain $\cdots E_{i+1} E_i \cdots$ in the first snake by $\cdots \tilde{E}_{i+1} \tilde{E}_i \cdots$ in the new snake. The canonical homs are related by $x_{\tilde{E}_i} x_{\tilde{E}_{i+1}} = r x_{E_i} x_{E_{i+1}}$.

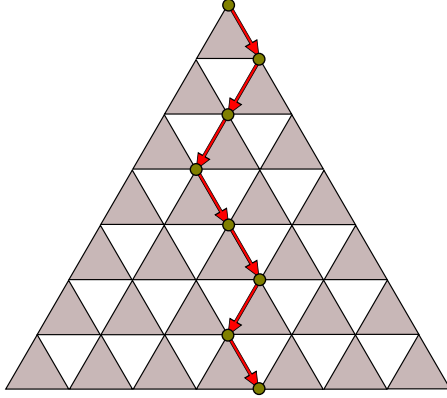


Figure 30. A typical snake, oriented from the B -vertex to the B -side.

A.4 Fock and Goncharov's snakes

In Section 9, especially subsections 7, and 8, p. 138 et. seq. of [2] Fock and Goncharov introduced the notion of a snake associated to a vector space with three flags:

Definition: A *snake* associated to a K -dimensional vector space V with three flags in general position is an oriented edge path of length $K - 1$, which begins at a vertex of the $(K - 1)$ -triangle of lines in V and terminates at the opposite edge. A typical example is shown in Figure 30.

There are 2^{K-1} different snakes from a fixed vertex to the opposite side. If we consider snakes from the B -vertex to the B -side, we can label each snake by a word in two letters, R and L , with the rightmost letter indicating the direction of the first edge and the leftmost letter indicating the direction of the last edge. Any two snakes can be related to each other by a series of elementary moves, of two basic types. (See [2], p. 140, Figure 9.11.) A move of type I is shown in Figure 28 and a move of type II is shown in Figure 29. Note that type I moves can only be made on the final edge of a snake.

To a snake we can associate a decomposition of V into lines. For example for a snake from the B -vertex we have:

$$V = \mathfrak{L}^{0,K-1,0} \oplus \bigoplus_{i=1}^{K-1} \mathfrak{L}^{t(E_i)}, \quad (\text{A.41})$$

where $t(E_i)$ is the target vertex of the i^{th} edge of the snake. Further, as we have explained, each oriented edge E on the $(K - 1)$ -triangle of lines is associated with a canonical hom, x_E . Therefore, to a snake we can associate a projective basis of V , as follows. We first choose a basis vector v_K in $\mathfrak{L}^{0,K-1,0}$ and then iterate:

$$v_{K-i} = v_{K+1-i} x_{E_i}, \quad 1 \leq i \leq K - 1. \quad (\text{A.42})$$

We write

$$\mathcal{B}^{\mathcal{SN}} = \begin{pmatrix} v_1 \\ v_2 \\ \vdots \\ v_{K-1} \\ v_K \end{pmatrix} \quad (\text{A.43})$$

for the basis determined by a snake \mathcal{SN} .

As discussed in [2], given two snakes, it is of interest to describe explicitly the linear transformation between the corresponding projective bases. It suffices to describe the transformations for the two types of moves. For type I moves it is easy to see that only v_1 is changed:

$$v_1^{\mathcal{SN}_2} = v_1^{\mathcal{SN}_1} + v_2^{\mathcal{SN}_1}, \quad (\text{A.44})$$

and therefore¹⁹

$$\mathcal{B}^{\mathcal{SN}_2} = (1 + e_{1,2})\mathcal{B}^{\mathcal{SN}_1}. \quad (\text{A.45})$$

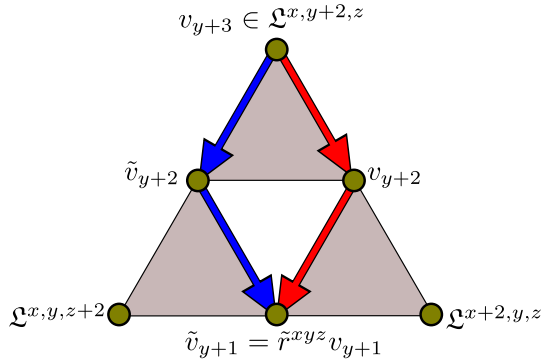


Figure 31. Computing the basis change from a type II move around the point (x, y, z) in the $(K-3)$ -triangle of spaces.

For a type II move centered on $\mathfrak{V}^{x,y,z}$, $x+y+z = K-3$, we first focus on the 2-triangle of 6 lines (A.28). As indicated in Figure 31, we choose basis vectors $v_{y+3}, v_{y+2}, v_{y+1}$ for the original snake \mathcal{SN}_1 . Then we have

$$v_{y+2} + v_{y+3} - \tilde{v}_{y+2} = 0, \quad (\text{A.46})$$

and using the key formula (A.19), $\tilde{v}_{y+1} = r^{x,y,z}v_{y+1}$. Thereafter the paths of the snakes \mathcal{SN}_1 and \mathcal{SN}_2 are the same, so the full change of basis is

$$\mathcal{B}^{\mathcal{SN}_2} = M(x, y+1, z)\mathcal{B}^{\mathcal{SN}_1}, \quad (\text{A.47})$$

¹⁹A word about conventions: Our linear transformations act from the right. Therefore, the matrix of a linear transformation T in a basis v_i is defined by $v_i T = \sum_j T_{ij} v_j$. If we change from a basis $\{v_i\}$ to a basis $\{v_i T\}$, the change of coordinates is obtained by acting on a row vector of coordinates x_i by right-multiplication with the matrix T_{ij} .

where

$$M(x, y+1, z) := \left(r^{x,y,z} \sum_{i=1}^{y+1} e_{ii} + \sum_{i=y+2}^K e_{ii} \right) (1 + e_{y+2,y+3}). \quad (\text{A.48})$$

We have labeled M by a point $(x, y+1, z)$ on the $(K-2)$ -triangle of planes. This is convenient, since if we define $r = 0$ for $y = -1$ then the formulae (A.47) and (A.48) also hold for $y = -1$, in which case we are considering a move of type I. In the application to spectral networks, the transformations (A.47), (A.48) correspond to \mathcal{S} -wall factors of type $S_{y+2,y+3}$, for $-1 \leq y \leq K-3$.

There are two canonical snakes beginning at the B -vertex, \mathcal{SN}_{BA} and \mathcal{SN}_{BC} , given respectively by the right and the left sides of the triangle of lines. The change of projective basis relating these canonical snakes is of particular importance for the spectral networks of the level K lift of the AD_1 theory. One can choose a path of $\frac{1}{2}K(K-1)+1$ snakes with each successive snake related to the previous one by a move of type I or type II. The total transformation between the two bases can therefore be written as

$$\mathcal{B}^{\mathcal{SN}_{BC}} = \prod_{(x,y,z) \in T(K-2)} M(x, y, z) \mathcal{B}^{\mathcal{SN}_{BA}}, \quad (\text{A.49})$$

where the product runs over the $\frac{1}{2}K(K-1)$ points (x, y, z) on the triangle $T(K-2)$ of planes. It is ordered so that later moves are further to the left. The formula (A.49) is equivalent to Proposition 9.2, p. 142, of [2].

Of course, there are many ways of using type I and type II moves to transform the snake \mathcal{SN}_{BA} into the snake \mathcal{SN}_{BC} , and any two such paths of snakes must lead to the same overall transformation (A.49). Nevertheless, it is useful to define a *canonical path of snakes*

$$\mathcal{SN}_{BA} \rightarrow \mathcal{SN}_{BC} \quad (\text{A.50})$$

as follows. We begin with the type I move with $y = -1$ on \mathcal{SN}_{BA} , and then proceed with type II moves up the right edge of the $(K-3)$ -triangle of spaces to $y = K-3$. The result is a snake that goes one step to the left to $(0, K-2, 1)$, and then proceeds parallel to the right hand side down to $(K-2, 0, 1)$. Next we begin again with a type I move at $y = -1$ and then proceed again up the edge to the left with type II moves to $y = K-4$, and so on. See Figure 9.14, p.142, of [2] for an illustration.

In terms of \mathcal{S} -transformations the canonical path of snakes is described by first implementing

$$S_{K-1,K} S_{K-2,K-1} \cdots S_{1,2}. \quad (\text{A.51})$$

(Remember that, since we are making a passive change of basis, this product is to be read from right to left; thus the first move is $S_{1,2}$, a type I move at the end of the snake, and the remaining factors are type II moves going successively up to the beginning of the snake.) Then the next set of moves is

$$S_{K-2,K-1} S_{K-3,K-2} \cdots S_{1,2}, \quad (\text{A.52})$$

and so on with the length of factors getting shorter by removing one \mathcal{S} -factor successively from the left until we have just $S_{1,2}$. The resulting product of \mathcal{S} -factors corresponds precisely to those in the product of \mathcal{S} -wall factors for the b -cable in (4.5) and (4.6).

The change of orientation from $\mathcal{SN}_{BC} \rightarrow \mathcal{SN}_{CB}$ multiplies the canonical homs along the snake by (-1) (because of the change of sign in the two lines in (A.8)). If we fix the overall scale by $v_K^{\mathcal{SN}_{CB}} = v_1^{\mathcal{SN}_{BC}}$, the effect of this orientation reversal is the transformation $W_0^{(K)}$ of (3.21):

$$v_i^{\mathcal{SN}_{CB}} = (-1)^{K+1-i} v_{K+1-i}^{\mathcal{SN}_{BC}}. \quad (\text{A.53})$$

Let us denote the total transformation in (A.49) by $M^{BA \rightarrow BC}$. Then it is clear that we have

$$M^{AC \rightarrow AB} W_0 M^{CB \rightarrow CA} W_0 M^{BA \rightarrow BC} = \kappa W_0, \quad (\text{A.54})$$

where κ is a constant. We must allow for such a constant because a snake only determines a *projective* basis. We claim that the constant is

$$\kappa = (-1)^{K-1} \prod_{(x,y,z) \in T(K-3)} r^{x,y,z}, \quad (\text{A.55})$$

where on the right hand side we take the product over the points in the $(K-3)$ -triangle of spaces. To prove (A.55) we take the determinant of (A.54). That determines κ up to a K^{th} root of unity. It is clear from the definition of the matrices that κ must also be a polynomial in the $r^{x,y,z}$. Therefore the root of unity is independent of the $r^{x,y,z}$, and can be determined by considering the special case $r^{x,y,z} = 1$. We write out the matrices explicitly for $r^{x,y,z} = 1$ in §B.3, and then (B.16) shows that the root of unity is $(-1)^{K-1}$.

The formula (A.48) provides an explicit solution of the monodromy constraint (3.24), when the mass parameters are equal to 1.

A.4.1 Examples of snakes for $K = 3$ and $K = 4$

As examples we consider the first two cases $K = 3$ and $K = 4$. Referring to the basis vectors defined in (A.14), (A.15), (A.16) (with $\tilde{v}^{011} = v^{011}$), we have the bases defined by the four snakes:

$$\begin{aligned} \mathcal{B}^{RR} &: \{v^{020}, v^{110}, v^{200}\} \\ \mathcal{B}^{LR} &: \{v^{020}, v^{110}, -v^{101}\} \\ \mathcal{B}^{RL} &: \{v^{020}, -v^{011}, -\tilde{v}^{101}\} \\ \mathcal{B}^{LL} &: \{v^{020}, -v^{011}, v^{002}\} \end{aligned} \quad (\text{A.56})$$

Then we have the basis changes:

$$\mathcal{B}^{LR} = \mathcal{B}^{RR} \begin{pmatrix} 1 & & \\ & 1 & 1 \\ & & 1 \end{pmatrix}, \quad (\text{A.57})$$

$$\mathcal{B}^{RL} = \mathcal{B}^{LR} \begin{pmatrix} r & & \\ & 1 & \\ & & 1 & 1 \end{pmatrix}, \quad (\text{A.58})$$

$$\mathcal{B}^{LL} = \mathcal{B}^{RL} \begin{pmatrix} 1 & & \\ & 1 & 1 \\ & & 1 \end{pmatrix}. \quad (\text{A.59})$$

Next let us consider the case $K = 4$. There are three sub-2-triangles we should focus on. In the top 2-triangle we can choose basis vectors

$$\begin{aligned} v^{030} + v^{021} + v^{120} &= 0 \\ v^{120} + v^{111} + v^{210} &= 0 \\ v^{021} + \tilde{v}^{111} + v^{012} &= 0 \end{aligned} \quad (\text{A.60})$$

with $\tilde{v}^{111} = r^{010}v^{111}$. On the bottom right 2-triangle we choose

$$\begin{aligned} v^{120} + v^{111} + v^{210} &= 0 \\ v^{210} + v^{201} + v^{300} &= 0 \\ v^{111} + v^{102} + \tilde{v}^{201} &= 0 \end{aligned} \quad (\text{A.61})$$

with $\tilde{v}^{201} = r^{100}v^{201}$. Finally, on the bottom left 2-triangle we choose:

$$\begin{aligned} v^{021} + v^{012} + \tilde{v}^{111} &= 0 \\ \tilde{v}^{111} + \hat{v}^{201} + \hat{v}^{102} &= 0 \\ v^{012} + v^{003} + \tilde{v}^{102} &= 0 \end{aligned} \quad (\text{A.62})$$

with $\tilde{v}^{102} = r^{001}\hat{v}^{102}$ and also $\hat{v}^{201} = r^{010}\tilde{v}^{201}$ and $\hat{v}^{102} = r^{010}v^{102}$. In terms of these vectors we can write the 7 snakes in the canonical path of snakes from RRR to LLL :²⁰

$$\begin{aligned} \mathcal{B}^{RRR} : & \{v^{030}, v^{120}, v^{210}, v^{300}\} \\ \mathcal{B}^{LRR} : & \{v^{030}, v^{120}, v^{210}, -v^{201}\} \\ \mathcal{B}^{RLR} : & \{v^{030}, v^{120}, -v^{111}, -\tilde{v}^{201}\} \\ \mathcal{B}^{RRL} : & \{v^{030}, -v^{021}, -\tilde{v}^{111}, -\hat{v}^{201}\} \\ \mathcal{B}^{LRL} : & \{v^{030}, -v^{021}, -\tilde{v}^{111}, \hat{v}^{102}\} \\ \mathcal{B}^{RLL} : & \{v^{030}, -v^{021}, v^{012}, \tilde{v}^{102}\} \\ \mathcal{B}^{LLL} : & \{v^{030}, -v^{021}, v^{012}, -v^{003}\} \end{aligned} \quad (\text{A.63})$$

From the linear relations among these bases, one can check that the changes of basis are as expected:

$$\mathcal{B}^{LRR} = \mathcal{B}^{RRR} \begin{pmatrix} 1 & & & \\ & 1 & 1 & \\ & & 1 & \\ & & & 1 \end{pmatrix}, \quad (\text{A.64})$$

²⁰Of course there are 8 snakes in total, but one of them does not occur in this canonical path. In general there are 2^{K-1} snakes but only $1 + \frac{1}{2}K(K-1)$ snakes in the canonical path. The overall change of basis is of course independent of which path of snakes from RRR to LLL we take. This fact is reflected in the spectral network, since one can freely pass an \mathcal{S} -wall of type ij through \mathcal{S} -walls and branch points of type kl as long as the indices do not overlap.

$$\mathcal{B}^{RLR} = \mathcal{B}^{LRR} \begin{pmatrix} r^{100} & & & \\ & 1 & & \\ & & 1 & 1 \\ & & & 1 \end{pmatrix}, \quad (\text{A.65})$$

$$\mathcal{B}^{RRL} = \mathcal{B}^{RLR} \begin{pmatrix} r^{010} & & & \\ & r^{010} & & \\ & & 1 & \\ & & & 1 & 1 \end{pmatrix}, \quad (\text{A.66})$$

$$\mathcal{B}^{LRL} = \mathcal{B}^{RRL} \begin{pmatrix} 1 & & & \\ & 1 & 1 & \\ & & 1 & \\ & & & 1 \end{pmatrix}, \quad (\text{A.67})$$

$$\mathcal{B}^{RLL} = \mathcal{B}^{LRL} \begin{pmatrix} r^{001} & & & \\ & 1 & & \\ & & 1 & 1 \\ & & & 1 \end{pmatrix}, \quad (\text{A.68})$$

$$\mathcal{B}^{LLL} = \mathcal{B}^{RLL} \begin{pmatrix} 1 & & & \\ & 1 & 1 & \\ & & 1 & \\ & & & 1 \end{pmatrix}. \quad (\text{A.69})$$

A.5 Duality

Finally we consider a basic and important question: how are the coordinates $r^{x,y,z}$ of a triple $(A_\bullet, B_\bullet, C_\bullet)$ related to the coordinates $\check{r}^{x,y,z}$ of the dual triple $(\check{A}_\bullet, \check{B}_\bullet, \check{C}_\bullet)$?

To answer this question, first note that the coordinates r^{xyz} can be read off²¹ from the cable transformation $M = M^{BA \rightarrow BC}$. For the dual flags we also have a cable transformation $\check{M} = M^{\check{B}\check{A} \rightarrow \check{B}\check{C}}$, from which we could similarly read off the dual coordinates $\check{r}^{x,y,z}$.

Let us define matrices α, β by

$$v_i^{\mathcal{SN}^{\check{B}\check{A}}} \cdot v_j^{\mathcal{SN}^{BA}} = \alpha_{ij}, \quad v_i^{\mathcal{SN}^{\check{B}\check{C}}} \cdot v_j^{\mathcal{SN}^{BC}} = \beta_{ij}. \quad (\text{A.70})$$

Then substituting $v_i^{\mathcal{SN}^{BC}} = M_{ij} v_j^{\mathcal{SN}^{BA}}$ and the dual relation into the formula for β reveals

$$\beta = M \alpha \check{M}^t. \quad (\text{A.71})$$

On the other hand, it follows directly from the definition of the snakes that α, β are antidiagonal. To see this note that $v_j^{\mathcal{SN}^{BA}}$ belongs to $A^{K-j} \cap B^{j-1}$, while $v_i^{\mathcal{SN}^{\check{B}\check{A}}}$ belongs to $\check{A}^{K-i} \cap \check{B}^{i-1}$; \check{B}^{i-1} annihilates B^{j-1} unless $i+j-2 < K$, i.e. $i+j < K+2$, while \check{A}^{K-i} annihilates A^{K-j} unless $2K-i-j < K$, i.e. $i+j > K$. Thus $v_i^{\mathcal{SN}^{\check{B}\check{A}}} \cdot v_j^{\mathcal{SN}^{BA}} = 0$ unless $i+j = K+1$.

²¹This is clear from the examples below. It seems likely one can give a rigorous proof by induction, but we did not do that.

Equation (A.71) can be rewritten as

$$\check{M} = \tilde{\beta} M^{-1,t} \tilde{\alpha} \quad (\text{A.72})$$

where $\tilde{\beta}$ and $\tilde{\alpha}$ are antidiagonal. This equation turns out to be strong enough to determine $\check{r}^{x,y,z}$ as a function of $r^{x,y,z}$, as well as determining $\tilde{\alpha}$ and $\tilde{\beta}$ up to an overall scale. To check that this is reasonable, let us count the parameters. M is an upper-triangular $K \times K$ matrix, with entries depending only on the $\frac{1}{2}(K-1)(K-2)$ independent variables $r^{x,y,z}$ — in other words its entries obey $2K-1$ nontrivial relations. The matrix \check{M} given by (A.72) is upper-triangular for any α, β . For general $\tilde{\alpha}, \tilde{\beta}$ though, \check{M} would not obey the same $2K-1$ relations; requiring that it does is just enough to fix $\tilde{\alpha}, \tilde{\beta}$ up to scale. The remaining $\frac{1}{2}(K-1)(K-2)$ equations in (A.72) are then enough to fix $\check{r}^{x,y,z}$.

In practice it is useful to rewrite (A.72) slightly as follows. We define a normalized matrix $T(r^{\mathfrak{v}})$ by left-multiplying M by a diagonal matrix so that the diagonal elements of $T(r^{\mathfrak{v}})$ are all 1, and similarly construct $T(\check{r}^{\mathfrak{v}})$ from \check{M} . Then we obtain

$$T(\check{r}^{\mathfrak{v}}) = \tilde{\beta} (T(r^{\mathfrak{v}}))^{-1,t} \tilde{\alpha} \quad (\text{A.73})$$

This easily implies that $\tilde{\beta} = \tilde{\alpha}^{-1}$. We can thus rewrite it as

$$T(\check{r}^{\mathfrak{v}}) = DW_0 (T(r^{\mathfrak{v}}))^{-1,t} W_0^{-1} D^{-1} \quad (\text{A.74})$$

where $W_0 = W_0^{(K)}$ and D is some diagonal matrix (uniquely determined up to scale as a function of $r^{\mathfrak{v}}$ by (A.74)).

B Explicit form of cable transformations

In this section we give explicit cable transformations in some tractable special cases.

B.1 $K = 3$

Writing out (A.48) explicitly we find that $M^{BA \rightarrow BC}$ is a product of three factors:

$$\begin{aligned} M^{BA \rightarrow BC}(1, 0, 0) &= (1 + e_{12}), \\ M^{BA \rightarrow BC}(0, 1, 0) &= (r^{000} e_{11} + e_{22} + e_{33})(1 + e_{23}), \\ M^{BA \rightarrow BC}(0, 0, 1) &= (1 + e_{12}), \end{aligned} \quad (\text{B.1})$$

where we have ordered the list so that the product from left to right is the product of factors from bottom to top. The explicit matrix is easily multiplied out. We find that $M^{BA \rightarrow BC}$ is

$$\begin{pmatrix} r^{000} & 1 + r^{000} & 1 \\ 0 & 1 & 1 \\ 0 & 0 & 1 \end{pmatrix}. \quad (\text{B.2})$$

The other cable transformations are identical, and we can multiply them out to find

$$M^{AC \rightarrow AB} W_0^{(3)} M^{CB \rightarrow CA} W_0^{(3)} M^{BA \rightarrow BC} = \kappa W_0^{(3)} \quad (\text{B.3})$$

with $\kappa = r^{000}$.

Now let us work out the relation between r and \hat{r} in this example. Writing out (A.74) longhand gives

$$\begin{pmatrix} \check{r}^{000} & 1 + \check{r}^{000} & 1 \\ 0 & 1 & 1 \\ 0 & 0 & 1 \end{pmatrix} = DW_0 \begin{pmatrix} r^{000} & 1 + r^{000} & 1 \\ 0 & 1 & 1 \\ 0 & 0 & 1 \end{pmatrix}^{-1,t} W_0^{-1} D^{-1} \quad (\text{B.4})$$

from which we easily read off

$$\hat{r}^{000} = 1/r^{000}. \quad (\text{B.5})$$

B.2 $K = 4$

Writing out (A.48) explicitly we find that $M^{BA \rightarrow BC}$ is a product of the following six factors:

$$\begin{aligned} M^{BA \rightarrow BC}(2, 0, 0) &= (1 + e_{12}), \\ M^{BA \rightarrow BC}(1, 1, 0) &= (r^{100}e_{11} + \sum_{i=2}^4 e_{ii})(1 + e_{23}), \\ M^{BA \rightarrow BC}(0, 2, 0) &= (r^{010}(e_{11} + e_{22}) + (e_{33} + e_{44}))(1 + e_{34}), \\ M^{BA \rightarrow BC}(1, 0, 1) &= (1 + e_{12}), \\ M^{BA \rightarrow BC}(0, 1, 1) &= (r^{001}e_{11} + \sum_{i=2}^4 e_{ii})(1 + e_{23}), \\ M^{BA \rightarrow BC}(0, 0, 2) &= (1 + e_{12}). \end{aligned} \quad (\text{B.6})$$

We have ordered the list so that the product from left to right is the product of factors from bottom to top.

The explicit matrix is easily multiplied out. For example, $M^{BA \rightarrow BC}$ is

$$\begin{pmatrix} r^{001}r^{010}r^{100} & (r^{001} + 1)r^{010} + r^{001}r^{100}r^{010} & (r^{001} + 1)r^{010} + 1 & 1 \\ 0 & r^{010} & r^{010} + 1 & 1 \\ 0 & 0 & 1 & 1 \\ 0 & 0 & 0 & 1 \end{pmatrix}. \quad (\text{B.7})$$

Similarly, $M^{CB \rightarrow CA}$ is

$$\begin{aligned} M^{CB \rightarrow CA}(0, 2, 0) &= (1 + e_{12}), \\ M^{CB \rightarrow CA}(0, 1, 1) &= (r^{010}e_{11} + \sum_{i=2}^4 e_{ii})(1 + e_{23}), \\ M^{CB \rightarrow CA}(0, 0, 2) &= (r^{001}(e_{11} + e_{22}) + (e_{33} + e_{44}))(1 + e_{34}), \\ M^{CB \rightarrow CA}(1, 1, 0) &= (1 + e_{12}), \\ M^{CB \rightarrow CA}(1, 0, 1) &= (r^{100}e_{11} + \sum_{i=2}^4 e_{ii})(1 + e_{23}), \\ M^{CB \rightarrow CA}(2, 0, 0) &= (1 + e_{12}). \end{aligned} \quad (\text{B.8})$$

Note particularly that we are using the same coordinates for the triangle $T(K-2)$, rather than a rotated set of coordinates which would put the C vertex on top. Also, note that the matrices (B.6) and (B.8) are the same except for a permutation of the coordinates r^v induced by a rotation of the triangle.

Similarly, we find the a -cable is a product of

$$\begin{aligned}
M^{AC \rightarrow AB}(0, 0, 2) &= (1 + e_{12}), \\
M^{AC \rightarrow AB}(1, 0, 1) &= (r^{001}e_{11} + \sum_{i=2}^4 e_{ii})(1 + e_{23}), \\
M^{AC \rightarrow AB}(2, 0, 0) &= (r^{100}(e_{11} + e_{22}) + (e_{33} + e_{44}))(1 + e_{34}), \\
M^{AC \rightarrow AB}(0, 1, 1) &= (1 + e_{12}), \\
M^{AC \rightarrow AB}(1, 1, 0) &= (r^{010}e_{11} + \sum_{i=2}^4 e_{ii})(1 + e_{23}), \\
M^{AC \rightarrow AB}(0, 2, 0) &= (1 + e_{12}).
\end{aligned} \tag{B.9}$$

The explicit matrices are easily multiplied out; we find that

$$M^{AC \rightarrow AB}W_0^{(4)}M^{CB \rightarrow CA}W_0^{(4)}M^{BA \rightarrow BC} = \kappa W_0^{(4)} \tag{B.10}$$

with $\kappa = -r^{100}r^{010}r^{001}$.

The formula (A.74) yields in this case

$$\begin{aligned}
\hat{r}^{100} &= \frac{1 + r^{100} + r^{100}r^{010}}{r^{010}(1 + r^{001} + r^{001}r^{100})}, \\
\hat{r}^{010} &= \frac{1 + r^{010} + r^{010}r^{001}}{r^{001}(1 + r^{100} + r^{100}r^{010})}, \\
\hat{r}^{001} &= \frac{1 + r^{001} + r^{001}r^{100}}{r^{100}(1 + r^{010} + r^{010}r^{001})}.
\end{aligned} \tag{B.11}$$

B.3 The point $r^{x,y,z} = 1$

At the point of \mathcal{C}_3 where all $r^{x,y,z} = 1$, it is possible to write explicit formulae for the cable factors T_a, T_b, T_c , valid for all K .

We find that $M^{BA \rightarrow BC}$, which can be written as

$$M^{BA \rightarrow BC} = S_{1,2}(S_{2,3}S_{1,2})(S_{3,4}S_{2,3}S_{1,2}) \cdots \tag{B.12}$$

with $S_{i,j} = 1 + e_{i,j}$, has Pascal's triangle embedded within it and is explicitly:

$$M^{BA \rightarrow BC} = \tau(K) = \sum_{i,j=1}^K \binom{K-i}{K-j} e_{i,j}. \tag{B.13}$$

The matrices $M^{CB \rightarrow CA}$ and $M^{AC \rightarrow AB}$ are also identically given by $\tau(K)$. The proof of (B.13) is easily given by induction after noting that

$$S_{K,K+1}S_{K-1,K} \cdots S_{1,2} = 1 + \sum_{j=1}^K e_{j,j+1}. \tag{B.14}$$

We can also compute

$$W_0^{(K)} \tau(K) W_0^{(K)} = \sum_{i,j=1}^K \binom{i-1}{j-1} (-1)^{K+1-i-j} e_{i,j}, \quad (\text{B.15})$$

and now the monodromy identity

$$(W_0^{(K)} \tau(K) W_0^{(K)}) \tau(K) (W_0^{(K)} \tau(K) W_0^{(K)}) = (-1)^{K-1} W_0^{(K)} \quad (\text{B.16})$$

boils down to an identity on sums of binomial coefficients:

$$\sum_{s,t=0}^n \binom{n-s}{a} \binom{t}{s} \binom{b}{n-t} (-1)^{s+t} = \delta_{a+b,n} (-1)^a, \quad (\text{B.17})$$

for a, b, n nonnegative integers. Equation (B.17) is proved by defining the left-hand side of (B.17) as $M(a, b)$ and then summing $\sum_{a=0}^n x^a M(a, b)$ successively using the binomial theorem to produce $(-1)^{n+b} x^{n-b}$.

References

- [1] D. Gaiotto, G. W. Moore, and A. Neitzke, “Spectral networks,” [1204.4824](#).
- [2] V. Fock and A. B. Goncharov, “Moduli spaces of local systems and higher Teichmüller theory,” *Publ. Math. Inst. Hautes Études Sci.* (2006), no. 103, 1–211, [math/0311149](#).
- [3] P. C. Argyres, M. Ronen Plesser, N. Seiberg, and E. Witten, “New $\mathcal{N} = 2$ Superconformal Field Theories in Four Dimensions,” *Nucl. Phys.* **B461** (1996) 71–84, [hep-th/9511154](#).
- [4] P. C. Argyres and M. R. Douglas, “New phenomena in $SU(3)$ supersymmetric gauge theory,” *Nucl. Phys.* **B448** (1995) 93–126, [hep-th/9505062](#).
- [5] A. D. Shapere and C. Vafa, “BPS structure of Argyres-Douglas superconformal theories,” [hep-th/9910182](#).
- [6] D. Gaiotto, G. W. Moore, and A. Neitzke, “Wall-Crossing in Coupled 2d-4d Systems,” [1103.2598](#).
- [7] D. Gaiotto, G. W. Moore, and A. Neitzke, “Wall-crossing, Hitchin Systems, and the WKB Approximation,” [0907.3987](#).
- [8] V. Fock and A. B. Goncharov, “Cluster X-varieties, amalgamation and Poisson-Lie groups,” [math/0508408](#).
- [9] M. Verbitsky, “Deformations of trianalytic subvarieties of hyperkähler manifolds,” *Selecta Math. (N.S.)* **3** (1998) 447–490, [alg-geom/9610010](#).
- [10] R. Bielawski, “Existence of closed geodesics on the moduli space of k -monopoles,” *Nonlinearity* **9** (1996), no. 6, 1463–1467.
- [11] D. Xie, “General Argyres-Douglas Theory,” [1204.2270](#).
- [12] D. Gaiotto, G. W. Moore, and A. Neitzke, “Framed BPS States,” [1006.0146](#).
- [13] M. Kontsevich and Y. Soibelman, “Stability structures, motivic Donaldson-Thomas invariants and cluster transformations,” [0811.2435](#).

- [14] D. Gaiotto, G. W. Moore, and A. Neitzke, “Four-dimensional wall-crossing via three-dimensional field theory,” *Commun. Math. Phys.* **299** (2010) 163–224, [0807.4723](#).
- [15] S. Cecotti and C. Vafa, “BPS Wall Crossing and Topological Strings,” [0910.2615](#).
- [16] T. Dimofte, S. Gukov, and Y. Soibelman, “Quantum Wall Crossing in $N=2$ Gauge Theories,” [0912.1346](#).
- [17] J. Manschot, B. Pioline, and A. Sen, “Wall Crossing from Boltzmann Black Hole Halos,” *JHEP* **1107** (2011) 059, [1011.1258](#).
- [18] B. Pioline, “Four ways across the wall,” *J.Phys.Conf.Ser.* **346** (2012) 012017, [1103.0261](#).
- [19] J. Caetano and J. Toledo, “ χ -Systems for Correlation Functions,” [1208.4548](#).
- [20] P. Longhi, “The BPS Spectrum Generator In 2d-4d Systems,” [1205.2512](#).
- [21] S. Cecotti, A. Neitzke, and C. Vafa, “R-Twisting and 4d/2d Correspondences,” [1006.3435](#).
- [22] D. Gaiotto, G. W. Moore, and A. Neitzke, “Spectral network movies.” Viewable at <http://www.ma.utexas.edu/users/neitzke/spectral-network-movies/> as of August 2012.
- [23] D. Gaiotto, “ $\mathcal{N} = 2$ dualities,” [0904.2715](#).
- [24] M. Alim, S. Cecotti, C. Cordova, S. Espahbodi, A. Rastogi, and C. Vafa, “BPS Quivers and Spectra of Complete $\mathcal{N} = 2$ Quantum Field Theories,” [1109.4941](#).
- [25] M. Alim, S. Cecotti, C. Cordova, S. Espahbodi, A. Rastogi, and C. Vafa, “ $\mathcal{N} = 2$ Quantum Field Theories and Their BPS Quivers,” [1112.3984](#).
- [26] I. Le and J. Kamnitzer. To appear.
- [27] G. W. Moore and Y. Tachikawa, “On 2d TQFTs whose values are holomorphic symplectic varieties,” [1106.5698](#).
- [28] D. Gaiotto, G. W. Moore, and Y. Tachikawa, “On 6d $\mathcal{N} = (2, 0)$ theory compactified on a Riemann surface with finite area,” [1110.2657](#).
- [29] O. Chacaltana and J. Distler, “Tinkertoys for Gaiotto Duality,” *JHEP* **1011** (2010) 099, [1008.5203](#).
- [30] O. Chacaltana and J. Distler, “Tinkertoys for the D_N series,” [1106.5410](#).
- [31] O. Chacaltana, J. Distler, and Y. Tachikawa, “Nilpotent orbits and codimension-two defects of 6d $\mathcal{N} = (2, 0)$ theories,” [1203.2930](#).
- [32] I. Brunner and D. Roggenkamp, “Defects and Bulk Perturbations of Boundary Landau-Ginzburg Orbifolds,” *JHEP* **0804:001,2008** (2007) [0712.0188](#).
- [33] T. Dimofte, D. Gaiotto, and R. van der Veen, “RG domain walls and hybrid triangulations.” To appear.
- [34] H.-Y. Chen, N. Dorey, and K. Petunin, “Moduli Space and Wall-Crossing Formulae in Higher-Rank Gauge Theories,” [1105.4584](#).
- [35] C. Fraser and T. J. Hollowood, “On the weak coupling spectrum of $\mathcal{N} = 2$ supersymmetric $SU(n)$ gauge theory,” *Nucl.Phys.* **B490** (1997) 217–238, [hep-th/9610142](#).
- [36] A. B. Goncharov, “Ideal webs and moduli spaces of local systems on surfaces.” To appear.
- [37] A. B. Goncharov and M. Kontsevich. To appear.

[38] N. Arkani-Hamed, J. Bourjaily, F. Cachazo, A. B. Goncharov, A. Postnikov, and J. Trnka, “Scattering Amplitudes and the Positive Grassmannian.” To appear.